A New Rheological Polymer Based on Boron Siloxane Cross-Linked by Isocyanate Groups

GEORGE SHMELIN

**Submitted in partial fulfilment of the
requirements of the University of
Hertfordshire
for the degree of Doctor of Philosophy**

February 2011

Abstract

The research described in this thesis originated from an idea to develop new body protection for the sport of fencing. The ultimate goal is to develop body armour which would be flexible, wearable, washable, light and breathable, offer protection from injuries and cover the entire body of a sportsman. A new material which exhibits shear thickening behaviour has been specially developed for this purpose in the process of this investigation. The material was designed and synthesised as a soft polymeric system which is flexible, chemically stable and able to increase the value of its modulus of elasticity upon impact at a high strain rate, while remaining in its soft gel-like elastomeric state when low strain rate deformation is applied.

The polymeric system that has been developed is based on interpenetrating polymeric networks (IPN) of immiscible polyurethane/urea-ester/ether and poly(boron)$_n$(dimethylsiloxane)$_m$ (where on average m $\approx$ 16 n). In addition, as the polydimethylsilane (PDMS) based polymeric system strongly tends to phase separation, the siloxane polymeric network was chemically cross-linked to the polyurethane polymeric network through polyurethane chemical cross-link-bridges. In order to introduce polyurethane cross-links to a siloxane-based polymeric network, some of the attached methyl groups in the PDMS polymeric backbone were substituted by ε-pentanol groups. The resulting polymeric system combines properties of an alternating copolymer with IPN.

The actual substitution of the methyl groups of PDMS into alternating ε-pentanol groups was performed by Grignard reaction of trifunctional chlorosilane monomers, magnesium and 1,5-dibromopentane. Chemical analytical techniques like FT-IR, ^{13}C NMR and ^{1}H NMR spectroscopy were used to reveal the chemical structure of the synthesised polymeric network. The mechanical and dynamical properties of the obtained polymeric system were analysed by dynamic mechanical analysis (DMA). This part of the investigation indicated that the novel polymeric system exhibited shear thickening behaviour, but only at a narrow diapason of deformations (i.e., deformations between 2 to 3 % of the length of the sample). At this limited diapason of deformation an effective increase of the modulus of elasticity from 6 MPa (at lower frequencies, i.e., up to ≤6 Hz of the applied oscillating stress) to 65 MPa (at frequencies between 12.5 to 25 Hz) was obtained. However, no increase in the modulus of elasticity was recorded at deformations below 1.5 % or above 3.5 % of length of the sample at the same frequencies (0 to 25Hz) of the applied oscillating stress.

__Acknowledgements__

I would like to thank all those who helped me in the execution of this research study. I would never have been able to work so hard and achieve reasonably promising results in key areas of this difficult and ambitious project without the significant and comprehensive support of my principal supervisor Dr Andreas Chrysanthou and the team of my second supervisors Dr Sharon Rossiter and Dr Guogang Ren.

In addition, I would like to thank Dr Suzanne Fergus, Dr Jacqueline Stair, Dr Sara Evans and particularly Dr Sharon Rossiter and Dr Joana Goral for their very high academic standards and guidance that enabled me to understand organic chemistry and not to see it as a science of mystery, but instead as an incredible science with logical rules where scientific predictions are possible and can be substantiated using various analytical techniques. I would also like to thank Dr Zhenxue Zhang for his comprehensive support particularly during the early stages of my work.

I would like to thank the entire group of technicians from the Chemistry laboratory of UH School of Pharmacy for their support in performing my experimental work. I strongly believe that without their help, completion of this study would have been almost impossible. I am particularly thankful to Mrs Judith Brooks, Mr Andrew Harman for his friendly help in correcting my written English in this thesis and also Mr Virendra Shah for passing onto me a part of his incredible skills in organic chemistry synthesis. In addition, I would like to thank Mr Peter Thomson of the School of Engineering and Technology for his permanent very friendly support.

My thanks is also expressed to the infinity of people who helped me during recent years including my University friends and Mrs Avis Cowley and Mrs Lorraine Nicholls from the Faculty Research Office. Most of all, I am thankful to my family for sharing my passion in this work.

Finally, I would like to thank Dr Ismail Jalisi from ICL for giving me the idea to continue my education and start my Ph.D. in May 2007. I also am particularly thankful to Mr Eamonn Swanton of Heales Enterprises Ltd for the financial support and unending confidence in this project.

Content

__Nomenclature__

__Physical Nomenclature__

A - nonlinearity strength of the tension in Indei's model

A_{cs} - cross section

a - length of the statistical polymeric segment ($a = l / N$) in Indei's model

C - normalization constant in Indei's model

$(DP)_w$ - degree of polymerization

D - tensile compliance

D_k - diffusion coefficient in de Gennes polymolecular viscosity model

E - Young's modulus

F - force

$G'(\omega)$ - the storage modulus

$G''(\omega)$ - the loss modulus

G - the Gibbs free energy

g - coupling intensity between the breakage rate and the middle-chain tension in Indei's model

H - enthalpy

K - constant in Ferry, Rouse and Beuche oligomeric viscosity model

k - the Boltzmann constant

L - length of a molecule

l - length

M - square of the molecular weight in de Gennes polymolecular viscosity model

N - number of segments in polymolecule

p_L - generation rate of the loop chains in Indei's model

q - electrical charge of an atom

R_{gk} - the gas constant

r - molecular end-to-end distance (overall coil size)

r_{dq} - distance between the electrical charges

ř - reduced end-to-end length of the chain in Indei's model $(ř = r / L)$

S - entropy

Sh - A Shore hardness

T - temperature

T_m - the crystalline melting temperature

t - time

β - breakage rate of the bridge chain in Indei's model

γ - strain of a shear stress

δ - stress-strain lag's phase angle $(\tan δ = G''(ω) / G'(ω))$

ε - strain of a tensile stress

ϵ - dielectric constant

$ϵ_0$ - electric permittivity of free space

η - viscosity

$ν^A(t)$ - number density of the active chains in Indei's model

$ν^D(t)$ - number density of the dangling chains in Indei's model

$ν^L(t)$ - number density of the loop chains in Indei's model

σ - tensile stress

τ - shear stress

$τ_t$ - relaxation time

υ - Poisson's ratio

$Φ_0$ - probability distribution function for a dangling chain in Indei's model

Ω - number of possible molecular confirmations

ω - the angular frequency of applied stress

w - width of the material

Ϝ(r, t) dr - number density of active chains having an end-to-end vector r ~ r + dr at time t in Indei's model

Б - free energy barrier

ч (ř) - (unitless) tension along the middle chain in Indei's model

Э - the Helmholtz free energy

Chemical Nomenclature

Al - aliphatic group

Ar - aromatic group

Et - ethyl group

Me - methyl group

R - organic group

X - halogen

List of Abbreviations

CR- constrain release

DMA- dynamic mechanical analysis

DP- degree of polymerization

EVA- ethylene vinyl acetate

FT-IR- Fourier transform infrared spectroscopy

GLC- gas liquid chromatography

GPC- gel permeation chromatography

HDI- hexamethylene diisocyanate

HPE- high density polyethylene

IPDI- isophorone diisocyanate

IPN- interpenetrating polymer networks

LDPE- low density polyethylene

MDI- methylene diphenyl diisocyanate

NMR- nuclear magnetic resonance

M_n- average molecular weight

PB- polybutadiene

PE- polyethylene

PEO- polyethylene-oxide (polyoxyethylene)

PDMS- polydimethylsilane

PDPS- polydiphenylsilane

PI- polyisoprene

PMMA- poly-(methyl-methacrylate)

PP- polypropylene

PPMS- polyphenylmethylsilane

PPO- polypropylene-oxide (polyoxypropylene)

PS- polystyrene

semi-IPN- scarcely cross-linked interpenetrating polymer networks

TDI- toluene diisocyanate

T_g- glass transition temperature

THF- tetrahydrofuran

T_m- crystalline melting temperature point

vs - versus

WLF- semi-empirical equation of Williams, Landel and Ferry, describing time-temperature superposition

List of Figures

List of Tables

1 <u>Introduction</u>

The research described in this thesis originated from an idea about new body protection for the sport of fencing. The ultimate goal is to develop body armour for fencing, which would be flexible, wearable, washable, light and breathable, offer protection from injuries and cover all the body of a sportsman.

A future development would be the ability to detect stress on its surface caused by a weapon of the opponent.

The first thing to consider for possible designs for body armour for use in modern fencing is the effect of a momentum pressure applied to a small section of the body's surface and the role of body armour in offering protection.
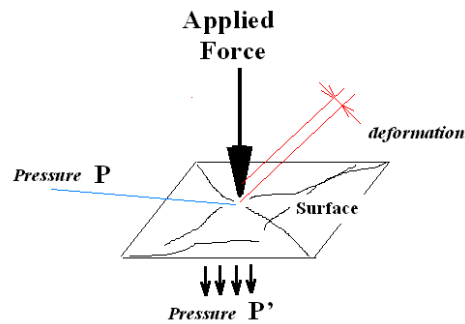
Figure 1: *Application of a Pressure on a Surface*

Following impact, the kinetic energy of a projectile will be transferred to the body armour it strikes. In order to effectively absorb the kinetic energy, the latter has to undergo deformation as suggested in Figure 1. In the absence of any body armour, the kinetic energy will be absorbed by the human body itself by undergoing elastic or permanent deformation, leading to possible rupture and penetration injuries. Needless to say, for the human body this could be life-threatening. The main aim of body armour is to spread the impact energy to effectively increase the surface area of the impact and thus decrease the applied pressure acting on the body to prevent possible penetration. In addition, it is also preferable that body armour should be able to absorb the impact energy by deforming [1, 2].

In the sport of fencing, the sharp edge of a foil, rapier or sword can impact with reasonably high speed on a very limited surface of application. The aim of the protective costume is to spread the pressure and also to reduce the speed of the foil's edge. Without a protective costume the impact from an unsharpened foil or rapier for the sportsman would still be able to cause quite serious injuries during competition.

The current protective costume available, as shown in Figure 2, is a composite of a conductive layer that registers the touch of a foil or rapier. It is a combination of a soft thick textile to protect the torso from the front. Because the costume is so bulky it does not cover the entire body of the sportsman and it is limited just to the torso [3]. Also this costume is suitable just for protection from a relatively low magnitude impact caused by a foil or rapier and is unsuitable for a protection from heavier weapons like a sword or an axe, etc.

Figure 2: Current Fencing Protective Costume

In the design of armour for sport applications, the main part of the sportsman's body, such as the torso and shoulders, could be covered by a number of flexible polymeric sheets made from vinyls or aramides and held by soft connections in a way similar to body armour of the Roman Legionaries (lightweight and reasonably cheap to produce armour "Lorica Segmentata" [4], as shown in Figure 3).

The design and material selection for the protection of the flexible and vulnerable parts of the body (knees and elbows) presents many challenges. It is clear to see from comparison of Figures 3 and 4, that progress in the attempt to cover those parts of the body effectively and to avoid a bulkiness in the design has been quite limited [5].

Figure 3: Roman Legionary's Body Amour "Lorica Segmentata"

Figure 4: Contemporary Armour of a Police Anti-Riot Detachment

Another ancient armour design to offer a possible solution for a flexible protection of elbows and knees is the "Chain Mail", as shown in Figure 5.
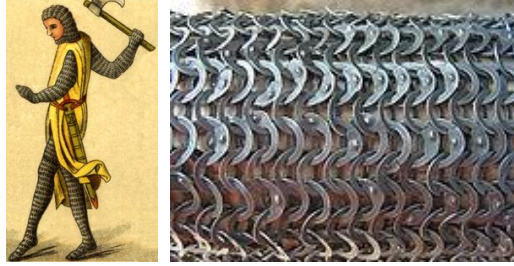
Figure 5: Chain Mail

Chain Mail is flexible armour and it is almost impossible to penetrate using any conventional medieval weapon. This construction can ward off a slashing blow from an edged weapon, preventing it from cutting through to the skin. On the other hand the flexibility of mail means that a particularly strong blow would often be transferred to the user, often causing fractures or serious bruising but preventing more serious injuries [6].

Metallic Chain Mail still finds application as protective gloves and aprons for butchers. In addition, the design based on Chain Mail gives needed breathability to the armour. A limitation could arise from the heavy weight of such armour and the technology of Chain Mail which requires excessive and skilful labour. On the other hand, based on the experiences of the composites industry, it is possible to combine the original design of Chain Mail with sewing/knitting of polymeric fibres to form fibre-networks in polymeric composites [7].

A recent patent and publication by the University of Exeter and Auxetix Ltd [8] can make a flexible design of the armour woven from yarns even more attractive. The idea is that a stretchy fibre provides the core of the yarn and a stiffer fibre is then wound around it, as shown in Figure 6.

Figure 6: an Example of an Auxetic Material

When the stiffer fibre is put under strain, it straightens. This causes the stretchy fibre to bulge out sideways, effectively increasing the diameter of the yarn. Scientifically speaking, the yarn is an auxetic material - one that gets thicker when stretched [9].

Also "Dragon Skin" as shown in Figure 7 is an ancient armour design which is in use for some of the latest bullet-proof armour. It is considered that "Dragon Skin" could be used in combinations of a segmented and a flexible part of the developing armour [5, 6].

Figure 7: Dragon Skin

After reviewing the previous and current possible designs of suitable armour, it became apparent that a self-stiffening polymeric material or composite could be the best choice for this application, hence it would be possible to avoid unnecessary bulkiness and excessive difficulties in the final design.

Acceptable polymeric candidates were looked at, sourced from recent patents and publications. During the last few years there has been increased commercial interest coupled with a better theoretical understanding of dynamic polymeric behaviour. A number of variable relevant publications and industrial patents have been launched in polymers suitable for a mechanical impact absorption and body or goods protection.

Current applications vary from a recent combined patent from a group of the leading Japanese plasma TV screen manufactures, as a 70 μm polyoxyalkylene-series polymer (generally polyoxybutylenes) for producing impact absorption sheets for thin flat glass panel displays [10], and a patent of footballers' shin protection by flexible sheets made from ethylene vinyl acetate (EVA) polymer [11]. Dow Corning has also published a patent of bikers' flexible protective suit based on poly-(boron-siloxane) resins, as shown in Figure 8 [12, 13]. There is also a patent from a locally based company Design

Blue, which has developed protective foam based on a polymeric alloy of poly-(boron-siloxane) gels and soft polyurethane foam "J-Foam" for a soft and flexible protective material for mountain skiers [14].
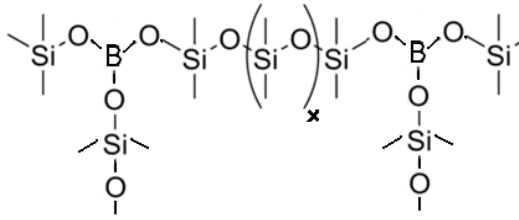
Figure 8: *Poly-(boron-siloxane)*   **Figure 9:** *Ethylene Vinyl Acetate (EVA)*
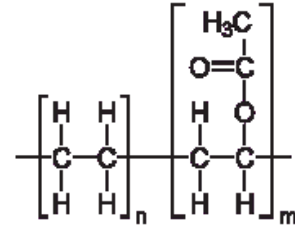
Despite progress in the area, currently only EVA based protective goods have been produced by Adidas commercially in an industrial scale [10]. All the other patented protective materials have been at a prototype stage. EVA, as shown in Figure 9, has been used as a drug delivery device polymer, even though the technological aspects of this material had been known [15].

EVA is a semi-flexible plastic at room temperature and is suitable for making protective sheets covering large and non-flexible parts of a sportsman's body like the shins, etc [16]. In the case of protecting such parts of a body as elbows and knees it is difficult to avoid a bulky design, as can be seen in the contemporary non-bullet-proof body armour designed for anti-riot police, shown in Figure 4.

After analysis of the contemporary market and patents on self-stiffening polymeric materials, it became apparent that none of the existing materials or patents entirely satisfies all the requirements, as none of the existing materials was able to provide a reliable and flexible protection for knees and elbows without serious compromises on wearability and bulkiness. Hence the decision was taken to develop a new self-stiffening polymeric material. The new polymer should be soft and elastic at room temperature, and able to significantly increase its tensile strength during fast deformation. The new developing polymer should also have high diapason of working temperatures, be chemically resistant as be washable, and have high values of tear resistance. Also it is preferable that the new polymer would be able to absorb high amounts of energy from an applied mechanical impact.

In addition, it was aimed to avoid already existing patents in the field. In the middle of the last century Bayer actively worked on nitrogen based rigid polyfibres not covered by the DuPont patent of Nylons and realized quickly that the new polymer could be a superior replacement of not just Nylon but also of natural rubber. This new polymer was polyurethane [17]. Research in this polymeric material is currently in a process of being patented as a novel semi-IPN (scarcely cross-linked Interpenetrating Polymeric Networks [18]) network of polyoxyalkenes (such as a combination of polyethylene oxide and polypropylene oxide) extended through urethane and urea links and cross-linked to a partly immiscible poly-(boron-siloxane) interpenetrating network.

It is expected that by using polymeric combinations of a few useful materials in a semi-IPN it is possible to avoid difficulties and limitations caused by these polymers and at the same time to have the best from the unique mechanical properties of both groups of those polymers [19].

In addition to being costly, polysiloxanes often exhibit insufficient tear resistance and tensile strength [20], while the very narrow range of possible working temperatures for polyoxyalkylenes, polyoxyalkenes and vinyls could potentially restrict their operation as self-stiffening materials [21].

In addition the use of scarcely cross-linked polymeric networks instead of non-cross-linked IPN of those immiscible and very flexible polymers would prevent possible phase separation [17].

In addition, we are expecting that the new developing polymeric material may have quite good damping characteristics. The benefits of such a light and effective shock absorbing polymer or foam could be welcomed by police forces in anti-riot detachments as flexible armoured material, or in the defence industry as part of body armour preventing soldiers from possible lethal shock wounds such as a blunt trauma caused by explosion, etc.

2 <u>Literature Review</u>

The topic of self-stiffening on relatively fast deformation polymeric materials which can be used for impact-protection is relatively new and covered in the existing literature just by a few recent patents and even fewer research articles. On the other hand, thorough analysis and investigation of data and models of known dynamic viscoelastic behaviour of polymers may lead this research towards developing material acceptable for body protection using self-stiffening on a fast deformation polymeric material.

2.1 Physical Properties of a Relaxed (non-Dynamic) Polymer

2.1.1 Effect of Intermolecular Secondary Forces

It is well known that some polymers at room temperature exhibit high tensile strength and are hard and brittle, while others are soft and very flexible. The variation of mechanical properties of different polymers lies in the affinity between the polymeric chains and in the ability of those chains to create interactions between them. It could be both kinds of interaction, such as chemical cross-links or physical cross-links - normally, the stronger the interaction between the chains the harder the polymeric material [22].

The interaction between the polymeric/oligomeric chains is influenced by the ability of the chains to build a strong hydrogen bond between the neighbouring polymolecules or be kept just by relatively weak Van der Waals forces. (In a polymolecular material additional intermolecular interaction effects could be caused by free volume and also molecular configuration, for example, the formation of molecular loops [19].)

An example can be presented by comparison of a boiling point difference between short molecules of methane, chloromethane and methanol, as shown in Figure 10. All three molecules are quite similar in their molecular mass and shape, but have huge differences in their boiling temperatures and hence in the amount of internal or secondary forces which are attracting the molecules together.

8

At atmospheric pressure, methane is a gas which boils at -161.6 °C, chloromethane boils at -24.2 °C and methanol just at 64.7 °C. The boiling temperature of methanol is significantly higher even though its molecular mass and the polarity of the valence bond is lower than in chloromethane.
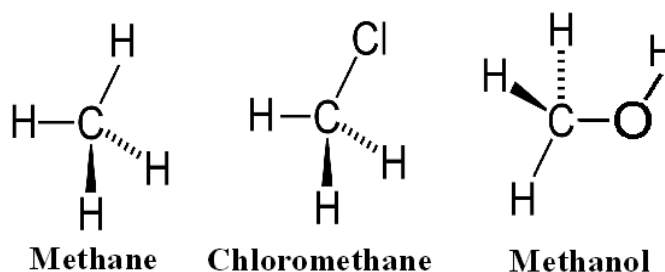
Figure 10: Methane, Chloromethane and Methanol

Methane is a short covalent molecule which is attracted to a neighbouring methane molecule by a weak Van der Waals force of about 0.2 kJ/mole.
In chloromethane, the chlorine atom is much more electronegative in comparison with carbon. Therefore, chlorine in the chloromethane covalent bond is attracting the bonding electrons much closer to it and creates an electrostatic dipole, as shown in Figure 11.

In chloromethane, the bonding electrons are closer to the electronegative chlorine atom and the positive charge to the carbon. Such dipoles create electrostatic attraction between neighbouring molecules. So the boiling temperature of chloromethane is significantly higher than in methane.
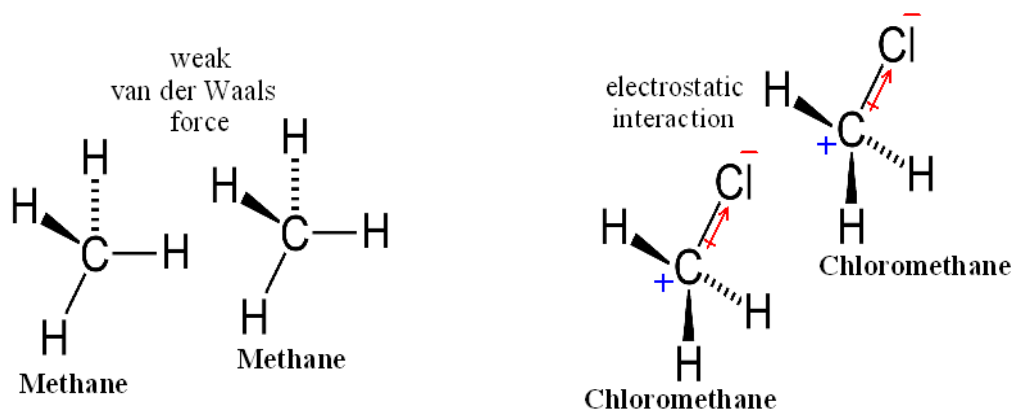
Figure 11: Van der Waals Force between Molecules of Methane and Chloromethane

The boiling temperature of methanol exceeds the boiling point of chloromethane, even though chlorine creates the bigger dipole with carbon than oxygen does, as shown in Figure 12.
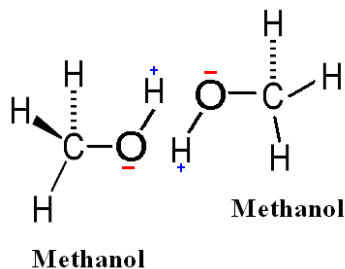
Figure 12: Hydrogen Force between Molecules of Methanol

The difference in the interaction between neighbouring molecules, and hence in the boiling temperatures lies in the possibility of a closer proximity of the electronegative charge to the positive charge of the neighbouring molecules. The electrostatic force of point charges has a reciprocal relationship to the square of the rising distance between the charges:

$$F = q_1 \, q_2 \, / \, 4\pi\epsilon\epsilon_0 \, (r_{dq})^2 \qquad (1)$$

where F is the force of the bond, q_1 and q_2 are the electrical charges of both atoms, ϵ is a dielectric constant, ϵ_0 is a constant called the permittivity of free space and r_{dq} is the distance between the electrical charges.

Between two molecules of methanol, the hydrogen attraction is so effective because a small atom of electronegative oxygen effectively allows a hydrogen proton attached to the neighbouring oxygen from another molecule to come close enough to create a strong bond. The bond is about 5 kJ/mole, which in comparison is 25 times higher than the Van der Waals bond between molecules of methane [23].

An atom of chlorine is much bigger in its size than an atom of oxygen and that effectively prevents chlorine from forming such a strong bond with hydrogen, as the comparatively small atoms of oxygen or nitrogen are able to.

In bromomethane the interaction between polar bonds of neighbouring molecules is even smaller in comparison to that between molecules of chloromethane, but because of a significantly higher molecular weight, the boiling temperature is higher and reaches -4 °C [23, 24].

Hence intermolecular interaction affects the physical properties of short molecules. It is possible to predict that it should be no less important for the mechanical properties of oligo/polymolecules. And therefore, the more polar the molecules, the stronger the connecting force. Polymers containing high numbers of polar groups in the chain normally exhibit much higher T_g, T_m and tensile strength at room temperature in comparison to those which are connected through weak Van der Waals forces [25].

In addition, the stress relaxation of polymers containing hydrogen bonds is strongly influenced by it. For example, a hydrogen bond (such as a bond between two molecules of methanol) is generally keeping both molecules strung together during thermal oscillations. In the event the hydrogen bond is broken, the bond can be reconnected with one of the neighbouring molecules. Therefore, for a melt of longer molecules containing strong hydrogen bonds, relaxation is available by bond rearrangements [17].

At room temperature for molecules of methanol, hydrogen bond rearrangement normally takes about 10^{-10} s and it is generally limited to receiving a suitable phonon of energy which is enough for such rearrangement [26]. For a longer molecule, a similar hydrogen bond rearrangement could take much longer, due to the fact that the molecular oscillations are limited by compression of the molecule into a "tunnel" of free volume by its neighbours. Therefore polymolecular materials containing high amount of hydrogen bonds in the chain normally exhibit very high values of T_g [17].

2.1.2 Effect of Crystallinity on a Mechanical Properties of a Polymer

The physical properties of a polymeric material (not cross-linked chemically) strongly depend on the cohesive energy density (i.e., how easily the molecules are able to form a number of consecutive strong hydrogen bonds with the neighbours). However, examples such as the polar and simultaneously very soft and flexible polyurethane/urea Spandex, and the non-polar polyethylene fibres of Dyneema (used for bullet-proof

armour), show that other factors are also involved in influencing the possible mechanical properties of a polymer [21].

Let us take polyethylene (PE) as an example, the repeating unit structure of which is shown in Figure 13. This polymer tends strongly to form a crystalline structure when it is slowly cooled from molten. If the crystalline structure of PE becomes ordered during its formation and the molecules are long and monodispersed enough (high density polyethylene HDPE), HDPE is able to form a material which is known as Spectra or Dyneema. This is the toughest thermoplastic material in existence and is extensively used in composite applications when exceptional toughness is required, as in the case of bullet-proof armour [19].
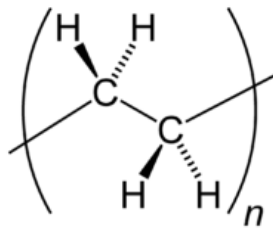
Figure 13: *the Repeating Unit of Polyethylene*

More commonly polyethylene is used as a packaging material where its molecules are much shorter. Since the molecules of polyethylene tend strongly to crystallize, they are deliberately branched or copolymerized to some extent with other vinyls (low density polyethylene LDPE). Hence the polymer does not form a perfect crystalline structure, and Van der Waals forces are effectively reduced in the areas of molecular chain defects. At room temperature the material is semicrystalline with quite flexible molecules (parts of molecules) in the amorphic areas. The density of the material drops and so does the tensile strength. The resulting polymer is soft, flexible and leathery [25].

Even more so, if ethylene is copolymerized randomly with 25 % of propylene in one resultant isotactic polymolecule, such molecules are effectively prevented from forming a crystalline structure and the polymer is elastic enough to be an elastomer, as shown in Figure 14.
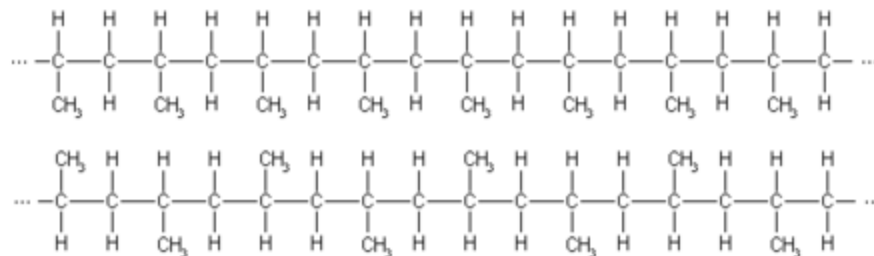
Figure 14: Polyethylene-polypropylene Rubber

In fact isotactic polyethylene-propylene normally forms a thermoplastic rubber which has enough crystalline areas to keep the polymer from flowing apart. It also has substantial amorphous areas which are able for easy flow on stress relaxation [17].

Other well known thermoplastic rubbers work on the same principle as polyethylene-propylene does. An example is the alternating copolymer of polydimethylsilane (PDMS) and polydiphenylsilane (PDPS), where PDMS does not form any crystalline structure at all until -40 °C and is kept together by the formation of some crystalline blocks of PDPS [20]. It is also possible to take the example of the alternating copolymer of Spandex, where long soft parts of the polymolecular chain stay in the amorphous stage when rigid and polar aryl-urethanes/ureas groups form effective physical cross-links to keep the material from flowing apart [25].

2.1.3   Geometry and Flexibility of a Polymeric Chain

In the example of high and low density polyethylene given below it is possible to see that if a polymeric chain is straight and free of possible defects it is able to form a crystalline structure and achieve high values of tensile strength. Therefore when a polymeric chain is not straight or includes a significant number of defects, such a chain would be unable to lie close enough to its neighbour (or itself in case of crystalline structure), hence its mechanical properties are lower [21]. As an illustration of this it is possible to consider the examples of two aramid materials: Kevlar, as shown in Figure 15, and Nylon, as shown in Figure 16.
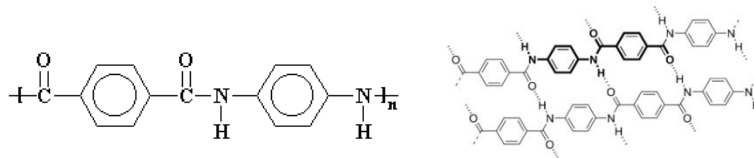
Figure 15: Aramid Kevlar

Aramid Nylon (Figure 16) is a much more flexible polymer than aramid Kevlar (Figure 15).
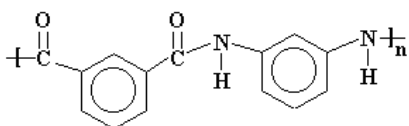
Figure 16: Aramid Nylon

Kevlar is stiffer than Nylon and has a higher T_m and T_g because the atoms of nitrogen are connected to the 1,4 (para) carbon of a phenyl group. This gives a much straighter molecular chain than in the case of the 1,3 (ortho) in Nylon [19]. The chain of Nylon tends to form coins and therefore the free polymeric volume is higher than in Kevlar. The straighter the chain, the closer to each other the polymolecules can lie in the polymer and so the stronger the secondary intermolecular force [17].

Quite often in the polymers industry a small amount of an incompatible monomer is added to a polymeric mass. These small particles of immiscible monomer/oligomer prevent two/few affinitive polymeric chains from reaching maximum proximity (i.e., giving an increase in free volume) and so prevent the formation of strong secondary forces interaction. Hence such monomer/oligomer would effectively work as a polymeric lubricant [25]. For example, for polyolefins it is the monomer/oligomer of styrene.

The rigidity of the polymeric chain is another important factor in the polymer behaviour. Molecules of PDMS are the most flexible, the majority of polyolefins give reasonably flexible materials while polyphenyls, polystyrenes, aramides are always rigid at room temperature. The essential differences in the polymer behaviour lies in the flexibility of the valence bonds (i.e., how easy it is to change the molecular shape by molecular thermal oscillations (IR phonons) - the conformational change of a molecule) [17, 26].

Silicon gives a very flexible bond with oxygen. Oxygen also gives quite a flexible valence bond with carbon. In a single carbon to carbon bond, such as in polyethylene, the energetical barrier of conformational change is about 3 kJ and even this bond is slightly more rigid than the bond of carbon to oxygen, but it still provides reasonable flexibility to the chain at room temperature, with a usual bond-rearrangement time about 10^{-10} s (which is similar to a force and rearrangement time of hydrogen-bond between two hydroxyl groups).

The energetical barrier of conformational change in the double carbon-to-carbon bond is about twenty times higher than in a single valence bond, and hence the chain normally stays absolutely rigid [23].

In aramides, urethanes and ureas a single bond between nitrogen and carbon is rigid and the energetical barrier is effectively closer to a double carbon-to-carbon bond, than to the single one. This is caused by a resonance structure of the nitrogen bond in those polymers [17, 23].

As an example, consider the fact that polyurethane can give a variety of flexible rubbers, while aramides just give stiff fibres, as shown in Figure 17.
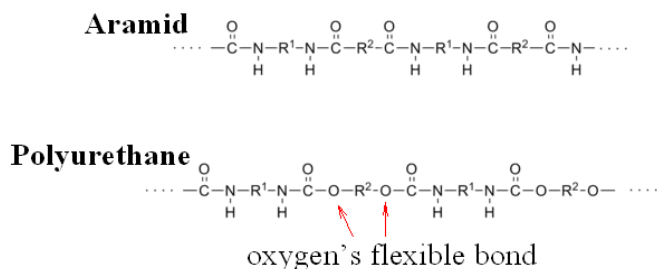
Figure 17: Molecules of Aramid and Polyurethane

Bulkiness and/or polarity of a polymeric chain are the factors which are normally reducing mobility of a chain and hence increase the tensile strength of a polymer. In the case of the alternating polyurethane copolymer, shown in Figure 17, polar and bulky groups of urethanes are affinitive to each other and effectively interact [21]. But in another example, shown below, the isotactic alternating copolymer of polyethylene-propylene, the ethylene or propylene groups do not have enough consequent chain length

to achieve high values of intermolecular interaction, lowering affinity. The material is therefore soft and flexible.

Looking at alternating polymer/copolymer (for example, such like Nylon 6,6): where each part of the chain is identical to the following, such equal blocks of polymer/copolymer are able to build strong intermolecular interactions, as shown in Figure 15. When all the parts of a copolymer have different lengths and are random and/or have differences in geometry, such interaction is on a much lower scale [25].

When blocks of a copolymer are quite different and have sufficient length, then such blocks of the copolymer start to behave as separate polymers and have different glass transition and melting point temperatures [21].

In some cases bulkiness of the chain or its substitution lead to a more flexible polymer, however, in some cases this could lead to the reverse effect. Polydimethylsilane (PDMS) is known as a polymer with the most flexible polymeric chain. But when methyl groups attached to the main polymeric chain are substituted by an ethyl or longer groups, the polymer gradually loses its chain's flexibility [20].

2.1.4   Copolymerization and Polymeric Compatibility

The majority of polymers are not compatible with other polymers, even when short molecules of the monomers or oligomers are absolutely miscible/compatible with each other [27]. This has found some useful engineering applications such as the creation of polyethylene-propylene rubbers from a blend of two reasonably rigid crystalline polymers, but it also brings enormous problems for the utilization of polymeric waste. Therefore it is impossible just to blend any polymeric waste and get something useful from it, as a careful separation of different polymers/polymeric-components is required before further processing. Unfortunately this is not always cost-effective and any polymer designer should consider this factor during the engineering of a new polymeric product [21].

A useful approximation to polymeric miscibility is the Flory-Huggins model where the change in the Gibbs free energy upon mixing ΔG (at temperature T) should be negative:

$$\Delta G = \Delta H - T \, \Delta S \qquad (2)$$

In the Flory-Huggins model ΔH (the change in enthalpy) and ΔS (the change in entropy) can be considered separately from each other. Here enthalpy would be considered as a molar (also polymer's chains fraction) fusion factor and entropy as a gain of freedom of the possible conformations of the molecule. Therefore when a polymer is dissolved in a short molecular solvent even with some losses in enthalpy, but a sufficient gain in entropy, it is immiscible with the polymer because two long molecular materials cannot give themselves a higher freedom of molecular movement [17, 27].

Even though the Flory-Huggins model is a quite effective and popular tool for a basic prediction of polymeric miscibility, and it is intensively used in the coating and dye industry, it is just a first approximation which does not include such factors as the specific polymeric geometry, strong hydrogen bond formation and most important a free volume of polymer. Later Freeman, Rowlinson and Siow [17] showed that polymers tend to a phase separation not just in lower temperatures, but also during high deformations or temperature increasing. This is due to the increasing difference in the free volume of the polymeric fractions. Therefore, each polymer has its different free volume and with increasing temperature or polymeric flow that difference in the free volume increases, and hence causes a polymeric phase separation [28, 29].

Recent work by Majumdar et al [30] shows a possible effect on a loosely cross-linked copolymer/semi-IPN of siloxane-urethane thermoset system formation by a solvent composition. PDMS is known as a polymer of the most flexible polymeric chain (and also the lowest after Teflon inter-chain adhesion [20]), because the energetic barrier of the chain conformation is extremely low, hence the time of the conformation is very short, therefore at any moment in time such a chain is able to take a conformation of the lowest possible energy [17].

PDMS/siloxane and urethane (or polyoxyalkylenes/polyesters as chain extenders) are immiscible, because of a great difference in their solubility parameters and also because of the significant difference in their polymeric free volume. In the case of copolymerization, siloxane generally tends to create a surface layer of a much higher concentration than in the main body of the polymer [20, 30]. Majumdar et al [30] showed that when a solvent system used in polymerization is immiscible or partly miscible with siloxane ("bad" solvent), siloxane does not form a layer of higher concentration on the

surface, and instead the lowest concentration of siloxane was found in the surface area of the polymer. Because siloxane affects the formation of the surface microstructure of a polyurethane polymer polymerized in a solvent, by a combination of solvent systems it is possible to effectively regulate the surface morphology of the resulting product.

2.1.5   Crystalline Melting Point T_m and Glass Transition Temperature T_g

Discussion of the crystalline melting point T_m and the glass transition temperature T_g cannot be separated from the dynamic properties of polymeric materials because of the similarities and strong co-influences of the processes [17].

The temperature at which the last standing and usually most perfect crystals are melted in a polymer is the crystalline melting point T_m. A semicrystalline or an amorphous polymer below this temperature tends to be leathery and rubbery, while above the melting point polymers are viscous liquids [25].

The crystalline melting temperature T_m may be described by the Gibbs free energy from equation 2:

$$T_m = \Delta H / \Delta S \qquad (3)$$

In this case, the change in enthalpy ΔH represents the difference in cohesive energies between chains in the crystalline and liquid states, while the change in entropy ΔS represents the difference in the degree of order between polymer molecules in the two states. A Schematic Representation of the free energy as a function of temperature is shown in Figure 18 [17, 31].

Enthalpy is generally independent of molecular weight. But polar groups on the chain, particularly if dispersed regularly in the chain, so as to encourage regions of extensive cooperative bonding, would enhance the magnitude of enthalpy. For example, for Nylon which exhibits high values of hydrogen bonds, and therefore cohesive energy (enthalpy), T_m will be significantly higher than in polyethylene [25].
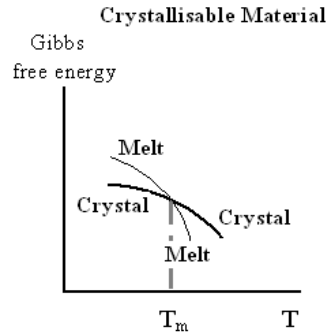
Figure 18: Schematic Representation of the Free Energy as a Function of Temperature

Table 1: Comparison of the Crystalline Melting Temperatures, T_m, of Common Polymers Having Quite Different Polymeric Chain Stiffness and Interchain Cohesive Energy

		T_m °C			T_m °C
polyethylene		135	polyethylene oxide		66
polydimethylsiloxane		unknown	Nylon 6,6		265
polypropylene		165	ureas		370
polystyrene		240	urethanes		200

The ends of molecules, or defects in the molecular geometry are unable to fit in a perfect crystalline structure and so will have more free volume and higher values of entropy. Therefore T_m of such polymers will always be lower than nominal. This is illustrated below in section 2.1.2 [21] using examples of LDPE or polyethylene-polypropylene rubber.

Entropy depends not only on molecular weight and chain geometry, but also on structural factors like chain stiffness. Chains that are flexible in the molten state would be capable of assuming a relatively larger number of conformations that stiffen and therefore result in a large ΔS. As shown in Table 1, polyethylene-oxide (PEO) has a more flexible chain than polyethylene (PE), and therefore T_m is significantly lower [25].

Also bulkiness of the chain would reduce mobility of the molecular chain. As an example take polystyrene, as shown in Table 1, where bulky benzene rings make the chain stiff [19]. On the other hand in some cases the opposite can be true (given as an illustration in section 2.1.2) as in a random copolymer of PDMS and PPMS, where bulky substitutions of phenyl groups in a main siloxane chain create more free volume and so increase the value of entropy. Hence T_m for the resulting polymer is 100 °C lower than for a linear PDMS [32].

Now consider an example of a molecule of an "ideal rubber" (an "Ideal rubber" like an "ideal gas", does not interact with its neighbours [17]). It has been shown experimentally that in an amorphous area, linear polymolecules do not lie straight but instead normally form coils, as shown in Figure 19. The overall coil size r or molecular end-to-end distance can be characterized statistically as the square root of the length of the molecule of its molecular length, the distance is given here in size of one polymeric segment (i.e., one methylene group for polyethylene polymer, etc) [33].

$$r = L^{-1/2}$$

r size of coil

L length of molecule
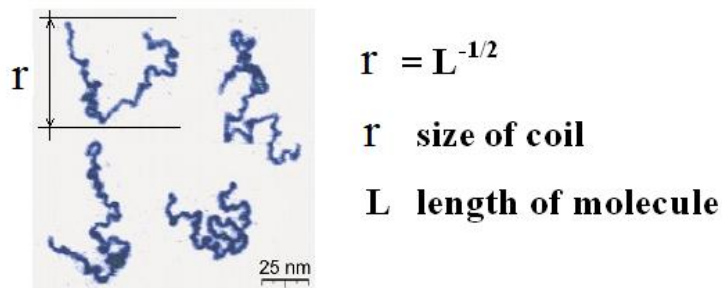
Figure 19: Appearance of Real Linear Polymer Chains

Therefore when a linear molecule contains more than 10,000 chain members, the end-to-end distance is just about 100 members. In such a case the maximum possible reversible elongation of such a molecule is 100 times. The Boltzmann equation for entropy, where entropy is a function of the possible molecular conformation:

$$S = k \ln \Omega \qquad (4)$$

where S is the entropy, k, the Boltzmann constant and Ω, the number of possible molecular conformations.

For the Helmholtz free energy $\Im$ (for "ideal rubber" volume, adhesion and temperature T holding constant), therefore:

$$\Im = - T S \qquad (5)$$

The force F required to give an extension dl is related to the change in free energy $d\Im$ by:

$$F = (d\Im / dl) \qquad (6)$$

$$F = - T (dS / dl) \qquad (7)$$

For real materials which consist of a collection of chains this "ideal rubber" elasticity equation 4 will be quite different, because when entropy S is dropping then using the Gibbs Free Energy equation 3, the crystalline melting temperature T_m would rise:

$$T_m = \Delta H / \Delta S \qquad (3)$$

For example, for a polyisoprene (PI) rubber elongation is impossible for more than 300 % because regular molecular chains tend to crystallize on elongation [34]. In reality just PDMS based rubbers are free from strain-induced crystallization at room temperature. Therefore this material is a natural choice for testing a new rheological hypothesis [35].

In contrast to crystallization, which is purely a thermodynamic process, glass transition is a kinetic process and is due to a free volume of molecular reconformations. The glass transition temperature, T_g, generally affects amorphous areas of polymer and pure crystalline areas stay virtually unaffected. Below T_g in amorphous areas, a polymolecule is fixed in place by secondary forces from neighbouring molecules in such way that only very short parts of the molecule are free enough for vibrational movements.

Such short parts of a polymolecule usually do not exceed more than a few atoms in a row [17].

When the temperature is higher and vibrational movement of the molecules is sufficiently intensive then they can move from one another and the molecules can start to move or slide past each other. If in the molecule about fifty members of the chain are free for conformational movement, the molecule will normally be free enough to move independently from the neighbouring molecules, then the temperature is above the glass transition [21].

For an ideally amorphous polymer a relaxation modulus dependence of temperature is shown in Figure 20.
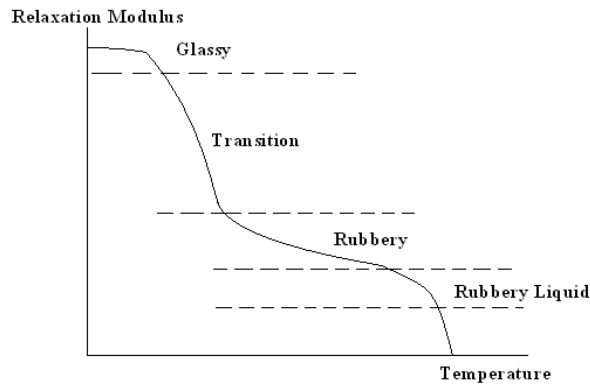
Figure 20: Schematic Plot of Relaxation Modulus vs Temperature for a Hypothetical Amorphous Polymer

When a linear amorphous polymer is frozen below T_g, relaxation is possible over a very long time. This is because for a chain reconformation of a polymolecule compressed between its neighbours, it is necessary for about fifty members of the chain to reconform and each such conformation requires a certain phonon of energy and also free volume [19]. Therefore the relaxation is exponential and the relaxation time τ_t at temperature T can be described through the Arrhenius equation where the activation energy of the reaction is substituted by the free energy barrier Б and R_{gk} is the gas constant:

$$\tau_t = f(\exp(-Б / R_{gk}T)) \qquad (8)$$
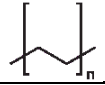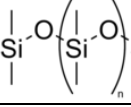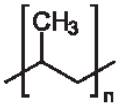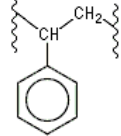
At the point where molecular thermal oscillations create enough free volume and conformations of the molecular chain are fast enough for an independent flow from its neighbours, such material starts to flow under stress. But when some crystalline structure is still in place the flow will be limited and the material will behave in a leathery and/or rubbery manner.

When the polymer is further heated, the last areas of perfect crystalline structure melt and the flow is further unlimited [33].

As molecules are squeezed in a "tunnel" of free volume, as in case of crystallisation, materials which have the most flexible molecular chain will have the lowest values of glass transition temperatures. A flexible chain would be able to reconform faster (and also use less heat on phonons of the reconformations) to slide through "open gates" between neighbouring molecules. Hence a polymolecule of PDMS which is the most flexible will have the lowest known T_g possible, as shown in Table 2 [19, 20].
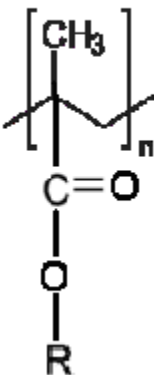
Table 2: *Comparison of the Glass Transition Temperature, T_g, of a few Common Polymers based on the Presence of Bulky Polymeric Chain Substitutions*

		T_g °C
polyethylene		-120
polydimethylsiloxane		-123
polypropylene		-10
polystyrene		100

Bulky chain substitution and the ends of a polymeric chain are also the factors which may strongly influence the glass transition temperature, because both molecular

ends and bulky substitutions inevitably occupy more space and so increase the free volume and therefore T_g normally becomes lower. The example of the influence of a molecular geometry on T_g is shown in Table 3 for polymethylacrylate [25]. But some opposite effects could be quite strong, because a bulky substitution may decrease the mobility of a polymeric chain, and also such a polymeric chain would inevitably require more empty space in order to be able to slide between its neighbours [20]. Hence polystyrene (PS), where a bulky benzene ring is attached to the polymeric chain, has a much higher T_g in comparison with polyethylene [25].

Table 3: Comparison of the Glass Transition Temperature, T_g, of Different Polymethylacrylate Polymers based on the Geometry Factors of the Polymeric Chain Substitution (i.e., lowering of T_g with Increase of the Free Polymeric Volume with Bulky Chain Substitution)

Generalized Formula	R	T_g °C
	methyl	105
	ethyl	65
	n-propyl	35
	n-butyl	21
	n-hexyl	-5
	n-octyl	-20
	n-dodecyl	-65

In the case of strong polar forces between molecules the mobility of a polymeric chain will have even more restricted movement. Such a chain cannot just slide through the "gates" between its neighbours but has to "jump" from one strong hydrogen bond to another (as was illustrated by the example of hydrogen bonding between molecules of methanol). Such hydrogen bond reconformation would require a very high amount of free volume. It is known that polymers containing hydrogen bonds have the highest glass

transition temperatures [17]. The example of aramid which exhibits strong hydrogen bond is shown in Figure 21.
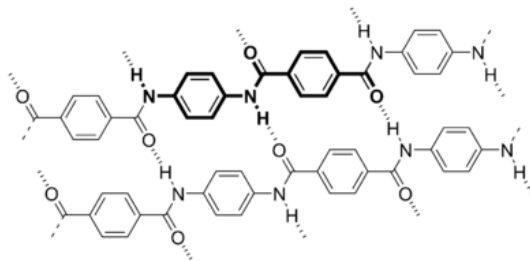
Figure 21: Example of Strong Hydrogen Bond in Aramid

Table 4: Comparison of the Glass Transition Temperature, T_g, of a some Vinyl-based polymers on the Difference in the Interchain Attractive Forces (i.e., Presence of Polar Groups)

		T_g °C
polypropylene	$\left[\begin{array}{c}CH_3\\ \end{array}\right]_n$	-10
poly(vinyl chloride)	$\left[\begin{array}{c}Cl\\ \end{array}\right]_n$	87
Polyacrylonitrile	$\left[\begin{array}{c}CN\\ \end{array}\right]_n$	103

An example of how the polarity of a group attached to a polyolefin chain changes its glass transition temperature is shown in Table 4 [25].

So far the glass transition has been discussed only in relation to amorphous polymers. For a semicrystalline polymer, such as low density polyethylene (LDPE), possible crystallinity will strongly constrain the molecular mobility of the polymer, as shown in Figure 22 where fast rubbery stress relaxation is able to start just when the amount of crystalline structure is significantly reduced above 120 °C [17].
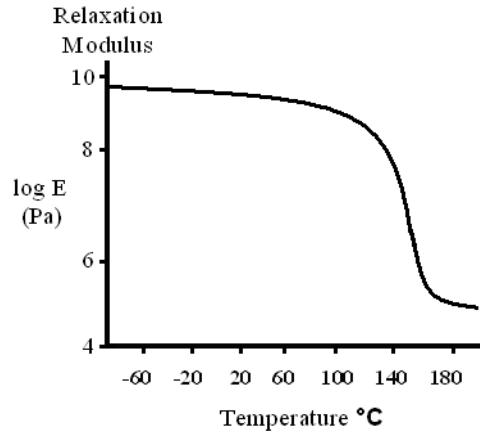
Figure 22: *Schematic Plot of the log of Relaxation Modulus*
vs Temperature for a LDPE

From section 2.1.5, it is possible to predict that at room temperature soft polymers based on polyalkenes or polyoxyalkenes tend to be self-stiffening upon the application of fast deformation due to an increase in volume of crystalline structure in the polymer caused by strain-induced crystallization [17, 35]. In the case of poly-(boron-siloxane) ("Silly Putty", as shown in Figure 23) the polysiloxane flexible chain does not tend toward strain-induced crystallization at room temperature [20]. But it is possible to predict that during fast deformation a strong hydrogen bond, caused by an atom of boron [36], will be unable to reconform fast enough due to increasing compression of the siloxane polychains. As well as in a melt of Nylon (shown below) [17], during stress the chain of polysiloxane containing atoms of boron atoms in the chain will be unable to slide freely between its molecular neighbours.
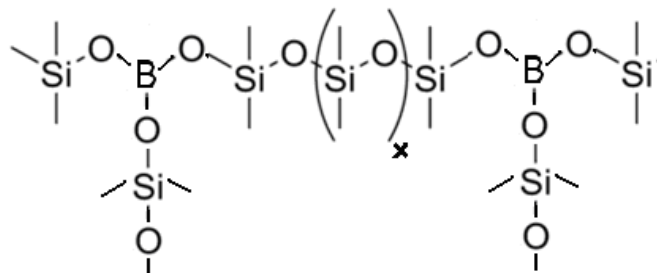
Figure 23: *Poly-(boron-siloxane) ("Silly Putty")*

2.1.6   Polymerization, Copolymerization

As mentioned earlier, continuous blocks of immiscible copolymer which exceed certain lengths start behaving as a separate polymeric material and would have separate T_g and T_m for the different phases of the polymer. Usually values of T_m and T_g of a polymer included in a block copolymer tend to increase by a couple of degrees when another block creating the polymeric material has its T_m and T_g higher (or decrease in opposite) [20]. In section 2.1.3 examples were given in the use of blocks of PEO as a soft chain extender for a soft polyurethane copolymer.

Flory and Kienle [17] studied the process of gelation during polymerization of molecular structures with a reactivity higher than two. In the original model Flory did not include such factors as intermolecular reactions which would lead to ring-structure formation and the possibility that reactive ends of some molecules would have quite different reactivity, for example primary and secondary hydroxyl groups in glycerol.

A gel does not form a molecule with an infinite weight, but rather a number of molecules with finite size existing in varying amounts, where a rate of termination would be a combination of factors, including such as solvent polarity, etc [17].

During fast gel formation, molecules of a solvent are stuck in the forming network of polymer. Complete evaporation of a solvent from such a system is difficult. An excessive amount of solvent would reduce mechanical properties of the resulting polymer [20].

2.1.7   Interpenetrating Polymer Networks (IPN)

The concept of interpenetrating polymer networks (IPN) is the subject of much research interest because of the numerous technological applications that are possible. IPN are usually a combination of two incompatible polymer networks, at least one of which is synthesized after another has already been formed. The content of IPN was first brought up by Mellar [37].

Usually, no chemical reaction occurs among the polymers in the networks. On the contrary, the polymers are coupled and interweaved into one another by interpenetrating and locking [38]. Often in the case of IPN containing PDMS (or another such immiscible and flexible polymer as a second polymeric network) some degree of chemical cross-

links between the networks is introduced. This prevents flow and produce of areas of different concentrations of polymeric components. Such cross-linked interpenetrating polymer networks are known as semi-IPN [39].

So far, polymers made by IPN technology have been increasingly used in strengthening rubbers, toughening plastics and composites [7, 40]. Most recent publications on IPN include some application in such areas as a mechanically self-supportive material for electro-active polymer [41] and electrolyte films [42] or proton exchange membranes [43].

Many studies are concerned with numerous medical applications of IPN. It has been shown that it is possible to build self-supporting porous IPNs of hydrogel [44] which would be able to deliver drugs as an oral drug device, which would not require any additional cover [45]. It is also possible to create a polymeric porous network of interpenetrating polymers of different miscibility with water (or stomach juice) where one of the components of the IPN would delay the solubility of the second. This way it would be possible to regulate the speed of drug absorption [46].

Another medical area where IPN may be a promising solution is in ophthalmology. Today, many people use soft contact lenses for vision correction. However, it has been reported that about half of soft contact lens wearers suffer from clinical symptoms such as eye infections and dry eyes, demonstrating a requirement soft and light conductive material with higher biocompatibility. The possible solution may be available by using IPN of super-hydrophilic silicone hydrogels with interpenetrating biocompatible polymers. Such lenses would have at least the same optical and mechanical properties and also offer higher water absorption, oxygen permeability and biocompatibility [47].

IPN also find applications as nano-composite sensors for temperature and pH- [48]. A recent publication by Wang et al [49] is concerned with pioneering research of three component IPN based on a nano- SiO_2/polymethylmethacrylate (PMM)/cyanate(CE) composite.

2.2   Constrain Release and Viscoelastic Properties of Polymers

2.2.1   Comparison of Viscoelastic Properties of Metals and Polymers

When discussing polymeric stress relaxation it is possible, and worthwhile, to start by comparing behaviour of a metal and a polymer under a stress. Uniaxial stress and elongation is shown in Figure 24, where the tensile stress σ, force F and cross section A_{cs}:

$$\sigma = F / A_{cs} \quad (9)$$

and ε is the strain:

$$\varepsilon = \Delta l / l_0 \quad (10)$$

Here Δl is the elongation and l_0 is the original length.

Hooke's law of the elastic behaviour says that strain is proportional to the applied stress:

$$\text{Stress} / \text{Strain} = \text{constant} \quad (11)$$
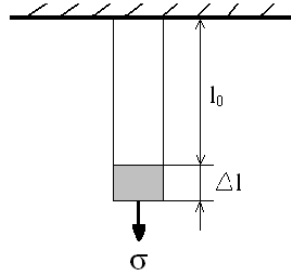
Figure 24: Uniaxial Elongation

where the constant E is a characteristic of the material and is called Young's modulus:

$$\sigma = E \, \varepsilon \quad (12)$$

It is possible to express equation 12 through a quantity called the tensile compliance D, where:

$$D = 1 / E \qquad (13)$$

$$D = \varepsilon / \sigma \qquad (14)$$

When a material is stretched it does not just deform in the direction of the applied load, but also in directions perpendicular to the applied load, as illustrated in Figure 25.
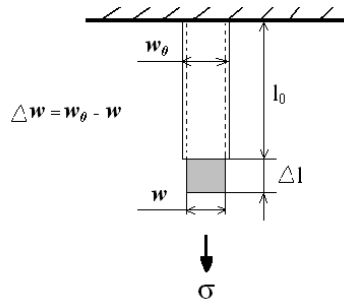
Figure 25: Contraction in the Perpendicular Direction upon Stretching

The amount of this contraction is proportional to the extension in the direction of the applied load, so that if Δw is the change in the width of the material and w_0 is original width, then:

$$\Delta w / w_0 = - \upsilon \, \Delta l / l_0 \qquad (15)$$

where υ is called Poisson's ratio.

Considering homogenous and isotropic materials, the Young's modulus E and Poisson's ratio υ are the only constant values needed in order to completely specify the elastic properties. The stress-strain curve for a hypothetical ideal material which breaks under a stress without yielding or plastic deformation is shown in Figure 26.
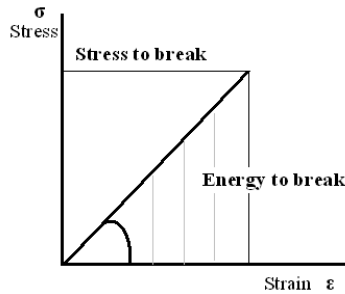
Figure 26: *Stress-strain Curve for a Hypothetical Material*

Real materials do not behave like the material shown in Figure 26. Some ceramics or perfect crystalline structures come close and display linear behaviour until failure. In fact, most materials are naturally imperfect in their structure and therefore even highly crystalline materials such as metals have some deviations from linearity and display some yielding and plastic deformation [1, 2]. Polymolecular materials normally do not give straight linear response upon the application of a mechanical stress, except in the case where the applied stress is very limited. Also any kind of mechanical oscillations may change the momentum dynamic response of a polymeric material. Therefore, processing of a polymeric material or prediction of its full mechanical properties could be an extremely difficult task. On the other hand there is a constant demand from industry for an increase of the speed of technological processing. One known way to achieve this is to increase the temperatures of processing, but there comes a limitation to the maximum possible working temperatures above which polymeric materials start to disintegrate upon thermal degradation. Hence a model for predicting possible dynamic behaviour of a polymeric material is needed - something that will be a very useful guide for engineering and technological processing of polymers. In particular, non-linear polymolecular mechanical response is a problem that extends beyond the scale of just moulding polymers, for example, where the demand to increase speed of moulding operations of "shark-skin" was an on-going problem [50]. Currently such areas as polymeric matrix composites exposed to an oscillating stress, hydraulics [51] and even the food processing industry are looking for suitable technological solutions to problems caused by non-linearity of dynamic behaviour of oligomeric and polymolecular materials [52].

The task of creating a credible mathematical model describing different aspects of the dynamic response of a polymeric material is currently incomplete. This is mainly because of a variety of possible dynamic processes in polymers and also because some key aspects of polymeric behaviour are still quite unclear. But at the same time the existing semiempirical models have shown they are useful approximations in the analysis and are able quite successfully to explain a lot of the experimental data [53].

The main names standing behind the contemporary theory of a dynamic polymeric behaviour are Ferry, Rouse and Beuche [54]. Their model is able quite well to describe the possible behaviour of an oligomeric material, but does not encounter an effect which is due to entanglement of polymolecules.

The suggested model of polymeric relaxation is based on the suggestion that a molecular chain works as a set of beads linked by springs. The springs vibrate with frequencies that depend upon the stiffness or force constant of the spring, but these vibrations are considered to be modified by frictional forces between the chain and the surrounding medium. There are various types of vibrations of a molecular chain which are normal modes of IR oscillation of a molecular chain and each is characterized by a certain frequency at given temperature.

These can be calculated using straightforward classical mechanics. There is a characteristic relaxation time associated with each of these damped normal modes and each of these contributes to the viscoelastic properties. In terms of this model it was found that the flow behaviour of polymer melts is dominated by the vibrational mode with the longest relaxation time, corresponding to a coordinated movement of the molecule as a whole [26].

This theory predicts that the viscosity η should be directly proportional to the molecular weight, which is only true to the entanglement limit, as shown in Figure 27 and equation 16:

$$\eta = K \, (DP)_w{}^{1.0} \qquad (16)$$

here K is constant and $(DP)_w$ is the degree of polymerization, beyond which the viscosity becomes proportional to the molecular weight to the power 3.4, as shown in equation 17:

$$\eta = K \, (DP)_w{}^{3.4} \qquad (17)$$

This is because in this model each chain is considered to be moving independently and it essentially allows chains to "pass through one another", so entanglements are neglected.
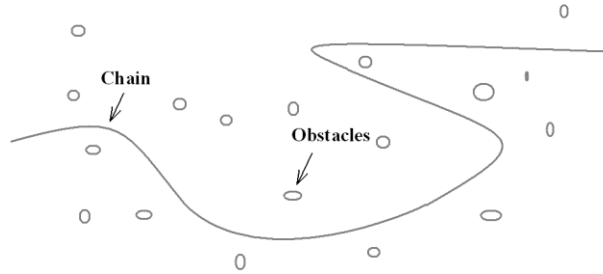
Figure 27: *The de Gennes Model of Reptation; the Chain Moves among the Fixed Obstacles with a Snake-like Motions, but cannot Cross any of them*

De Gennes [54] later suggested a different approach. He proposed a "reptation" relaxation model where he included the effect of polymolecular entanglement. In this model long flexible polymeric chains are deeply overlapping with each other to mutually constrain their large-scale motions. Therefore, a polymolecular chain is "trapped" by other chains that are considered to act as a set of obstacles, as shown in Figure 27. The chain is not allowed to cross these obstacles, but can slither through them with motion similar to a snake moving through the grass, hence the name reptation. Here de Gennes found that the diffusion coefficient D_k of a chain in the melt should depend inversely on the square of the molecular weight M:

$$D_k \sim f \, (1 \, / \, M^2) \qquad (18)$$

which it does. Also de Gennes obtained a relationship between melt viscosity η and molecular weight M:

$$\eta \sim f \, (\, M^3) \qquad (19)$$

which is not quite right, because $\eta \sim f(\mathrm{M}^{3.4})$ from equation 17. At this time it is still not exactly clear whether this is just a minor problem that can be fixed by "tinkering" with the model, or if there is a more fundamental difficulty [17, 54].

Therefore for describing dynamic polymeric relaxation of those polymers whose molecules on average do not reach certain values of a molecular weight (which is necessary for effective polymolecular entanglements) it is possible to use the relaxation model known as a Rouse-like constrain release (CR) relaxation. For a polymeric relaxation which involves the added effect of polymolecular entanglements the reptation model is used [17].

Sawada et al [55] have worked on an experimental proof of some of the theoretical model of polymeric relaxation, suggested originally by de Gennes and later extended by Edwards, Graessley and other researchers [56]. The experiment was run on a series of binary monodispersed blends of linear polyisoprene (PI). Those binary blends contained high molecular weight probe component chains of PI with $M_n \sim 626,000$. Those high molecular weight probe component chains were diluted and entangled with series of blends of lower molecular weight PI (M_n varied from 14,000 to $\sim 329,000$) matrix chains. The PI/PI blends were exposed to an oscillatory stress of different frequencies. The probe exhibited the Rouse-like constrain release relaxation in the matrix chains which were much shorter than the probe. CR-dominant relaxation was gradually overwhelmed by competing relaxation mechanisms, such as reptation, when the matrix molecules moderately increased in their molecular masses.

Sawada also run a series quite similar to the PI/PI blends experiments for binary blends of linear polystyrene (PS). The blends of PI/PI and PS/PS showed qualitatively similar relaxation features, but quantitatively different. The CR-dominance was more easily achieved in PI/PI blends than in PS/PS blends. It was suggested that the entanglement dynamics are not uniquely determined by the numbers of entanglement segments per chain and the relaxation time within this segments, but is affected by additional molecular factors such as the local CR gate number.

Takahashi et al [35] ran quite similar experiments to those which were performed earlier by Sawada et al [55] for blends of PI/PI and PS/PS. Takahashi used scarcely cross-linked gels of monodispersed polydimethylsiloxane (PDMS). PDMS is a particularly

useful material for such experiments, because it the only known polymeric material which is free from a strain-induced crystallization at room temperature [17].

The results of those series of experiments was that Takahashi and Sawada came to a similar suggestion, that constrain release (CR) gates and its number are affected by the heterogeneity of polymeric probes, although this hypothesis has not been entirely proven yet [55].

2.2.2 Relaxation in Polymers

For this discussion it may be useful to restate some fundamental principles of polymeric behaviour given above in previous sections. First perhaps it is necessary to rephrase the meaning of temperature, which is a measure of the mean kinetic energy of a molecule. So if heat is added to a material the molecules start to move faster on average. Second, in polymer molecules there are energy barriers inhibiting bond rotation, so that at low temperatures the atoms largely vibrate around their mean positions, but at higher temperatures they might have sufficient energy to rotate over these barriers and adopt new conformations. Therefore if there is sufficient thermal energy then it is possible to predict that each bond "clicking" between each of these conformations, but on average more bonds will be found in the lowest energy conformation (trans) than in higher energy arrangements (gauche) at any instant of time. If the energy of each of these states is known, then it is possible to use methods of statistical mechanics to calculate the relative population of the conformational states. This distribution will change with temperature, where more bonds will be found in the higher energy states at higher temperatures rather than at lower temperatures.

Now consider a hypothetical single chain, isolated in space, in equilibrium at a given temperature. There is a certain distribution of trans and gauche states and an average distance between the ends of a chain as it flops around over time. Now imagine that it were possible to grasp the ends of the molecular chain and apply a stretching force. The chain would no longer be at equilibrium, in that a more stretched-out overall chain conformation would be now favoured. This, in turn would favour a new distribution of trans and gauche local bond conformations.

However, for a molecular chain sitting in a viscous medium that approximates the effect of the other chains, then because of frictional forces it would not be able to follow the applied load immediately, as it would take time for the bonds to rearrange themselves to the new equilibrium population of states. The chain relaxes to this new equilibrium state. If rotations around each backbone bond in a polymer chain were totally independent of one another, and if in addition it was necessary to consider only the transition between two local states such as trans and gauche, then the relaxation process could be described in terms of a single relaxation time, which characterizes the time scale necessary for the rearrangements to take place [57].

Of course, in a real polymeric material the situation is far more complex. It is only an approximation to consider two allowed bond conformational states. Bond rotations are not independent of one another but are affected by both short and long range static interactions. The polymeric chains are not isolated and those are acted on by simple viscous forces, while the effect of entanglements needs to be considered, and so on.

Therefore there are various types of complex coupled motions or relaxation processes and these are usually referred to as "modes". Each of these modes will have a different characteristic relaxation time or range of times. Even this is a simplification and it has been argued by de Gennes [55, 58] that the actual concept of modes might be invalid. The various relaxation processes that occur in entangled chains may be so complex and coupled that only smooth distribution or spectrum of relaxation times may actually exist.

Relaxation of a polymer is a strong function of temperature. In low molecular weight liquids relaxations are very fast and normally reach about 10^{-10} sec. In a polymeric melt (the temperature is much higher than T_g) the relaxation is much slower. In neutron scattering experiments to detect the relaxation time for polystyrene samples (M_n - 144,000) the result was about five minutes to approach completion. At temperatures close to the T_g or below the T_g, relaxation times are obviously much longer [17].

In the glassy state, conformational changes involving coupled bond rotations are severely inhibited, although they can occur over very long time periods, and local conformational transitions and side chain motions can occur. Nevertheless, for small strains and short times the response can be regarded as essentially elastic.

In the region of the glass transition there is now sufficient thermal energy that various cooperative motions involving longer chain sequences occur. Frictional forces are such that motions are sluggish, however, and retarded or inelastic responses are observed. In dynamic mechanical experiments there is severe mismatch between the imposed frequency of oscillation and the time scale of the relaxation process. Frictional losses then rise to a maximum.

As temperature is raised the time scale of conformational relaxation processes becomes shorter. In other words the chains can adjust their shape to an imposed deformation in the material as a whole more rapidly. The time scale for disentanglement of the chains is longer than the time scale for these conformational adjustments, however, so in this region the entanglements act something like cross-links. The chain can stretch out between the entanglement points and a rubbery plateau is observed in the appropriate experiments. Finally, as the temperature is increased still further, the time necessary for disentanglement decreases, chains diffusion becomes faster than the measurement time of the experiment and the material enters to a terminal flow [59, 60].

Similar results are obtained if the stress relaxation time is made variable and the temperature is held constant. A schematic representation of the modulus versus time is shown in the right-hand part of Figure 28.

At short time periods (how short depends on the nature of the polymer, for example rubber or glassy polymer, at the temperature of the experiment) the measured stress relaxation modulus is high, characteristic of the glassy state and the polymer is characterized by the modulus, usually larger than 10^9 Pa. As time goes on, the stress required to maintain the given strain starts to decrease sharply until it reaches the rubbery plateau.

For a glassy polymeric sample which is below its T_g at the temperature of the experiment, the time required for the stress to relax to the point that is considered to be rubbery could be exceptionally long and could reach an order of hundreds of years [17, 56].
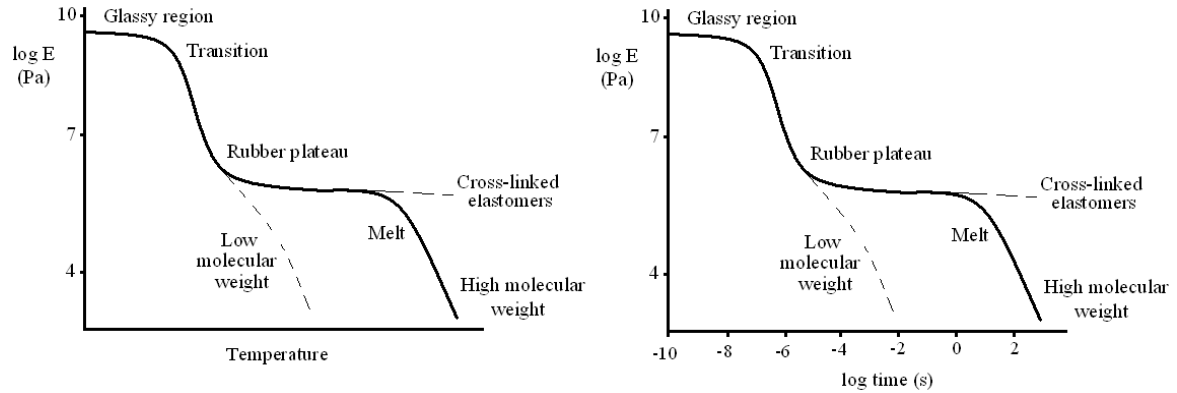
Figure 28: Schematic Diagram of log of Relaxation Modulus vs Temperature (left) and Relaxation Modulus vs log of Time (right) for a Hypothetical Amorphous Polymer

Perhaps one of the most useful methods for determining viscoelastic behaviour is the measurement of dynamic mechanical properties. In this type of experiment an oscillatory stress is applied to the sample. The frequency of the oscillation can be varied over an enormous range. If the sample happens to be perfectly elastic and if the applied stress varies sinusoidally, then the strain γ would be completely in-phase with the applied stress and would vary as:

$$\gamma = \gamma_0 \sin(\omega t) \qquad (20)$$

where ω is the angular frequency of the applied stress, t is the time and γ_0 is the original strain. If we are to consider experiments involving shear stresses and strains and small amplitudes of vibration then it possible to write Hooke's law as:

$$\tau(t) = G\,\gamma_0 \sin(\omega t) \qquad (21)$$

where the symbol $\tau(t)$ indicates that the applied shear stress varies with time.

For a Newtonian viscous liquid with viscosity η, the resulting strain γ will be exactly 90° out-of-phase with the stress, because:

$$\tau(t) = \eta\,\gamma(\tau) = \eta\,{}^{d}\!/dt\,[\gamma_0 \sin(\omega t)] \qquad (22)$$

38

It follows that for a viscoelastic material the response expected to be characterized by a phase angle somewhere between 0° and 90° should be related to the dissipation of energy (viscous type response) relative to its storage (elastic type response). If a sinusoidal stress is applied to a viscoelastic material such as a polymer it should be expected for the resulting measured strain to lag behind by some degree, which is possible to define in terms of phase angle δ, so it is possible to express the stress in terms of an in-phase component and an out-of-phase component with respect to the strain. The relationship between stress and strain can now be defined in terms of these in-phase and out-of-phase components by:

$$\tau\,(t) = \gamma_0\,[G'\,(\omega)\,\sin\,(\omega\,t) + G''\,(\omega)\,\cos\,(\omega\,t)] \qquad (23)$$

where:

$$G'\,(\omega) = \tau_0\,/\,\gamma_0\,\cos\,\delta \qquad (24)$$

and:

$$G''\,(\omega) = \tau_0\,/\,\gamma_0\,\sin\,\delta \qquad (25)$$

The in-phase component, $G'\,(\omega)$ is called the storage modulus, while the out-of-phase component, $G''\,(\omega)$ is called the loss modulus:

$$\tan\,\delta = G''\,(\omega)\,/\,G'\,(\omega) \qquad (26)$$

A schematic representation of the dependence of $G''\,(\omega)$, $G'\,(\omega)$ and $\tan\,\delta$ upon the frequency of oscillation ω is shown in Figure 29 for an amorphous polymer. This is an idealized representation and real data can often appear more complex. Nevertheless, the key features correspond to those observed for all amorphous polymers. At a constant temperature, firstly, at low frequencies the storage modulus $G'\,(\omega)$ is characteristic of that found in rubbers. As the frequency increases this modulus increases several orders of magnitude and levels out at a value of the modulus characteristic of the glassy state. At

room temperature both a glassy polymer and a rubber would give this type of curve, and these curves would be shifted along the frequency axis to one another.
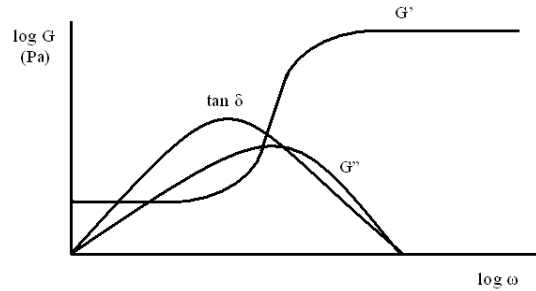
Figure 29: Schematic Diagram of log of the Frequency Dependence of log of the Modules G', G'' and their Ratio $\tan \delta$

It can also be seen that the loss modulus $G''(\omega)$ starts at low values and also increases with frequency, while $\tan \delta$ goes through a maximum and displays a peak in the range where $G'(\omega)$ is changing its value from one characteristic of rubber to one characteristic of the glassy state [54, 57].

Clearly $\tan \delta$ is showing a maximum at a position that is characteristic of a T_g. If a sample was subjected to an oscillatory stress at a specific frequency and the temperatures were allowed to vary, then a typical result would be shown as in Figure 30 [59].
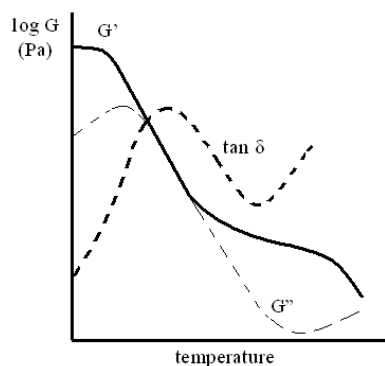
Figure 30: Schematic Diagram of the Temperature Dependence of log of the Modules G', G'' and $\tan \delta$ for an Amorphous Polymer

So far relaxation in a purely amorphous polymer has been discussed and one would expect similar relaxation processes to occur in the amorphous domains of semi-crystalline polymers, but here motion is suppressed and constrained by crystallites. The viscoelastic behaviour of semicrystalline polymers is far more complex, because of the superposition of behaviour of the crystalline and amorphous domains. In some polymers, where the degree of crystallinity is not too high, transitions characteristic of amorphous state can be observed superimposed upon those due to the crystalline domains. This superposition is not necessarily linear (as mentioned in section 2.1.5), however, and coupling of responses can occur, particularly as the degree of crystallinity of a sample is increased and the amorphous regions become constrained by the crystalline domains. Because of these factors the behaviour of semicrystalline polymers is much less uniform than those that are purely amorphous, displaying individual idiosyncrasies that often have to be described separately. There is one generalization that it is possible to make, however, and that concerns the large change in the modulus that is observed at the crystalline melting point T_m.
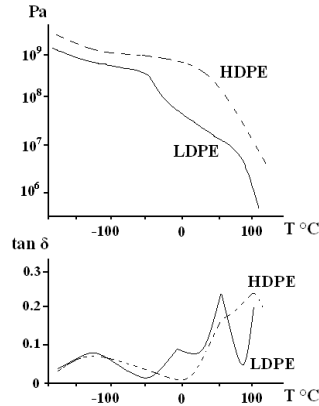
Figure 31: *Temperature Dependence Schematic Diagram of log of the Storage Modulus (top) and tan δ (bottom) of High Density Polyethylene (HDPE) and Low Density Polyethylene (LDPE)*

Figure 31 displays schematically the type of storage modulus and tan δ versus temperature behaviour for high and low density polyethylene polymers, which are highly crystalline polymers [17]. There are small regions of amorphous material that are

constrained by hard crystalline domains, so at low temperatures both samples display a high modulus. As discussed in the previous sections, melting of smaller and less perfect crystals can occur at temperatures below the melting of the bulk of the crystalline domains, so the modulus decreases somewhat as the temperature is raised, but the largest change in modulus occurs at what is define as T_m. At this temperature the polymer becomes entirely amorphous and subsequently displays a rubbery plateau.

More advanced contemporary mathematical models have been developed, for example that proposed by Gotlib et al [61, 62] for IPN of two scarcely cross-linked networks. A possible spectrum of relaxation process in IPN is inevitably much more complicated and diverse than for a network of monodispersed linear polymeric chains which are taking a Gaussian conformation (where the distance from end-to-end of a polymolecule is equal on average to a square-mean of the full molecular length, as discussed in section 2.1.5). Also in his model Gotlib suggested that when one polymeric network is formed on the top of the existing cross-linked polymeric network, polymolecules of the second network would be effectively prevented from taking Gaussian confirmations and would stay further stretched. This and some other factors, such as the number, bulkiness and distance between junctions in both polymeric networks, may affect the dynamics of entanglements during relaxation. In his model for IPN, consisting of two homogenous networks with junctions of both networks of functionality equal to six, Gotlib suggested that the relaxation for a couple of different junctions would give a spectrum of relaxation time. But the spectrum of relaxation times would still exhibit some quite narrow possible time limits.

2.2.3   Some Other Contemporary Theoretical and Experimental Models of Polymeric Viscoelasticity of Interest of this Project

During a flow of melts of polymolecular materials, shear thinning is generally observed. Shear thickening phenomena are rarer and often just observed in cases of flow of melts of polymers which tend to stress-induced crystallization, such as polyethylene. In some cases polymeric melts which exhibit strong hydrogen bond formation, for example PDMS based Silly Putty, tend to form an associated gel-network during flow. Such telechelic associated polymers are able to increase their viscosity during a

deformational flow. But if the speed of flow of a polymeric melt exceeds certain values, the viscosity of polymeric melt can only decrease further - and during very fast flow all known polymeric materials tend only to shear thinning [63].

Indei [64] studied shear thickening phenomena on examples of telechelic associating polymers on the basis of the transient network theory. He investigated how a nonlinearity of the tension along the middle chains affects the stationary shear viscosity of the network under different conditions (i.e., when a dissociation rate of the end chains from the network junctions was coupled to the middle-chain tension) and also when a generation rate of the chain-in-loop conformation was enhanced by middle-chain tension.

On the basis of the transient network theory Indei introduced nonlinear models for the elongational properties of the middle chain with the (unitless) tension along the middle chain ч $(\check{r})$:

$$\text{ч} (\check{r}) = 3 \check{r} [1 + (2A / 3) \check{r}^2 / (1 - \check{r}^2)] \qquad (27)$$

where $\check{r} = r / L$ and represent the reduced end-to-end length of the chain (r is the length and the L is the contour length, as it was mentioned previously), and A represents the nonlinearity strength of the tension. He also introduced the breakage rate of the bridge chain $\beta (r)$ (i.e., the elastically active chain that sustains the stress of the network), which is given as follow:

$$\beta (r) = \beta_0 [1 + g (\text{ч} (\check{r}))^2] \qquad (28)$$

where g represents the coupling intensity between the breakage rate and the middle-chain tension, and β_0 represents the dissociation rate of the end chains resulting from their own thermal agitation. Equation 28 shows that the higher the tension in the active chain, the higher the probability that the end chains will dissociate from the network.

Telechelic polymers are able to take a closed-loop conformation, when their two ends connect to form flower-like micelles, as shown in Figure 32. For simplicity, p_L is the generation rate of the loop chains (where p is the transition rate from the dangling chain to the active chain and p_{L0} is a constant which represents the original generation

rate of the loop chains) were assumed in this model by Indei to be constant. Also he assumed that the strong nonlinearity of the tension in the active chain, caused by a large value of A, leads to shear thickening, if the dissociation rate is weakly coupled to the tension. However, if A exceeds a certain value, the active chains break before sufficient elongation occurs to cause thickening. This is because the nonlinear term of the tension is strongly coupled to the dissociation rate even for a small g value. Therefore, only thinning occurs in this case.

$$\beta(r) = \beta_0 (1 + g r^2)$$

$$p_L = p_{L0} \, a^3 \, \Phi_0(0)$$

active chain   (p = constant)   dangling chain   (β_L = constant)   loop chain
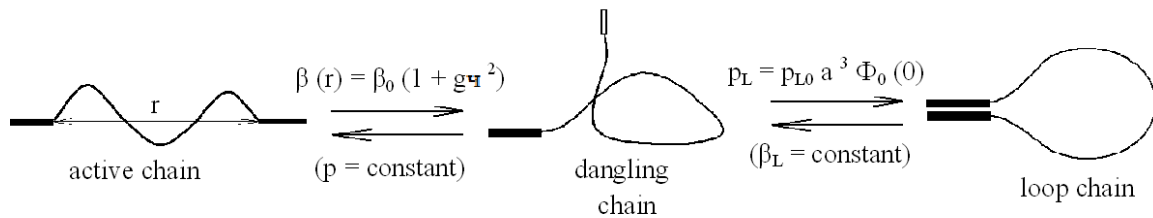
Figure 32: Three States of the Chain. Ends Chains Associated with Junctions are Shown in Black. The Transition Rates between the Different Chains States are Shown beside each Arrow

A chain having a large value of A tends to shrink due to the strong tension along the middle chain. Since the end-to-end distance is narrow, there is a high probability that such a chain might take a loop conformation. A high generation rate of the loop chain diminishes the population of the active chains in the networks and therefore affects the viscoelastic properties of system (i.e., a high generation rate of the loop chain caused by a high value of A) and influences the necessary conditions for thickening and the viscosity profile of the telechelic polymer networks on the basis of the transient network theory.

Indei in his theoretical model considered polymeric networks comprised of n (where n is the number of chains involved) primary chains carrying short "sticky" chains at both their ends, where the primary chains are monodispersed and each primary chain is comprised of N statistical segments. The molecular weight of a primary chain is assumed to be lower than the entanglement molecular weight, so that the reptation dynamics of the chains are not dominant. Further, he assumed that the specific time of deformation applied to the system is much longer that the single-chain Rouse relaxation time.

The primary chains in the network were categorized into three types according to the manner in which their end chains are connected to the network junctions: active chains, dangling chains and loop chains, as shown in Figure 32. The active chains bridge two distinct junctions in the network. They are components of the network backbone and hence sustain the stress stored in the network. Indei assumed the affine deformation for active chains. If one end of the active chain is disconnected from the junction, it becomes a dangling chain with only one end connected to the junction. The probability of the occurrence of this event per unit time Φ_0 (i.e., dissociation rate) is give by equation 28. The dangling chains are practically always in the equilibrium state despite the deformation applied to the system. The probability distribution function for a dangling chain with end-to-end vector $r = (x, y, z)$ is expressed as:

$$\Phi_0 = C \exp [-1/ k_B T \int dr\, f(r)] = C (1- ř^2)^{NA} \exp [- (3 / 2 - A)\, N\, ř^2] \quad (29)$$

where $r = (x^2 + y^2 + z^2)^{½}$ represents the end-to-end chain length; and $f(r) = (k_B T / a)\, ч(ř)$ represents the tension along the middle chain ($a = l / N$ is the length of the statistical segment and $ч(ř)$ is given by equation 27); k_B the Boltzmann constant; T the temperature. The normalization constant C is given by:

$$C = (4\pi \int dr\, r^2 (1- ř^2)^{NA} \exp [- (3 / 2 - A)\, N\, ř^2])^{-1} \quad (30)$$

The loop is formed by incorporating both ends of the chains into the same junction, and it is created from a dangling chain if an unbound end of the dangling chain is connected to the other end. It was assumed that the probability of the occurrence of this event per unit time (loop generation rate p_L) is given by:

$$p_L = p_{L0}\, a^3\, \Phi_0(0) \quad (31)$$

where p_{L0} is a constant, and $a^3 \Phi_0(0)$ represents the probability of an unbound end of the dangling chain being inside the volume a^3 around the other end. Figure 33 shows the loop generation rate expressed by equation 31 as a function of the nonlinearity amplitude

A of the middle-chain tension with N varying from curve to curve. The loop generation rate p_L increases with A, because the dangling chain with a high A tends to have a short end-to-end length and hence a large value of $\Phi_0 (0)$ due to the high tension along the backbone. It was also observed that that the magnitude of p_L decreases as N increases, because the longer the chain, the lower the probability that the chain will form a loop.
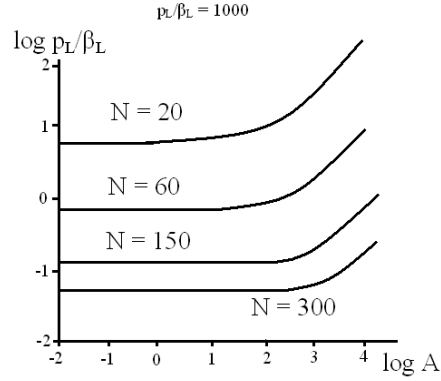
Figure 33: Log of the Loop Generation Rate Plotted vs log of the Nonlinearity Amplitude of the Middle-chain Tension for Several Molecular Weights

For simplicity, isolated chains were ignored because they contribute only indirectly to the viscoelastic properties of the system. Then, the total number density n of the chain can be expressed as:

$$n = v^A(t) + v^D(t) + v^L(t) \qquad (32)$$

where $v^A(t)$, $v^D(t)$ and $v^L(t)$ represent the number density of the active chains, dangling chains and loop chains at time t, respectively.

Now let $F(r, t)$ dr be the number density of active chains having an end-to-end vector $r \sim r + dr$ at time. The time development equation for $F(r ,t)$ dr, $v^D(t)$ and $v^L(t)$ are given follows:

$$dF(r,t) / dt + \Delta (k(t) r F (r,t)) = - \beta F(r,t) + p \, v^D(t) \, \Phi_0 (r) \qquad (33)$$

46

$$dv^{D}(t) / dt = - p\, v^{D}(t) + \int dr\, \beta\, F\,(r,t) - p_{L}\, v^{D}(t) + \beta_{L}\, v^{L}(t) \qquad (34)$$

$$dv^{L}(t) / dt = - \beta_{L}\, v^{L}(t) + p_{L}\, v^{D}(t) \qquad (35)$$

where $k(t)$ is the velocity gradient tensor applied to the system, $k_{xy}(t) = \gamma$ (where γ is the strain) and the other components are 0 for a steady flow along the x-axis (the direction of the velocity in this model is along y-axis); p is the transition rate from the dangling chain to the active chain and β_{L} is the transition rate from the loop chain to the dangling chain, as shown in Figure 32.

So, if for a very limited time p and β_{L} are assumed constant, a momentum shear stress τ_{xy} at time $t + dt$ is expressed:

$$\tau_{xy} = \int dr\, xy\, /\, r\, f(r)\, F(r,\, t) = v^{A}\, k_{B}\, T/a\, f(\gamma)\, [(xy\, /\, r)\, (ч\, (\check{r}))\,] \qquad (36)$$

Then the shear viscosity is:

$$\eta = \tau_{xy} / \gamma \qquad (37)$$
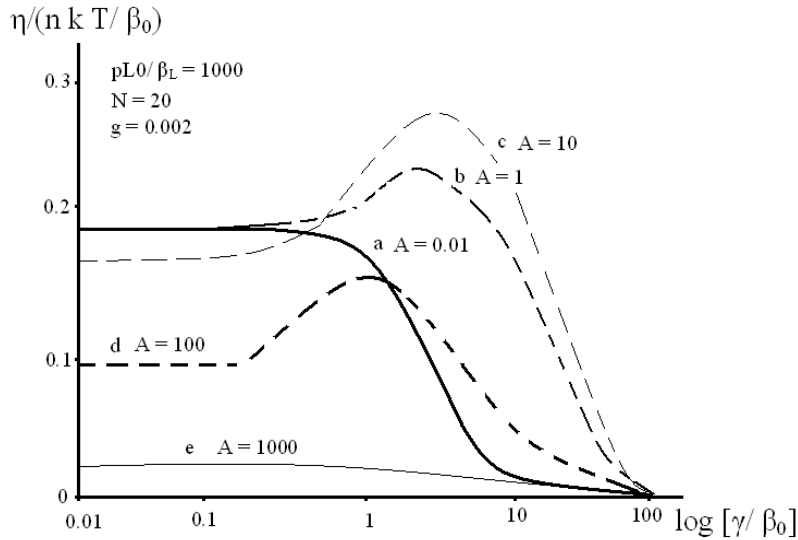
Figure 34: The Nonlinear Stationary Viscosity Plotted vs log of the Shear Rate, the Nonlinear Amplitude of the Middle-chain Tension Varies from Curve to Curve

Figure 34 shows the (unitless) nonlinear stationary viscosity as a function of the (unitless) shear rate with the nonlinearity strength A varying from curve to curve for $p_{L0} = 1000 \, \beta_L$.

When A is close to zero as shown by line *a*, only thinning occurs; however, peaks appear in the viscosity curves for a higher value of A (lines *b*, *c*, *d* and very limited peak for line *e*). Thus, the transition from thinning to thickening occurs with an increase in A, indicating that the cause of thickening is the nonlinear strong tension in the middle chain. But also the number of active chains ν^A decreases linearly with an increase in A, because more dangling chains tend to become loop chains rather than active chains. Therefore, the line *e* shows almost shear thinning alone.

In other words, shear thickening can occur if the nonlinearity strength A overcomes the coupling intensity, when dangling chains prefer to become loop chains rather than active chains and hence the population of active chains is small for a large value of A. Hence, the thickening conditions are mainly determined by the coupling intensity between the tension and the dissociation rate of the end chains for a given nonlinearity strength.

Indei et al [64] ran an experiment where they measured the dynamic viscosity of an aqueous solution of telechelic polyethylene oxide (PEO $M_n \sim 10,000$) and an aqueous solution containing a comparable number of repeated units of a telechelic oligomer N-isopropylacrylamide. In this experiment PEO exhibited strong shear thickening, when N-isopropylacrylamide (which has very polar amide groups in the chain) showed only shear thinning.

Sunarso et al [65] investigated a complex rheology of associative polymers on an example of an aqueous solution of urethane containing hydrophobic ethoxy groups in the molecular chain. In their numerical simulation model Sunarso et al [65] tried to simplify the existing mathematical model of transient networks where molecules are represented by a network of beads and spring chains, because a simulation of the original model is computationaly very intensive even for a quite simple calculation of rheological properties. Therefore, they replaced, for example, the different populations of active chains given in the original model (i.e., active chains, dangling chains and loop chains)

by a simplified model containing just two sets of populations, active chains and dangling chains, where the sizes of both sets of populations and the constant rate of association and dissociation is a function of velocity of the flow.

The suggested model quite successfully predicted a steady shear viscosity characterized by a Newtonian plateau at low shear rates, followed by shear thickening at moderate shear rates, and shear thinning at high shear rates. The model showed quite remarkable agreement with experimental data, but also the model had some qualitative disagreement with the data obtained in the experiment in the area of the curves where shear thickening of moderate rates is changing to a shear thinning of the high rates.

Because the goal of this project is in a developing an IPN or a block copolymer with a specific viscoelasticity, another area of a great interest for this work are models which predict a possible viscoelasticity of a heterogeneous polymeric system.

The models given above in this section describe viscoelastic behaviour of homogenous entanglements-free polymeric materials. In the case of a sample of a polymeric material which consists of longer than average molecules, which are sufficiently long to form entanglements and tend to a reptation relaxation, viscoelastic behaviour of such a polymeric sample may be significantly different. This is particularly true if a sample of polymeric material is not homogenous. For example, the introduction of a small quantity of solvent into a physically entangled polymeric matrix will lead to a swelling of the polymer chains and hence an increase in the number of chain-chain interactions. Therefore, viscoelastic behaviour will differ with a greater probability of polymer-polymer contacts and reflects the growth rather than depletion of interactions. When there is a further increase in the amount of solvent this leads to a decrease in the observed viscosity with there being a reduction in the number of chain-chain contacts [66].

In the case when a polymeric matrix interacts with a material containing longer molecules than a solvent a possible viscoelastic relaxation will differ more strongly than in the case of interaction with relatively short molecules of a solvent. (As it was shown earlier, the majority of polymeric materials are immiscible with other blends of polymers.)

In the case of a polymeric blend of two immiscible Newtonian polymeric liquids, the resulting polymeric blend will exhibit a non-Newtonian viscoelasticity.

In a blend of two polymeric liquids, molecules of one of the polymers will be in the form of droplets of a different size in a matrix of another polymer. In the case of a deformation (a flow) of such material, molecules of the polymeric matrix will be unable to obtain a new position freely because of obstacles caused by the droplets. Chains of polymolecules of the polymeric matrix will be unable to pass through the droplets dispersed in the polymeric matrix, as shown in Figure 35. On the other hand during a deformational flow of such material, the droplets will be constantly exposed to a shear stress caused by frictional forces at the interface. And it was shown experimentally that a distribution of populations of sizes of the droplets will change during a deformation towards an increase in the population of smaller droplets and a significant decrease in the population of larger droplets.
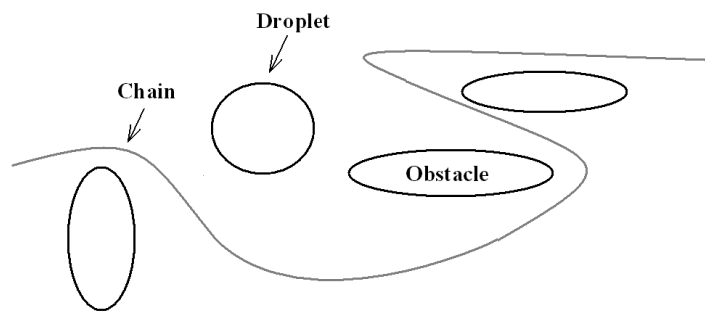
Figure 35: *Schematic Representation of Blend of Two Immiscible Polymeric Liquids*

During a deformation the average size of droplets will became smaller, so the average size of obstacles will be smaller. The chains of the polymeric matrix will be able to obtain a new position faster and hence, the effective viscosity of the polymeric blend will be lower during a deformation. When the blend is left for a sufficiently long relaxation time the droplet will gradually obtain their original sizes [67].

Okamoto et al [68] studied this model using experimental data of a blend of polyisobutylene and polydimethylsiloxane while Takahashi et al [69] used copolymers of immiscible blocks, polystyrene-block-polyisoprene-block-polystyrene and polystyrene-block-polyisoprene-block-poly (2-vinylpyridine). Both groups of researchers obtained

quite similar results in that the viscosity of samples decreased during a first shear stress, when the viscosity of pre-sheared sample was closer to the viscosity of Newtonian liquid.

Some qualitative disagreement was found in both models between the theoretical prediction and the experimental data which may be caused by some additional factors involved, such as interactions between adjacent droplets.

Xu et al [70] studied viscoelastic behaviour of hydroxyl-terminated polydimethylsiloxane (PDMS) filled with calcium carbonate ($CaCO_3$), with diameter of particles about 50 nm.

In contrast to the system of colloidal droplets presented earlier, the particles of calcium carbonate did not change their geometry during deformational stress. Some shear thickening was obtained during low frequency oscillating stress deformations, whilst during a high frequency stress a shear thinning was observed.

The initial shear thickening area may be explained by the fact that during deformation, polymolecular chains of PDMS were forced to obtain a new position but also to avoid the obstacles (particles of calcium carbonate filler). Therefore, in the areas between the filler particles, the polymolecular chains were somewhat compressed together which caused an increase in the number of entanglements and in strain-induced crystallization. Also it is believed that particles of the filler are able to create some sort of a gel-matrix due to entanglements between adjacent calcium carbonate particles.

Shear thinning during a high frequency stress can be explained by the fact that the gel-matrix of calcium carbonate particles effectively disappeared when the particles were covered by substantial number of PDMS polymolecules (chains of PDMS were forced to change their initial geometry due to the stress). Hence the stress-relaxation was dominated further by a flow of a polymolecular matrix of PDMS and the particles of calcium carbonate did not play such a significant role as that during low frequency deformation.

See et al [71] came to a similar conclusion as Xu et al [70] when they studied a response under step changes in the magnetic flux density of a magneto-rheological suspension consisting of carbonyl iron particles in silicone oil, where the sample was subjected to a constant stress. It was found that the magnetic suspension showed significant changes in shear rate under a strong magnetic field in comparison to the shear

rate without the field, just when a fraction of the magnetic particles was higher than 30 % of the volume of the suspension. The change of shear rate under a constant magnetic field was increased just for a short period and then reduced to the original value.

The result is in agreement with a suggestion of Xu et al [70] that on the first step of the stress caused by magnetic particles a gel-matrix of the dispersed particles appeared which is soon replaced by a flowing matrix of polychain siloxane.

2.3 Review of Possible Chemistry behind the Polymerization Process of the Developing Polymer

The polydimethylsiloxane (PDMS) based polymer poly-(boron)$_n$-poly(dimethylsiloxane)$_m$ [where m ≈ 15 n] is known as a shear thickening polymeric material at room temperature during low intensity deformation. So far in this research polyboron-PDMS (commonly known as a "Bouncy" or "Silly Putty" [72]) oligomeric material has been considered as a main polymeric candidate for further polymerization or copolymerization to form a foam or an elastomer suitable for the final application as a protective material.

Due to a significantly higher than average cost of an elastomeric material, possible insufficient tear resistance and also some technological difficulties in the production of a rubber based on a pure polyboron-PDMS, it was decided that the best possible application may be by introducing polyboron-PDMS into a kind of a block copolymer where polyboron-PDMS would be able to exhibit high shear thickening and the final material be able to obtain an acceptable level of tear resistance.

2.3.1 Chemistry of Siloxanes

PDMS has the most flexible bond of the main polymeric chain amongst all known polymers. As pointed out earlier in this work, a polymeric chain of PDMS at room temperature is able almost momentarily to obtain a position of minimum energy. Usually oligomers of PDMS tend to form cycles. However, when in polymolecules the probability of obtaining a ring form is always lower and polymolecules of PDMS take a coil form, where the end-to-end distance can be characterized statistically as the square root of the molecular length [20].

The main polymeric bond of a siloxane polymer consists of a continuous line of silicon-oxygen bonds (368 kJ/mol and 1.64 Å), as shown in Figure 36 [23].

Siloxane polymers are chemically very stable polymers and are normally able to withstand a temperature of 200 °C without breaking the silicon-oxygen bond even though the bond is quite long and polar (60 % polarity of the silicon-oxygen bond). The explanation lies in the fact that a flexible polymeric chain normally obtains a coil position

where the silicon-oxygen chain is effectively hidden, by the attachment to the main chain, from the methyl groups outside.
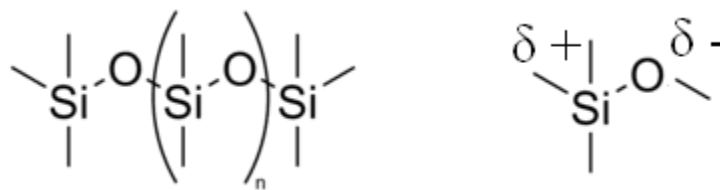
Figure 36: *Chain of Siloxane*

Normally PDMS is immiscible with water and strongly tends to a phase separation which is energetically much more efficient. But when a small amount of PDMS forms a film on the water surface, it tends to lie by exposing its polar silicon-oxygen bond towards the water molecules. In such a case the PDMS chain is very vulnerable to a cationic or anionic attack on its polar silicon-oxygen bond. In fact a PDMS chain in the presence of water is vulnerable at reasonably mild acidic conditions of pH 4 or basic conditions of pH 9. In the absence of water molecules PDMS is normally able to withstand quite harsh conditions of pH lower than pH 3 or higher than pH 11. Water vapour with acidic or basic traces is particularly effective in breaking the silicon-oxygen bond of siloxanes [20].

The main starting monomer for the polymerization of a PDMS chain is dichlorodimethylsilane, as shown in Figure 37.
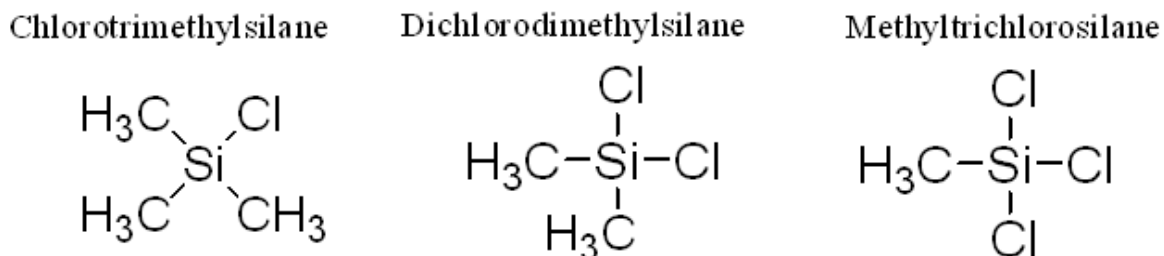
Figure 37: *Siloxane Monomers, Chlorotrimethylsilane,*
Dichlorodimethylsilane and Methyltrichlorosilane

A polycondensation reaction between dimethyldichlorosilane $Si(CH_3)_2Cl_2$ and water (H_2O) is fairly fast and exothermic. The relevant final product of the reaction is PDMS, as shown Figure 36.

$$n\ [Si(CH_3)_2Cl_2] + n\ [H_2O] \rightarrow [Si(CH_3)_2O]_n + 2n\ HCl \qquad (37)$$

In reality this is the result of two condensation reactions: the first is a fairly fast reaction:

$$ClSi(CH_3)_2Cl + H_2O \rightarrow ClSi(CH_3)_2OH + HCl \qquad (38)$$

The second is a slow polycondensation reaction:

$$RSi(CH_3)_2OH + R^1Si(CH_3)_2OH \rightarrow RSi(CH_3)_2O\ Si(CH_3)_2R^1 + H_2O \qquad (39)$$

This polycondensation reaction results in just about half of the silane producing the linear form of the polymer (as shown earlier, short siloxane molecules tend to form rings). Without additional solvent, about half of the silane is a cyclic silane, as shown in Figure 38, where half of the formed short cyclic siloxanes are octamethyltetrasilane and the rest is a mix of five, six, seven, eight or more atoms of silicon members rings (where lower numbers are predominant). If the polycondensation reaction is run in a non-polar solvent, particularly in dimethylether, about 80 % of the resulting product is cyclic. Instead, when the reaction is run in an excess of water, it may reach a much higher proportion of the straight polymer form.

In industry polymers with monodispersed molecular weight are normally made from separating cyclic silanes by careful evaporation and following with a further ring-opening reaction. The ring-opening reaction is usually carried out in a small amount of base or acid catalyst and/or at elevated temperatures of 160-220 °C. A high concentration of a strong base or acid leads to predominantly cyclic compounds, however, a lower concentration gives a higher amount of straight molecular chain polymers. Boric acid is one of the Lewis acids used in a chain opening reaction, the result being a polyboron-PDMS [73].
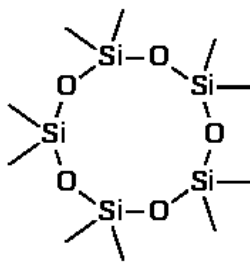
Figure 38: *The Cyclic Polysiloxane, Molecule of Decamethylcyclopentasiloxane*

In order to stop the growth of the polymeric chain for monodispersed weight polymers or to increase the chemical stability of the resulting polymer (for example, silicone oil for high temperature baths or lubricants for a jet engine, etc), one-side reactive chlorotrimethylsilane is often added to the polymerization bath.

In order to obtain a cross-linked resin, three-side reactive methyltrichlorosilane or four-side reactive tetrachlorosilane are often used [20].

The use of other halo-silanes instead of chloro-silanes is normally limited to a specific synthesis, such as the formulation of tetraorgano-silane (for example, it is impossible to obtain tetraorgano-silane by Grignard reaction of tetrachlorosilane), because of their much higher price.

Monomers of halosilanes are used as starting materials for the synthesis of PDMS other siloxanes. For example, polydiphenylsilane (PDPS) is synthesised from dichlorodiphenylsilane, as shown in Figure 39 [71].
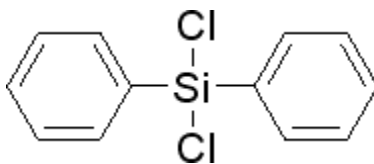
Figure 39: *Dichlorodiphenylsilane*

A block copolymer of PDPS and PDMS is able to form a thermoplastic siloxane elastomer. A copolymer of polymethylphenylsilane (PMPS) and PDMS is also used in the synthesis of new synthetic lubricants. As a pure linear oligomeric PDMS is almost a Newtonian liquid. With the addition of PMPS or PDPS to the polymeric chain the

resulting polymer is slightly shear thickened. This can be used to improve adhesion to heavy duty parts of engines during the compression of the polymeric lubricant between moving parts.

Simultaneous polymerization can be achieved in one bath (in order to obtain a random copolymer) by reacting together dichlorodimethylsilane and other monomers of organohalosilanes. All monomers of organohalosilanes, (for example dichlorodiphenylsilane) with a group larger than the methyl group attached to the silicon atom, will have higher reactivity. Therefore, during simultaneous polymerization in one bath of dichlorodimethylsilane and dichlorodiphenylsilane, dichlorodiphenylsilane will tend to react first, and will also form blocks of polymer first and dichlorodimethylsilane will follow. The resulting copolymer may not be absolutely random, as dichlorodiphenylsilane would have been able to form quite substantial blocks before dichlorodimethylsilane would be introduced to the polymerization [20].

In general, the rule for the reactivity of organohalosilanes is as follows: the stronger electron the withdrawing group (i.e., the reactivity is promoted by the decrease of electron density at the silicon atom) that is introduced into the organohalosilane (i.e., directly attached to the silicon atom), the stronger the reactivity of the monomer of that organohalosilane. Therefore, dihalo-ethylmethylsilane will be more reactive than dihalo-dimethylsilane, while dichlorodiphenylsilane will be more reactive than dichloromethylphenylsilane, etc [73]. (In the case of the difference in the reactivity of different vinyls, the rule of the reactivity is quite similar to the organohalosilanes. Hence, the stronger the electron withdrawing group attached to the monomer, the more reactive the resulting vinyl monomer. For example, vinylidene-acetate or styrene-vinyls react much more readily than propylene-vinyl, etc [23].)

The chemical stability of a bond between carbon and silicon of a polymeric chain of organosiloxane may significantly differ with different kinds of groups attached to the silicon. The methyl group attached to the silicon in polyorganosiloxane (about 290 kJ/mol and 1.89 Å) will be even more chemically stable than the methyl group attached to a carbon in polypropylene (about 373 kJ/mol and 1.54 Å), and a silicon-ethyl bond in the ethyl group attached to a siloxane chain will be much more reactive [20, 23].

The long and polar bond between the carbon of the ethyl group and silicon is quite open and can be cleaved quite readily by the S_N2 mechanism by either nucleophilic attack on the silicon, or electrophilic attack on the carbon, where nucleophilic attack on the silicon by a strong anion is particularly effective, as shown in Figure 40 [23, 74].
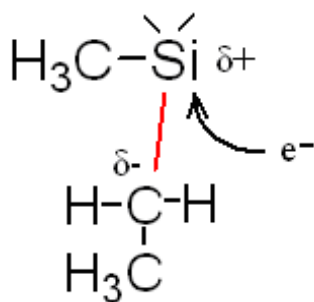
Figure 40: Mechanism of Nucleophilic Attack on a Silicon Atom of a Siloxane Chain

In general, the more electronegative the α-carbon atom (directly attached to the silicon on the polychain), the lower the stability of such a bond. Therefore, if a strongly electron withdrawing group is present (for example amine or hydroxyl) and is close enough to the α-carbon, such a bond may be quite readily cleaved [75, 76].

In addition, the reactivity of hydrogen atoms attached to the α-carbon, as shown in Figure 40, will differ strongly with an attachment to the group. For example, if on the β-carbon of this group one of the hydrogens is substituted with an electron withdrawing group such as chlorine or hydroxyl, the reactivity of the α-carbon will be much higher and substitution of a hydrogen will be easy available by the S_N2 mechanism. But because of the extremely high reactivity of the resulting bond between the α-carbon and silicon of a polychain such syntheses have not found any practical use in polymeric siloxanes. As a result any organofunctional attachment to the silicon should have an aliphatic bridge of at least three carbon atoms in a row between the silicon and a strongly electron withdrawing group to be stable enough for practical use in a polymer. Any organofunctional group, such as a double carbon-carbon bond, can be attached to the silicon, however it should be no closer than to γ-carbon atom [20, 71].

2.3.2 Possible Alternatively Polycondensation Reaction of PDMS

During the polycondensation reaction of an organochlorosilane with water, hydrochloric acid is a byproduct of the reaction. In some cases it is preferable to avoid the formation of corrosive hydrochloric acid. Alternatively, for polymer extension, it is possible to use reactive α, ω hydroxyl groups attached to a silicon atom of an organosiloxane molecular chain. Siloxane-hydroxyl groups are quite reactive and readily perform polycondensation reactions giving a silicon-oxygen-siloxane bond and a water molecule. This occurs even in the presence of very small traces of cations or anions (for example the polycondensation reaction of PDMS between $MeSi(CH_3)_2OH$ and $MeSi(CH_3)_2OH$ which occurs readily in the presence of hydrochloric acid as a catalyst) [20].

Siloxane methoxys $RSiOMe$ (or sometimes ethoxys $RSiOEt$, etc) are much more stable than hydroxyl-ended siloxanes because of the required presence of water for the reaction to occur. Siloxane-methoxys are the most stable, and the longer the alkoxy group, the more reactive is the alkoxy-siloxane.

$$RSiOMe + H_2O \rightarrow RSiOH \rightarrow RSiOSiR \qquad (40)$$

Therefore, it is much easier to store and/or to mix in a blend of these polymers than hydroxyl-ended-siloxanes. The polymerization conditions are mild; the reaction requires water (moisture from air) and often some catalyst (either cationic or anionic), and/or elevated temperature to start [71].

In recent years it has been increasingly popular to use this mild reaction of hydrating the alkoxy-silanes moiety for copolymerization or polymer prolongation of modified organic polymers, where another possible reaction may be considered technically less desirable. Other reactions are less desirable for reasons such as the need for high temperatures or that the byproduct of the reaction (or the required catalyst, etc) could be too corrosive and hence may cause decomposition of polymer. One of the commercial applications was SIOPLAS technology which involves the grafting of triethoxy-silane functionality onto linear polyethylene. The resulting modified polyethylene undergoes cross-linking on exposure to moisture which increases its

operating temperatures and allows its use in hot water piping and superior cable insulation applications which are outside the range of unmodified linear polyethylene [20, 77].

Thus, in general, incorporation of siloxane condensation cross-linking into organic thermoplastic polymers will increase the operational range of these materials. A similar approach has been employed by a Japanese corporation to develop a range of curable polypropylene oxide polymers by incorporating a trifunctional alkoxy-silane moiety into the polypropylene oxide polymers by hydrosilylation. α, ω allyloxy polypropylene oxides and hydridosilane functional alkoxy-silanes or siloxanes were reacted to produce a functional polypropylene oxide polymer which cross-linked on exposure to moisture. These materials have been formulated into very satisfactory room temperature curing sealants [78].

In the case of reaction of alkoxy-silanes with chlorosilane the resulting byproduct of siloxane polycondensation reaction is non-corrosive chloromethane or chloroethane, which are quite easily vaporizable from the polymer and can be recycled [20, 71].

2.3.3 Introduction of Cross-links into Polysiloxanes

In order to obtain a polymeric siloxane matrix from a mixture of linear polysilanes some cross-links are introduced. It is possible to introduce some monomers with functionality higher than two, such as methyltrichlorosilane or tetrachlorosilane, in a stage polycondensation reaction of organohalosilanes.

In some applications it is more convenient to first obtain a linear oligomeric mixture which is further able to react by exposure to atmospheric moisture to form a cross-linked product. In such a linear oligomeric mixture (usually with α, ω reactive allyloxy ends) it is possible to add some amount of trifunctional alkoxy-silane or tetrafunctional alkoxy-silane for polycondensation curing [20, 71].

Another popular way to obtain a cross-linked polysiloxane matrix is the use of a peroxide-induced free radical reaction. In this case three quite different kinds of vulcanization of polysilicones by organo-peroxides are possible.

The first method uses such highly reactive organo-peroxide as

2,4-dichlorobenzoyl peroxide, which is able to break the bond between the carbon and hydrogen in the methyl group attached to the siloxane chain. Two siloxane chains will be cross-linked through random ethylene bridges, where the number of cross-links will be proportional to the quantity of the peroxide used.

$$ArOOAr \rightarrow 2ArO\cdot \quad (41)$$

$$2ArO\cdot + CH_3SiR \rightarrow ArOH + \cdot CH_2SiR \quad (42)$$

$$RSiCH_2\cdot + \cdot CH_2SiR \rightarrow RSiCH_2CH_2SiR \quad (43)$$
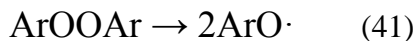
The problems caused by this method of peroxide-induced free radical vulcanization are the inability to control it and more importantly, an excessive use of highly reactive peroxide which gives volatile byproducts. These volatile byproducts should be removed by post-curing to prevent a decomposition of polymer.

Alternatively it is possible to use organo-functional polysiloxanes, where some reactive vinyl groups are attached to a polysiloxane chain. These are able to react in the presence of a milder organo-peroxide such as di-*t*-butyl peroxide. Free radicals of such organo-peroxides as di-*t*-butyl peroxide are unable to break a carbon-hydrogen bond of a methyl group of polysiloxane on its own, but readily break a double carbon-carbon bond of the attached vinyl group.

$$t\text{-butyl OO } t\text{-butyl} \rightarrow 2\ t\text{-butyl O}\cdot \quad (44)$$

$$t\text{-butyl O}\cdot + CH_2CH(CH_2)_3SiR \rightarrow t\text{-butyl OH} + \cdot CH_2(CH_2)_4SiR \quad (45)$$

$$RSi(CH_2)_4CH_2\cdot + \cdot CH_2(CH_2)_4SiR \rightarrow RSi(CH_2)_{10}SiR \quad (46)$$
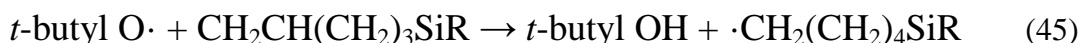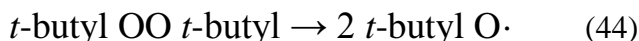
In such a case the number of cross-links will be practically proportional to the number of vinyl groups attached to the polymeric siloxane chain and less proportional to the amount of the peroxide used. Such a method is more expensive, but allows control of the length of the polychain between cross-links and also requires a significantly smaller amount of peroxide, hence the post-cure is faster. The problem of this method is the higher level of organic incorporations into the polysiloxane polymer, where the higher proportion of purely organic parts of the polymer can significantly change possible

mechanical properties of the resulting polymer. But in applications where this factor is not important such vinyl-through free radical siloxane vulcanization may be very useful.

The third method is a combination of the two methods described above. Here alongside the use of vinyl groups attached to a polysiloxane chain, a strong organo-peroxide is used, such as 2,4-dichlorobenzoyl peroxide, which is able to break a carbon-hydrogen bond. Therefore, a cross-link between siloxane polymolecules can be introduced from a broken double bond of a vinyl attached to the methyl radical of the second molecule. Such a polysiloxane vulcanization method requires less vinyl substitution.

It was also observed experimentally that the introduction of short organic vinyls into a mixture of PDMS and a mild organic-peroxide, such as di-*t*-butyl peroxide gives a cross-linked polymer. The exact mechanism is not understood entirely, but it is thought, that a vinyl radical is able somehow to break a carbon-hydrogen bond of a methyl group attached to a polysiloxane chain. Hence, in a polysiloxane cross-linked through vinyl groups and a mild organo-peroxide there will always be an insignificant amount of cross-links caused by carbon-hydrogen bonds broken by methyl radicals.

In spite of much research and development, covering a whole range of peroxides, no single peroxide has yet been identified which will satisfy all the various requirements.

The silicone rubber technologist, therefore, normally employs a range of siloxane polymers and a limited range of peroxides, typically, 2,4-dichlorobenzoyl peroxide, dicumyl peroxide and di-*t*-butyl peroxide to achieve the required rubber properties [20, 74].

It is also important to notice here that a pure cross-linked PDMS rubber does not give a product with satisfactory mechanical properties because of the near total absence of an intermolecular force between the molecules of PDMS. Mechanical properties of such PDMS polymer will be more a function of the amount of reinforcing filler, such as silica fines or calcium carbonate, rather than proportional to the number of cross-links introduced into the pure polymer [73].

2.3.4   Organofunctional Siloxanes

In order to modify a semi-organic siloxane polymer to be a part of an organic polymer or to introduce an organic polymer into a siloxane chain it is necessary to introduce some organofunctional groups into the siloxane chain. A good example of such an organofunctional siloxane may be a vinyl siloxane. This is able to react further with organic compounds having a double carbon-carbon bond, etc, where the chemistry of the possible reaction for the vinyl group attached to the siloxane chain will be similar to that of the purely organic polymers.

A convenient reaction to obtain a vinyl-functional siloxane is a hydrosilylation reaction, which involves the addition of a hydrogen-silicon bond (where hydrogen is attached straight to a silicon atom of siloxane chain (R_3SiH)) to an unsaturated carbon-carbon bond, catalyzed by a noble metal, typically Pt. This is a well-known and versatile reaction in organo-silicon chemistry. It has been widely used in the synthesis of different kinds of organofunctional siloxanes as an organic group attached to a silicon of a siloxane chain may contain different kinds of functional groups, for example amine or halogen, etc.

As a starting monomeric material for the polycondensation of siloxane containing hydrosilanes (R_3SiH) in the polymeric chain, hydrohalosilane monomers are used which often contain one methyl group, such as dichloromethylsilane (Cl_2MeSiH). The polycondensation reaction should be run in mild acidic conditions, as the hydrogen attached to the silicon is slightly acidic and can be readily cleaved in basic conditions [20, 72].

Another useful method to achieve organofunctional silanes is by Grignard reaction [23]. In such a reaction the halogen of a monomeric organohalosilane can be substituted to the organic group:

$$CH_3SiCl_3 + ClMg(CH_2)_2CH_3 \rightarrow CH_3SiCl_2(CH_2)_2CH_3 + ClMgCl \qquad (47)$$

Using this method for the introduction of organofunctional groups, it is possible, selectively, to displace the halogen from the $Si\text{-}X$ bonds of halosilanes in preference to the halogen from the $C\text{-}X$ bonds of organohalosilanes simply because the $Si\text{-}X$ bond is

more reactive in organo-metallic substitution than the $C\text{-}X$ bond. In fact, if a substrate contains both types of bond, it is possible to replace the halogen in the $C\text{-}X$ bond only after all the $Si\text{-}X$ bonds have been similarly reacted. This difference in the reaction rates has made it possible to attach both halogen-substituted aromatic and halogen-substituted aliphatic groups to the silicon:

$$CH_3SiCl_3 + ClMg(CH_2)_2CH_2Cl \rightarrow CH_3SiCl_2(CH_2)_2CH_2Cl + ClMgCl \qquad (48)$$
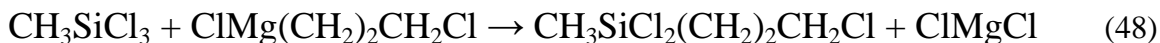
The mechanism of Grignard reaction is best expressed as involving coordination between the magnesium atom and the halogen linked to the silicon, resulting in the formation of a four-centre transition state, as shown in Figure 41.
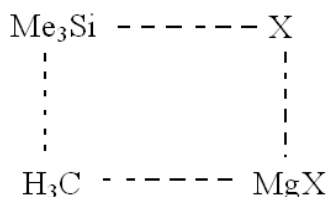
Figure 41: The Formation of a Four-centre Transition State in Grignard Reaction

The rigid four-centre complex explains the strong steric effects observed in Grignard reactions. These steric effects are caused not only by bulky atoms or groups on the silicon, but also by those linked to magnesium. Steric hindrance may necessitate the use of elevated temperatures, as is the case in the synthesis of bulky aromatic silanes such as naphthyl-chlorosilane.

Grignard reactions are promoted by a decrease of the electron density at silicon, so that tetra-halosilanes X_4Si and tri-halosilanes X_3MeSi have their reactivity much higher than the reactivity of di-halosilanes X_2Me_2Si or particularly mono-halosilanes XMe_3Si (i.e., chlorophenyldimethylsilane is more reactive than chlorotrimethylsilane) [23, 72].

Grignard reactions result in a mixture of silanes invariably containing the mono- and di-substituted products and often also tri- and, some cases, even tetra- substituted products. The product containing halogen atoms always subsequently reacts with the

Grignard reagent. The relative quantities of the various products can be altered by appropriate choice of the reagents' molar ratios. The amount of the di-substituted silane obtained is, however, often appreciably greater than expected on the basis of the statistical distribution of the products [20]. Also, many tetraorganosilanes have been synthesized by the use of an excess of Grignard reagent. Similarly to the rate of reaction, the distribution of the product is greatly influenced by steric effects, as exemplified by the alkylation of a silicon tetrahalide by methyl, ethyl and propyl magnesium halide. Steric effects also operate in the alkylation of trichlorosilane by isopropyl or tert-butyl magnesium chloride. The tri- and tetra-substituted silanes are then often difficult to prepare. The preparation of tri-organohalosilanes is easier when the starting material is tetrafluorosilane, though the presence of bulky groups again leads to products with a smaller number of alkylgroups, for example diisopropyldifluorosilane.

Owing to its availability, tetrachlorosilane is often used as the starting material, although tetrafluorosilane also has a wide application. Bromides and iodides are employed as well, but they react slower than tetrachlorosilanes [72, 75].

Halosilanes containing hydrogen linked to the silicon can also be used as the starting material for Grignard synthesis, because the $Si-H$ bond is hardly ever affected in this reaction. This enables one to carry out reactions of the type:

$$SiHCl_3 + 2RMgX \rightarrow R_2SiHCl + 2MgClX \qquad (49)$$

Alkoxides are also suitable starting materials for Grignard synthesis, and tetramethoxysilane is in fact often used. The advantage of these starting materials is that it is possible to dispense with solvent properly since the excess of tetra-alkoxysilane itself can act as such. By doing this, it avoids the complications associated with the use of ether as the solvent. The use of alkoxysilanes also facilitates filtration of the resulting magnesium salts. The poisonous nature of many alkoxysilanes is, however, inconvenient. Alkoxysilanes react somewhat more slowly than the chlorosilanes and the steric effects exert a greater influence on their reactions. It is often difficult to substitute the last group. The reactivity of the alkoxysilanes decrease along the series $Et > n\text{-}Pr > n\text{-}Bu > iso\text{-}Bu$

$>$ sec-Bu. The advantage of the use of partially substituted alkoxysilanes is that hydrolysis leads to non-corrosive alcohols instead of hydrochloric acid.

Grignard synthesis can be carried out either in one stage or in two stages. In the second case, the Grignard reagent is prepared first. The solvent is usually diethyl ether, but other ethers may also be employed if a higher temperature is required or if diethyl ether would present difficulties in the distillation products. Tetraethoxysilane and chlorobezene can act simultaneously as reagent and solvent. A solvent other than ethers, benzene or petroleum ether may also be used provided that tetraethoxysilane is present as a catalyst in small quantities. The Grignard reagent and the silane are brought together by the dropwise addition of one to the other, the order of the addition being suitably chosen. In the alternative method, the synthesis is carried out in one step by suspending the magnesium in an ethereal solution of the silane and by adding the organic halide dropwise to an ethereal suspension of magnesium from two dropping funnels. After the reaction has reached completion, the liquid product can be separated from the solid magnesium salts by distillation, or the salt can be filtered off.

Certain properties of Grignard reagents and the halosilanes may interfere with the success of the synthesis. An example of considerable importance is the ether-splitting action of the halosilanes, which is strongly promoted by traces of aluminium chloride and ferric chloride. Bromosilanes and iodosilanes in particular react rather quickly with ethers in some cases. Tetrahydrofuran (THF) is prone to reacting with halosilanes and reacts with bromides and iodides even at room temperature:

$$THF + SiBr_4 \rightarrow Br(CH_2)_4OSiBr_3 \qquad (50)$$

Halogen-exchange takes place with the chlorosilanes when the Grignard reagent contains bromine or iodine. Under these conditions, THF is cleaved as well. If bromine or iodine is absent from the system, the chlorosilanes react only at 65 °C. Hence, under somewhat more vigorous conditions (refluxing for a few hours) the use of THF leads to a practically quantitative conversion of trimethylhalosilane into 4-halo-butoxytrimethylsilane [72].

For the preparation of Grignard reagent the reaction of a metal (normally Mg, but often Zn or Hg) and an alkyl halide is used. The reaction should be run in a solution

where the alkyl halide must react with magnesium on the surface of solid metal. In such a reaction the surface area and its character are important in allowing maximum contact between the elemental magnesium and alkyl halide. In the preparation of Grignard reagents, the magnesium is usually in the form of metal shavings or lathe "turnings". The reaction mechanism consists of the following steps:

$$R\text{-}X + \text{-Mg-Mg-Mg-} \rightarrow \text{-Mg-Mg-Mg} + R\cdot + X\cdot \qquad (51)$$

$$\text{-Mg-Mg}^+\text{-Mg-} + R\cdot + X^- \rightarrow \text{-Mg}^+\text{-Mg}^+\text{-Mg-} + R^- - X^- \qquad (52)$$

$$R^- + Mg^{2+} + X^- \rightarrow RMgX \qquad (53)$$
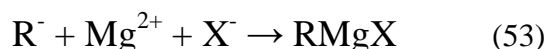
Reaction of RX at the magnesium surface produces an alkyl radical and $Mg\text{-}X$ species, probably still associated with the metal surface. The resulting free radical $R\cdot$ then reacts with the $\cdot Mg\text{-}X$ to produce the Grignard reagent. The principal side reactions involve alternative reactions of organic radicals, mostly dimerization and disproportion:

$$CH_3(CH_2)_2CH_2\cdot + CH_3(CH_2)_2CH_2\cdot \rightarrow CH_3(CH_2)_6CH_3 \qquad (54)$$

$$CH_3(CH_2)_2CH_2\cdot + CH_3(CH_2)_2CH_2\cdot \rightarrow CH_3(CH_2)_2CH_3 +$$
$$CH_3CH_2CH=CH_2 \qquad (55)$$
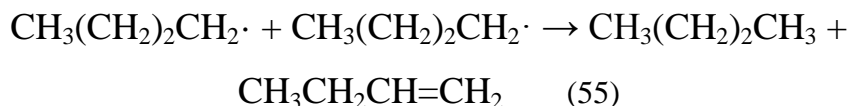
However, for simple alkyl halides the yield of alkylmagnesium halides is quite high and normally is above 90 %. The reaction works well with chlorides, bromides and iodides. Reaction with chlorides is frequently somewhat sluggish and iodides are generally expensive. Hence, alkyl bromides are common laboratory reagent in Grignard synthesis.

A suitable amount of the solvent is essential for the success of Grignard synthesis, because in dilute ether solution (about 0.1 M) alkyl-Grignard reagents exist as monomers in which the magnesium is coordinated to two solvent molecules. However, in more concentrated solutions (0.5-1 M) the principal species is a dimer in which two magnesium atoms are bridged by two bromines, as shown in Figure 42. In this structure each magnesium acquires its octet by additional coordination with one bromine from the other $RMgBr$ and ether oxygen [23].
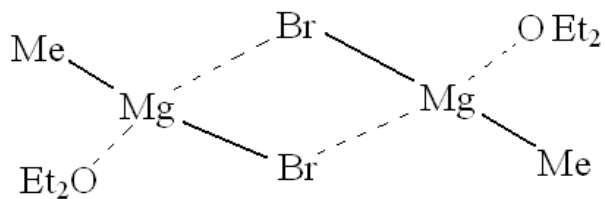
Figure 42: *Methylmagnesium-bromide Dimer in Ether*

In order to obtain a siloxane-prepolymer suitable for a possible further copolymerization with organic polymers, the alkyl group attached to a siloxane polymeric chain by Grignard synthesis should contain some reactive ends which can be readily transformed to a suitable organic group. For example, a halogen group is quite easily replaceable by S_N2 by a hydroxyl (therefore this is suitable for polyester or polyurethane polymerization), etc. Here a bond between the carbon of the alkyl group and the hydrogen may be too stable to be considered for a modification of the attached alkyl group into an appropriate reactive end. This is because the alkyl group could be potentially cleaved from the siloxane chain by harsh conditions of the possible reaction [72].

As pointed out earlier, a Grignard reagent first selectively reacts with $Si\text{-}X$ and starts to react with $C\text{-}X$ only when $Si\text{-}X$ has disappeared from the reaction. Hence, it is relatively easy by Grignard synthesis to introduce a halogen-ended alkyl group into a siloxane polychain. In the case of the preparation of the Grignard reagent, the reaction between short α,ω-dihaloalkyl and magnesium will always be faster on one side of α,ω-dihaloalkyl (in the case where the alkyl group is short enough for the electron withdrawing effect, $2 < n < 7$), as the ω-haloalkyl is able to form a much more stable cation. So $^{+}CH_2(CH_2)_{n-1}X$ forms faster than $^{+}CH_2(CH_2)_{n-1}MgX$, because MgX group (in contrast to a halogen) is not an electron withdrawing group. Hence, the first halogen in such a short α,ω-dihaloalkyl group will be a much easier leaving group and therefore, will be more reactive [72, 74].

2.3.5 Heterosiloxanes

Heterosiloxanes are polysiloxanes in which some of the silicon atoms in the siloxane chain have been replaced by other atoms. One of the best known examples is the boron-silicon polymer whose extraordinary rheological properties are applied in this work.

Also the following hetero-atoms and groups are known to have been incorporated in the siloxane polymeric chain: B, Al, Ga, Ti, Ge, Sn, Pb, P, As, Sb, V, Nb, Ta , Cr, W and most recently Ar. These polymers show a certain resemblance to silicates and may be regarded as their organic derivatives. The thermal stability of heterosiloxanes is generally good and occasionally better than that of the siloxanes. Heterosiloxanes containing V, Nb, Ta, Cr, W, P, Sn or Ar are stable between 300-600 °C. Efficient heat resistance has also been observed in the case of heterosiloxanes containing aluminium, phosphorus and boron atoms [72, 79].

Recently heterosiloxanes based on boron-silicones have found additional applications as precursors of amorphous SiBCO ceramics, where SiBCO ceramics are obtained by pyrolysis of the polyorgano-boron-siloxane gels under inert atmosphere at 1200-1300 °C. The main advantage of such a novel method is the formation of ceramics with well-defined molecular units controlling the structure. Moreover, the final ceramics can be significantly lower in price than existing ones [80, 81].

Boron is just slightly more electronegative than silicon, so the polarity of the boron-oxygen bond reminds us of the silicon-oxygen bond of siloxane [82, 83]. But in contrast with silicon, boron gives a planar structure with a bond angle of 120° when it is bonded to three neighbouring oxygen atoms. Also, the boron-oxygen bond is just 1.365 Å in comparison with 1.64 Å for the silicon-oxygen bond. Additionally this bond is less flexible [84]. Hence the structure of the backbone of polyboron-siloxane may significantly differ from the original structure of pure siloxane, and the difference will be greater as the proportion of boron rises. As shown earlier in section 2.2.3, the rheological properties of heterosiloxane may differ with the amount of substitution in such polymeric chain, because of the increasing rigidity of the main backbone.

The rheological properties of boron-siloxane polymer can be explained by the fact that boron is much less shielded to intermolecular interaction than silicon, and moreover, boron does not have a full octet of electrons and has only 3 pairs of electrons on the valent (*p*) orbital. Hence boron incorporated in a siloxane polymeric chain is always attracted to a strong intermolecular bond with a neighbouring nucleophile, such as oxygen (or nitrogen) [85].

This strong affinity of boron when incorporated in a polysiloxane has recently found some applications in electronics as a film-forming material able to show selective cation permeability, when an anion is left trapped by the polymer [86]. Also such a polymeric film may be potentially used as a proton fuel cell, where acidic anions can be effectively trapped by the boron atoms of such a heterosiloxane [87].

Kurono et al [86] have been investigating the electro-permeability of amorphous boron-siloxane, where the ratio between silicon and boron $Si:B$ was varied from 1:2 to 2:1. The electro-conductivity of such an amorphous polymer was directly related to the ability of this material to trap an anion, and was governed by the WLF equation. Because of the poor mechanical properties of the amorphous polyboronsiloxane with the ratio of $Si:B$ ~1:1, Kurono et al [86] introduced a polyethylene-oxide (PEO) to the polymer. As a result, the mechanical properties of such a film-forming polymer improved, but the electro-conductivity was no longer a function governed by the WLF equation, and was much more the function of polymeric entanglements.

Poly-boron-siloxane can be synthesised by the hydrolysis of alkoxy-siloxanes and alkoxy-borates in catalyzed conditions in the presence of hydrochloric or hydrobromic acids [88]. Alternatively it can be prepared by the polycondensation reaction between boric acid and silanol or halosilanes. Also poly-boron-silane can be obtained by the incorporation of boron (at elevated temperatures ~180-220 °C and/or under harsh catalyzing conditions) into an existing polysiloxane chain, where an existing siloxane polymeric chain is no longer stable. Therefore, a broken polymeric chain of poly-siloxane readily undergoes a polycondensation reaction with boric acid and gives a more stable polyboron-siloxane product [73, 89].

Poly-organo-boron-silanes can be characterized by the typical Fourier transform infrared spectroscopy (FT-IR) bands associated with the $Si\text{-}O$ bonds at 1120-1020 cm^{-1}

and 840-790 cm^{-1}, Si-O-Si 460-400 cm^{-1}. Absorptions at 920-950 cm^{-1} (Si-OH) and at 1620 cm^{-1} (H-O-H) and 3600-3100 cm^{-1} (O-H) suggest the presence of terminal hydroxyl groups as well as absorbed water. The presence of boron gives rise to peaks at 1500-1300 cm^{-1} (B-O) and at 1195 cm^{-1} (B-OH), and also bands due to borosiloxane bridges at 930-915 cm^{-1} (B-O-Si) and at 675 cm^{-1} (B-O-Si) [93]. Also, weaker peaks of the resonance area of the second harmonic of the infrared (B-O-Si) oscillations at 2430-2580 cm^{-1} may often be more informative, because of the absence of another strong absorption in this spectrum [20].

Another group of FT-IR absorption bands which are of a great importance in this work is the spectrum of infrared absorption of organic compounds directly attached to a silicon on an organo-siloxane. So, Si-Me moieties lead to a sharp peak at 1275 cm^{-1}, 800 cm^{-1} (Si-C) and 780 cm^{-1} (Me-Si) [91]. Moreover, in the area of FT-IR absorption at ~3000-2900 cm^{-1} due to the C-H bond, there are normally no other strong peaks present. Hence, it is possible to recognize this as a fingerprint (CH_2-H) - a sharp peak at 2965-2960 cm^{-1} and a less intensive peak 2860 cm^{-1} from the Si-Me bond. Additionally a carbon-carbon double bond (C=C) gives an increase in (C-H) frequency, moving it to a 3100-3000 cm^{-1} absorption [24]. Also important in this work is an absorption spectrum of olefin groups attached to a silicon (Si-$(CH_2)_n$) of a siloxane, where the normal absorption spectrum of hydroxyl attached to a methylene (CH_2) of an olefin gives rise to a sharp peak at 2926 cm^{-1} and a less intensive one at 2853 cm^{-1}. In addition it can be characterized by the bands at 1463 cm^{-1} (CH_3-C), 1410 cm^{-1} (CH_2-Si), 1255 cm^{-1} (CH_2-Si), 960 cm^{-1} (Si-C_2H_5), 760 cm^{-1} (Si-C) and due to vibrations of the (CH_2-Si) 697 cm^{-1} [92]. In the case where such an olefin group is stretched (i.e., for example is formed a closed cycle, etc) therefore, the bond will be additionally stretched, and this will give an absorption band slightly higher (at ~10 cm^{-1} higher than normal) [23, 93].

Another popular analytical technique for heterosiloxanes is NMR spectroscopy. Both ^{13}C NMR and ^{1}H NMR are known as the most important analytical tools of

contemporary organic chemistry. In analysis of heterosiloxanes, as well as ^{13}C NMR and ^{1}H NMR, are often involved relatively novel techniques of ^{11}B NMR and ^{29}Si NMR [20].

In siloxanes both ^{13}C NMR and ^{1}H NMR would normally show quite similar chemical shifts to their analogous purely organic compounds, with the greater exception to those carbon atoms (and also for ^{1}H NMR, hydrogens atoms attached to such carbon atom) which are directly attached to the silicon. Such carbon normally will have a significantly smaller chemical shift (usually close to 0) as the neighbouring silicon will effectively supply the carbon with the shielding electrons. For those carbon atoms which are situated further from the silicon, this effect gets smaller with the distance, and on a γ-carbon atom it usually does not have any significant effect.

However, a precise identification of the various components is quite difficult due to the large overlap of the signals, as well as the broadening mechanism due to polymeric entanglements [20, 86-92].

2.3.6 Polymeric Copolymerization Candidates

PDMS based polysiloxanes have already successfully formed the base of soft elastomers for a number of decades, but the mechanical properties are often significantly lower than in purely organic rubbers, because of the near-absence of intermolecular attraction at room temperature between polymolecules. The main technological approach to achieve an acceptable level of such mechanical properties as tensile strength in PDMS-based polymers was the introduction of reinforcing filler (usually silica fines). Also, such a siloxane polymer should be built on a base of polymolecules much larger than in conventional organic polymers. For example an effective polyurethane elastomer may contain molecules on average of only ~5,000 g/mole, when for a PDMS-based elastomer a molecular mass of ≥100,000 g/mole is essential. Also, if any rheologic heterogeneity is introduced to PDMS (say the formation of poly-(boron)$_n$-(siloxane)$_m$) this makes the resulting polymer significantly less processable). Hence, the final price of such elastomeric material may be too high to be competitive.

A possible option to obtain a polymer with simultaneously acceptable rheological properties, mechanical properties and convenient technology is the copolymerization of polyboron-PDMS with a conventional organic polymer to form an elastomer. Alternating "hard block" - "soft block" structures have already proven to be suitable to increase the mechanical properties of many polymers. Generally, a polymer containing bulky and polar junctions could play the role of a reinforcing filler in a soft PDMS polymer [94]. But as shown earlier, in an organic-siloxane copolymer, siloxane normally loses its unique mechanical properties, in proportion to the amount of the organic phase of the polymeric segment in the resulting copolymer.

Alternatively, it may be possible to form an effective IPN based on a cross-linked poly-(boron)$_n$-(siloxane)$_m$ network with an acceptable cross-linked network of polymer with suitable mechanical properties. In such IPN, the network of polyboron-PDMS would be free enough to exhibit the unique rheological properties, where the second polymeric network would play a role of the polymeric matrix with sufficient mechanical properties. But since PDMS is highly incompatible with any other existing polymer and also exhibits enormous flexibility in the backbone chain, such PDMS based uncross-linked IPN may undergo to a phase separation [20].

Therefore at this stage, an achievable option looks like the formation of a scarcely cross-linked IPN (semi-IPN) of poly-(boron)$_n$-(siloxane)$_m$ network with a flexible cross-linked polymeric network, which is able to perform the role of a polymeric matrix with suitable mechanical properties.

Currently, polyurethane is the most prominent candidate to form the matrix polymeric network for such semi-IPN. This polymer is slightly more expensive than other similar polymers (i.e., natural rubber), but instead it forms an enormous variety of products (i.e., forms a very soft and flexible elastomer, or a fibre comparable with an aramid, etc). Also this polymer is relatively easy to form into a flexible cross-linked elastomeric network, which can exhibit a very high tear resistance up to 1 GPa [95].

2.3.7   Chemical Properties of Polyurethanes

Generally all polyurethanes are based on a reaction between reactive isocyanate $RN=C=O$ and R^1OH reactive hydroxyl ends.

The reaction occurs at elevated temperatures from 70 °C to 180 °C and depends on the isocyanate reactivity, geometry and choice of catalyst.

Another important reaction for the formation of polyurethane polymer is that of a primary amine with an isocyanate, which gives a substituted urea:

$$R^1NH_2 + RN{=}C{=}O \rightarrow R^1NH\text{-}CO\text{-}NH\text{-}R \text{ (substituted urea)} \qquad (56)$$

No less important is the reaction of isocyanate with water:

$$RN{=}C{=}O + H_2O \rightarrow R\text{-}NH\text{-}CO\text{-}OH \rightarrow RNH_2 + CO_2 \qquad (57)$$

where a molecule of unstable carbamic acid breaks readily and gives a molecule of carbon dioxide and a molecule (reactive end) of primary amine, which is able to further react with an isocyanate to give a urea link, as shown in Figure 43:

$$R^1NH_2 + RN{=}C{=}O \rightarrow R^1NH\text{-}CO\text{-}NH\text{-}R \text{ (substituted urea)} \qquad (56)$$

This is a basic reaction for any foam production. In some foams where it is necessary to achieve a higher level of bubbles, low-temperature boiling point liquids are added to the pre-polymer [96].
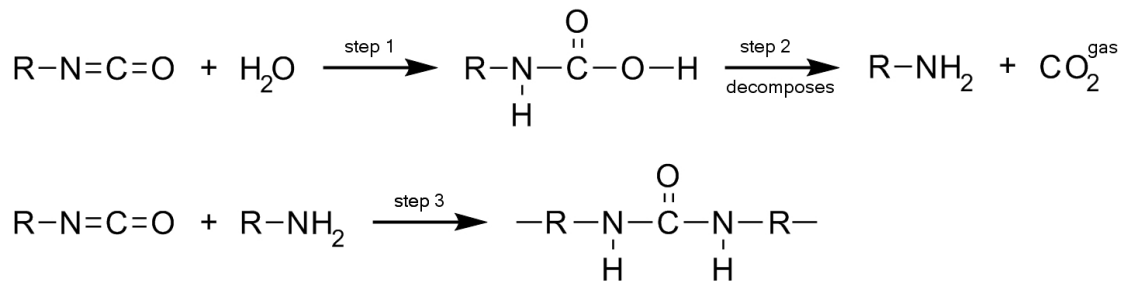
Figure 43: Carbon-dioxide Gas and Polyurea Link Formed by Reacting Water and Isocyanate

A secondary amine such as substituted urea is also able to react with isocyanate. The reaction normally requires a higher temperature than for the reaction between isocyanate and hydroxyl groups. But in the case of the reaction of substituted urea with

isocyanate group, the result is a cross-linked polymer. Therefore, in foam production, it is usual to use a stoichiometry of 1 mole of water to 3 mole of isocyanate [97].

$$R^1NH\text{-}CO\text{-}NH\text{-}R^2 + RN=C=O \rightarrow R^1NH\text{-}CO\text{-}N(R)\text{-}R^2 \qquad (58)$$
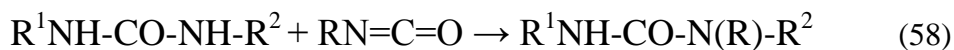
FT-IR is a convenient method for the analysis of these reactions. As an isocyanate gives a finger-print oscillating frequency at 2273 cm^{-1} [98], these spectra progressively decrease, until it disappears upon completion of the reaction. These spectral changes are normally accompanied by the growth of a series of new bands produced by urethane in the 1760-1510 cm^{-1} spectral region [99]. Frequencies at 1760-1720 cm^{-1} spectral region are due to carbonyl $C=O$ vibration absorption, while peaks at ~1580 cm^{-1} and 1510 cm^{-1} are characteristic of the amide $C\text{-}N$ stretching vibration and the in-plane $N\text{-}H$ bending respectively. Urea instead can be easily recognized by spectra at 1630 cm^{-1} and 1577 cm^{-1} [100], and also by UV and visual spectra. Because urea has a strong absorption in the visual spectra up to ~460 nm, it gives an intense yellow colour to a polyureas/polyureas-urethane polymer [92, 95].

The reactivity of isocyanates is higher in more electro-negative aromatic isocyanates $ArN=C=O$ and lower in aliphatics $AlN=C=O$. The reactivity of amines is opposite to this. The aliphatic is more reactive than the aromatic amines since the isocyanate nitrogen accepts hydrogen and the amine donates it [95].

Also different reactive groups have very different ranking orders of the reactivity of compounds towards isocyanate: primary amine > water/primary alcohol > carboxylic acids > ureas > phenol > active CH_2 groups. Additionally, the geometric factors of isocyanate may also play a role in reactivity. For example, toluene 2,4 diisocyanate (2,4-TDI) as shown in Figure 44, has a much higher reactivity for isocyanate 4 than 2. In 2 isocyanate the access is closed by the methyl group attached to the ring. When a hydroxyl reacts with isocyanate it works as a self-catalyst. In the case of 2,4-TDI the access to 2 is more difficult than to the open isocyanate 4 [97].
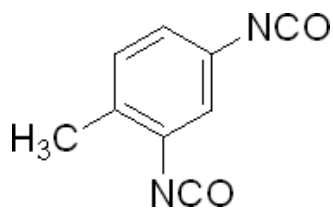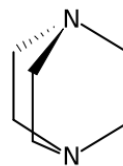
Figure 44: 2,4-TDI   *Figure 45: DABCO*

The use of a suitable catalyst can increase the reactivity of a group by hundreds of times. The most suitable catalysts for polyurethanes are tertiary amines and metal-organic salts, such as organo-tin salts. In some cases the organo-metal salts can speed the reaction a couple of thousand times. (If the reaction is reversible the catalyst accelerates the reaction in both directions.) The reaction mechanism catalyzed by a tertiary amine is shown in Figure 46.

Since the experiments in this work used reasonably unreactive aliphatic diisocyanates, such as hexamethane diisocyanate (HDI), which normally requires elevated temperatures (about 160-180 °C) to start the reaction, a catalyst was needed. 1,4-diazabicyclo(2,2,2)octane (DABCO) catalyst was used, as is shown in Figure 45. With the use of an acceptable catalyst (or often group of catalysts) aliphatic HDI may be as reactive as aromatic TDI (about 80 °C) [96].
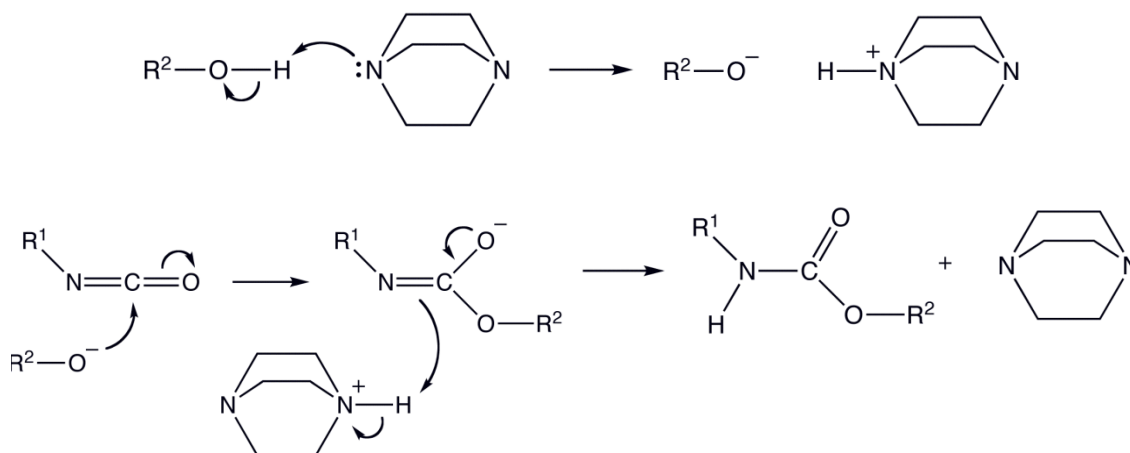
Figure 46: Polyurethane Reaction Mechanism Catalyzed by DABCO

The limitation of the thermal and chemical stability of polyurethanes and polyureas also may not be ignored. An aromatic diisocyanate such as TDI (i.e., without catalyst) requires just ~80 °C to start the endothermic reaction, in comparison with the elevated temperatures required to start the reaction of aliphatic diisocyanates such as HDI or isophorone diisocyanate (IPDI). Also, TDI-based polyurethane links tend to undergo thermal degradation at temperatures of 180-200 °C (in the absence of catalyst), hence it is technologically advisable to avoid formation of a prepolymer built on a base of aromatic diisocyanates (particularly TDI) with a prospect of the further polymerization through aliphatic isocyanates [101].

The presence in the reaction bath of a weak anion such as a tertiary amine will normally speed the polymerization reaction of polyurethane, whereas the presence of a cation may facilitate decomposition of the isocyanate to carbon dioxide and amine [102]. Hence, the presence of 1 molecule of strong acid would be able to decompose up to 500 isocyanate reactive ends [96].

2.3.8   Mechanical Properties of Polyurethanes

The mechanical properties of polyurethanes depend on the isocyanate group. An aromatic isocyanate would normally give more rigid polymers because of the bulkiness and polarity of the ring. A comparably flexible aliphatic group, such as IPDI would give a more flexible polymer.
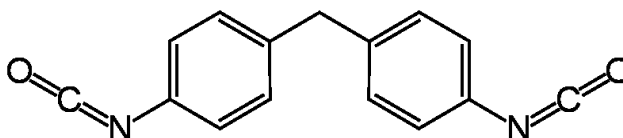
Figure 47: 4,4-MDI

Polymers based on different aromatic isocyanates show different mechanical properties. In general, the most rigid polymers are based on phenyl 1,4-diisocyanate because of its flat and straight molecular geometry. This provides the possibility to obtain a maximum degree of secondary intermolecular forces. While a molecule of 4,4-diphenyl methyl diisocyanate (4,4-MDI), as shown in Figure 47, is not as entirely straight as a

molecule of phenyl 1,4-diisocyanate, 4,4-MDI gives more flexible products due to the presence of a 60° angle on the connecting methylene group.
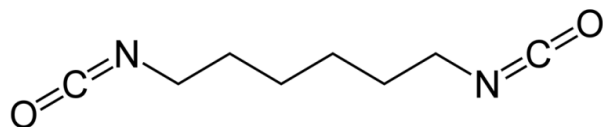
Figure 48: HDI

TDI is a monomer well suited to form soft and flexible foams and elastomers, because it cannot give straight polymeric chains and reduce the degree of crystallinity in the resulting polymer [95]. This is a similar effect to that seen between Kevlar and Nylon, as was discussed in section 2.1.3. Therefore, in some cases a relatively straight molecule of aliphatic HDI, which is shown in Figure 48, can give a resultant polymer with higher tensile strength than a similar polymer based on aromatic TDI [104].
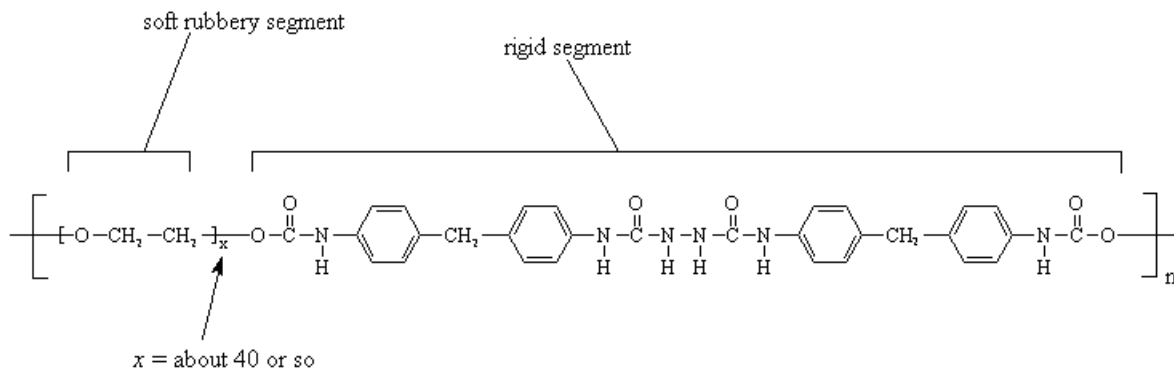
Figure 49: Spandex

Also it is possible to vary the mechanical properties of the polymer by simply varying the proportion (length) of the soft block-copolymer (segment). Hence, a polyurethane polymer containing a higher proportion of bulky and polar urethane segment will have a higher value of tensile strength and lower T_g and T_m than a similar polymer containing a lower proportion of polyurethane and a higher proportion of a soft segment in it. Also urea gives significantly less flexible polymeric link than urethane [103]. A suitable example is Spandex fibres developed by DuPont, as shown in

Figure 49. Spandex has quite a complicated structure, with both urea and urethane polymeric linkages in the backbone chain [96].

An appropriate choice of a suitable soft segment for a polyurethane backbone chain would be no less important for the final mechanical properties, as a flexible isotactic copolymer of polyethylene oxide (PEO) and polypropylene oxide (PPO), shown in Figure 50, will give at room temperature a soft and rubbery product. While long segments of polyether or polyester with repeatable units in the backbone, which tend to a give strong intermolecular interaction (such as tetra-octamethyl polyester) will give a harder and less flexible polymeric material [95].
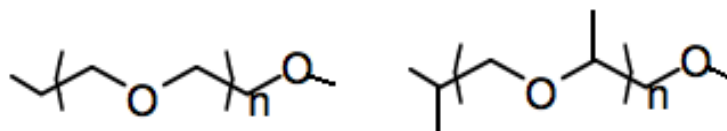
Figure 50: Polyethylene Oxide and Polypropylene Oxide

It is not a general rule in polyurethanes that a polymer with high values of tensile strength or heavily cross-linked product gives a better tear resistance than a soft linear polymer, as in the case of linear soft Spandex which exhibits outstanding tear resistance. It is often convenient to introduce some polyols into the formulation, therefore, to increase the degree of cross-links and to improve the tear resistance and solvent resistance of a final product. A number of such polyols have found applications in polyurethanes. So far, the most important are castor oil, glycerol and sorbitol, as shown in Figure 51. For example, an addition of just 15 % of castor oil by the mass of all the components of the polymerization usually gives about a 50 % rise in the tear resistance [96].
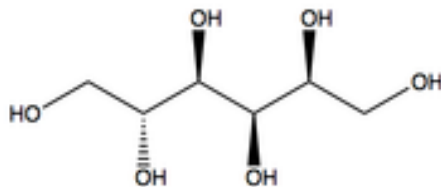
Figure 51: Sorbitol

In the case of an elastic polyurethane polymer, short polyols, like sorbitol or glycerol, with a number of attached urethane groups on it, create "hard" heterogeneous centres in a flexible and amorphous body of a polymer. Therefore, such cross-linked polyurethane polymer would normally behave in a dynamically similar way to a soft polymer with a reinforcing filler. The relaxation spectrum of the resulting polymer is usually relatively wide, but limited to certain values. In the case of stress relaxation above its T_g, such soft heterogeneous polyurethane would also often exhibit relatively high values of $\tan \delta$ (~0.3) [104].

A major technological difficulty with such heavily cross-linked polyurethane structure may be the fact that some bulky urethanes (particularly TDI 4) cannot effectively reach all hydroxyl reactive ends of a hydroxyl-ended polyol $R(OH)_n$. Hence, the right stoichiometry would not be obtained. The right stoichiometry would be even less achievable in the case of the designed reaction between hydroxyls of a polyol $R(OH)_n$ and oligomeric prepolymer isocyanate-ended molecules $(O=C=N-R^1)_n$, where a gelation has taken place.

$$R(OH)_n + (O=C=N-R^1)_n \rightarrow R(O(CO)NR^1N=C=O)_{n-m} + \textit{unreacted } R(OH)_m + \textit{unreacted } (R^1N=C=O)_m \qquad (59)$$
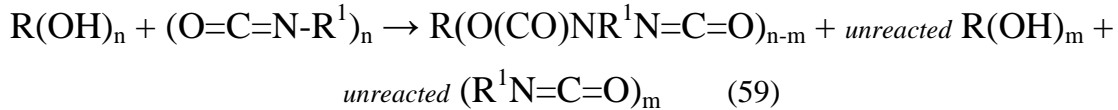
In some cases it is possible to prepare a prepolymer built on a polyol and the number of diisocyanates equal to the functionality of the chosen polyol (i.e., if the polyol is glycerol then it should react with 3 diisocyanate molecules).

$$R(OH)_n + (O=C=N-R^1N=C=O)_n \rightarrow R(O(CO)NR^1N=C=O)_n \qquad (60)$$
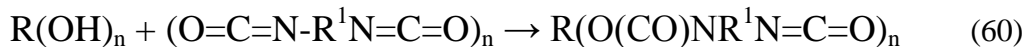
In such a case a multi-functional isocyanate-ended prepolymer can be obtained [101].

2.3.9 Existing Copolymers and IPN Materials of Poly-(urethane/urea-siloxanes)

Copolymers of polyurethane and siloxane are a group of reasonably novel polymeric materials. Now such "soft" and "hard" segmented polyurethanes have found commercial applications as coatings, adhesives, gas and liquid selective permeability

membranes, cosmetics and are particularly important as biomaterials because of their biocompatibility, elasticity and possible high mechanical stability [105]. (Also, a fine example was given in section 2.1.7 in the discussion of the existing novel IPN, i.e., the recent Japanese research on a novel siloxane based IPN material for application in ophthalmology [43].)

Riess et al [106] have developed a polyurea-siloxane segmented copolymer for use in the cosmetic industry based on a reaction between silane γ-primary amine and an isocyanate of HDI.

$$H_2N(CH_2)_3SiMe_2(OMe_2Si)_n(CH_2)_3NH_2 + 2(O=C=N(CH_2)_6N=C=O) \rightarrow$$
$$O=C=N-R-N=C=O \qquad (61)$$
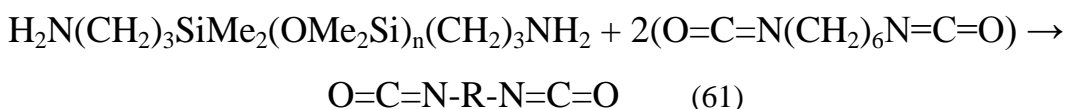
The polymerization was completed by the introduction of aliphatic di-amines and the formation of a poly-(urea-siloxane) polymer:

$$n(O=C=N-R-N=C=O) + n(H_2NR^1NH_2) \rightarrow -R(N(CO)NR^1N(CO)_n- \qquad (62)$$

Riess et al [106] used a number of aliphatic di-amine polymer extenders of different lengths, from short 1,6-hexane di-amine to long prepolymers with molecular mass about 2,000 g/mole. The influence of a "hard" urea segment was reported as gradually decreasing in the obtained block-copolymers with the rise in the proportion of the "soft" aliphatic or siloxane segment.

Epoxy-ended siloxanes are often used in order for a siloxane prepolymer to be chemically attached to an organic copolymer. (An epoxy group is shown in Figure 52.) It is a convenient way to copolymerize an epoxy-ended siloxane with ureas or urethanes, as epoxy readily reacts with primary and secondary amines. The reaction with secondary amines is slower, but gives a cross-linked polymer/prepolymer [107].

Huag et al [20] have synthesized a semi-IPN of siloxane-polyurethane by introducing triethoxysilil groups into polytetramethylene oxide by the reaction of isocyanatopropyl-triethoxy silane with the free hydroxyl-groups on the polytetramethylene oxide. This material was further mixed with tetraethoxysilane and

hydrolyzed under careful conditions in a sol-gel system to produce a range of novel organic/inorganic hybrid materials.
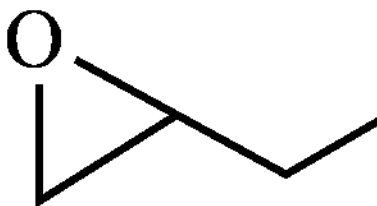
Figure 52: Epoxy Group

More recently, Pathak et al [108] synthesized a siloxane-polyurethane waterborne coating for protecting the surface of metallic alloys from the aggressive conditions of sea water. The short siloxanes chosen for this polymerization had 3 functional methoxy groups ($-Si(OMe)_3$) and 1 epoxy group ($(OMe)_3Si(CH_2)_5OCH_2(C_2H_3O)$) attached to a silicon atom through the δ-ether bridge. Those epoxy-ended siloxanes were allowed to react with amine groups of the polyurethane prepolymer. The obtained siloxane-urethane prepolymer was further hydrolyzed to form a coating. But also, even where a siloxane polymer is not predicted to come into contact with water (i.e., electronics), there are other applications for some polyester materials containing siloxy-bridges ($-SiMe_2$-$O-CH_2$-) in their backbone [109].

Nunes et al [110] studied vibrational IR spectra and the microstructure of polysiloxane organic hybrids doped with metal-organo salts. The results of these experiments on polysiloxane organic/inorganic hybrid IPN/semi-IPN materials led to the formation of an entire range of different polymers, from clear and light-transparent polymers to absolutely opaque ones. A homogenous polymer tends to be clear and light transparent, while heterogeneous polymers are opaque because of light dispersion by the numerous phase separations in such a polymeric body.

Also the IR spectra of the carbonyl and amine groups in the urethane cross-links of the polymer had slightly different oscillating frequencies than in a purely amorphous polymer. Normally the $C=O$ bond of urethane has an absorption at 1762 cm^{-1} band where no hydrogen bond is present, 1720 cm^{-1} in the presence of a hydrogen bond and

finally at 1692 cm^{-1} in ordered hydrogen/(cation)-bonded aggregates. In a secondary amine of a urethane group the normal absorption frequency of amide C-N stretching drops from 1737 cm^{-1} to a 1714 cm^{-1}, and the in-plane N-H bending drops from 1574 cm^{-1} to a 1520 cm^{-1} in the presence of strong hydrogen bond.

3 Experimental Strategy behind this Research Project

The work conducted during the process of the investigation consisted of a group of interconnected studies. The overall experimental strategy that was undertaken to achieve the project aims is summarised in Figure 53. The aim of the Experimental Phase 1 (as shown in Figure 53) was to form an effective shear thickening poly-(boron-siloxane) polymer. Heterogeneous polysiloxane normally includes a cross-link that involves the incorporated tri-functional boron atoms. Therefore, boron-polysiloxane tends to create a polymeric network when the number of boron substitutions in the polymeric backbone is sufficiently high. The heterogeneous boron-polysiloxane polymeric network gives a soft "liquid like" material under the application of relatively slow deformations. However, during fast deformation this material exhibits a non-Newtonian liquid behaviour and shows complex relaxation dynamics including molecular entanglements and hydrogen bond rearrangements.

The literature review has shown some critical cases where a high number of heterogeneous substitutions (i.e., incorporation of bulky, inflexible or polar groups) in a flexible polymeric backbone could significantly decrease flexibility of such a polymeric backbone (i.e., in this project PDMS). Therefore, such a resulting polymer can be predicted to no longer to give a soft and flexible polymer with "liquid like" behaviour. Additionally, according to the theoretical model of Indei and others [64, 65], such polymers may also no longer be able to exhibit shear thickening behaviour, as a significantly increasing tension of the polymeric backbone could lead to strictly shear thinning behaviour. Therefore, in order to be an effective shear thickening polymeric material, poly-(boron-siloxane) should be a soft and a flexible polymeric material able to exhibit "liquid like" behaviour at slow deformation rates.

As siloxanes often give polymeric materials with insufficient tear resistance [20], it was decided that such a poly-(boron-siloxane) soft polymeric network could be further incorporated into a non-siloxane based polymeric network in order to give the acceptable final mechanical properties. Such a protective non-siloxane based polymeric network should not restrict the "liquid like" behaviour found in a poly-(boron-siloxane) network, as it would inevitably restrict its shear thickening effect. Therefore, both polymeric

networks may be incorporated into interpenetrating polymeric networks (IPN), where both polymeric networks are not chemically cross-linked, but also are unable to undergo a separation [37].
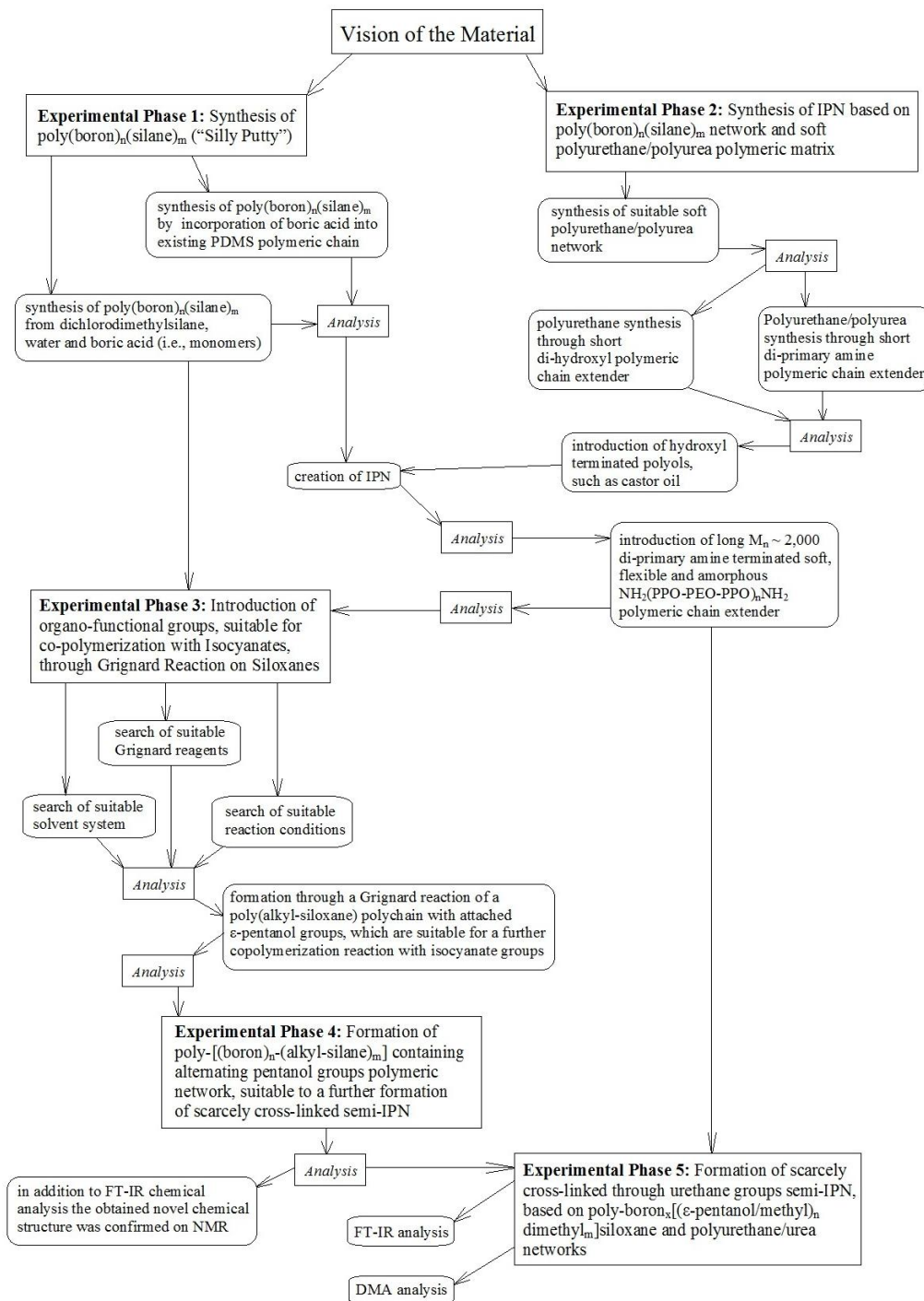
Figure 53: *Schematic Diagram Representation of the Key Stages of the Experimental Strategy behind this Research Project*

An essential requirement for the formation of a successful IPN is the fact that at least one of the polymeric networks must be at least partially formed before the formation of IPN (i.e., final polymerisation/copolymerization) [38]. As polyurethane soft block polymers are able to exhibit high tear resistance and readily form soft polymeric networks at an acceptable temperature range under mild chemical conditions (i.e., for PDMS based polymers), a soft polyurethane cross-linked network was selected to be the second component of the IPN in Experimental Phase 2. (Analytical technique which was used in order to compare possible mechanical properties of the obtained polyurethane/urea elastomers is discussed in section 3.1.)

A number of attempts in Experimental Phase 2 to synthesise the IPN based on fully cured polyborosilane and partially cured polyurethane (where polyurethane was finally cured during formation of the IPN) proved unsuccessful, as the soft and immiscible polyborosilane (based on PDMS) tends to phase separation. Hence, the decision was taken to introduce some chemical cross-links between these two immiscible polymeric networks of the IPN.

The chemical cross-links were successfully introduced by modification of the PDMS based polyborosilane, where some of the methyl groups that were attached to the polymeric siloxane backbone were substituted by ε-pentanol groups by using Grignard reaction, as shown in Figure 53, in Experimental Phase 3. The ε-pentanol groups are active hydroxyl groups attached to olefin and are therefore suitable for use for further copolymerization reaction with isocyanates of a polyurethane polymeric network. The resulting polymeric structure was confirmed by FT-IR analysis (FT-IR chemical analytical technique is discussed in section 3.2).

In Experimental Phase 4 (as shown in Figure 53), boron polymeric chain substitutions were successfully incorporated into the polymeric backbone of the poly-(alkyl-siloxane) with attached alternating ε-pentanol groups (that was obtained in Experimental Phase 3). FT-IR analysis showed that there was no visual decrease in the magnitude of the absorption in the fingerprint of ε-pentanol groups in the infrared absorption spectrum of the obtained oligomeric/polymeric borosiloxane material. Hence, the proportion of the lost ε-pentanol groups can be neglected. Additionally, this novel

polymeric structure was confirmed by ^{1}H NMR and ^{13}C NMR spectra (NMR chemical analytical technique is discussed in section 3.2).

In Experimental Phase 5, the resulting polyborosiloxane with the attached polychain alternating ε-pentanol groups and soft polyurethane/urea polymeric networks were successfully copolymerized in THF/methyl-ethyl ketone solvent system, where the solvent system was then slowly evaporated at room temperature. This approach was adopted in order to avoid producing a foam-like polymeric system (i.e., the presence of a solvent with low-boiling temperature may act as a blowing agent leading to the creation of a foam).

The obtained scarcely cross-linked IPN was further analysed by dynamic mechanical analysis (DMA, this analytical technique is discussed in the Literature Review, section 2.2.2). The DMA test was used to analyse dynamic behaviour of the obtained samples of poly-(boron$_n$-dimethylsilane$_m$-urea/urethane) from Experimental Phase 5, a sample of polyurethane soft elastomer which is appropriately similar to the polyurethane matrix used in the formation of those semi-IPN samples and, in addition, a random sample of silica-fines reinforced natural rubber (i.e., natural rubber reinforced by silica-fines is a heterogeneous polymeric system). By the comparison of the dynamic behaviour of the pure polyurethane matrix with the scarcely cross-linked IPN containing high polyborosilane proportion (up to 50 % of the polymer's mass) it was possible to estimate the actual effect in the polymeric relaxation caused by the polyborosiloxane incorporation. In addition, the comparison of the dynamical behaviour of the pure polyurethane matrix and the sample of a reinforced natural rubber shows very strong similarities in the relaxation processes in those chemically different soft and heterogeneous polymeric systems (i.e., conglomerates of rigid urea and urethane groups normally behave as a kind of reinforcing filler inside soft polyurethane elastomers [101]).

3.1 Analytical Techniques Used in Order to Compare Mechanical Properties of the Obtained Polyurethane/urea Elastomers

In order to compare the essential mechanical properties of the number of the polyurethane/urea elastomers obtained in Experimental Phase 2 were introduced two separate mechanical tests.

The first mechanical test was designed to compare possible tear resistance of the obtained polyurethane samples. In the Literature Review was discussed that possible tear resistance of a soft elastomer depends on the number of introduced cross-links into the polymer. Chemical cross-links tend to be permanent and usually stay until the polymer starts to disintegrate chemically. By contrast physical cross-links are polymolecular entanglements which tend to disintegrate (or rearrange in a case of a strong polar bond) with time. An elevated temperature accelerates such a process of disintegration and/or rearrangement of polymeric entanglements [19].

Therefore, a possible tear resistance of a soft polyurethane elastomer cross-linked predominantly by chemical cross-links tends to be higher than in a polymer predominantly cross-linked by physical cross-links [101]. Hence, introduced in this research tear resistance test was designed to compare possible tear resistance of the obtained polyurethane elastomers under a uniaxial stress applied for a relatively long time (120 s). Therefore, it was possible to estimate the proportion of the introduced into the polymer chemical cross-links (i.e., degree of polymerization [17]). Therefore, all the obtained (synthesised) in this project polyurethane elastomers after been fully cured and dried out of solvent, were cut in 20 mm length and 5 mm / 5 mm cross-section strips and a vertical load was applied for 120 s, as shown in Figure 54.
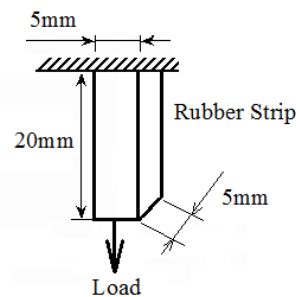
Figure 54: *Schematic Drawing of the Introduced Tear Resistance Test*

The polyurethane samples with a high proportion of physical cross-links (i.e., based on short polymeric chain extenders [97]) and reasonably low degree of polymerization tended to tear (at room temperature) at very low magnitude stress ≤ 0.058 MPa (150 g of the applied load). By a contrast, when later on in the research, the proportion of physical cross-links was effectively reduced (i.e., introduction of long and flexible polymeric chain extenders based on polypropylene-oxide and/or polyethylene-oxide, etc) and the degree of polymerization was sufficient, such samples tended to deform but withstood without tearing up to 3.14 MPa (8 kg of the load) of the applied uniaxial stress. These results are in good agreement with literature [101].

The second mechanical test was designed to compare the possible hardness of the obtained polymeric samples. As the final application of the developing polymer is a soft and flexible polymeric material which is suitable for a body protection in the sport of fencing, a hardness test based on the standard industrial A Shore durometer test was chosen. This hardness test measures the depth of an indetation in a polymeric soft elastomer created by a hardened steel rod (1.1 mm diameter, with a truncated 35° corner, and a spherical edge of 0.79 mm diameter, as shown in Figure 55) and applied force of 8.064 N [111]. The depth of indentation is dependent on the hardness (i.e., storage modulus G', as discussed in the Literature Review, section 2.2.2) of the material. In order to eliminate/minimize possible polymeric viscoelastic effects (i.e., loss modulus G'') during this test, the force was applied in a consistent manner, without shock and the force was continuously applied for 30 s before the measurements were taken. These samples of the material were uniformly 6.4 mm thick.
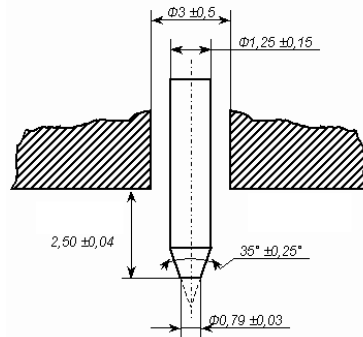
Figure 55: Steel Rod of A Shore Durometer's Test

This durometer test gives quite limited information, as it gives only information of the possible storage modulus values. In addition, the experimental data obtained from the A Shore test (where Sh is the obtained A Shore hardness) was converted into the storage modulus G' data by semi-empirical approximate relation:

$$G' = 0.0981(56 + 7.6234\ Sh)\ /\ 0.1375(254 - 2.54\ Sh) \qquad (63)$$

This gives quite limited information of the possible mechanical properties of the obtained polymers. On the other hand, it was the most time-effective method (due to the time-limitation of the project), which enable to compare the properties of the numerous polyurethane samples obtained in Experimental Phase 2. (Therefore, the final samples of semi-IPN obtained in Experimental Phase 5 were fully analysed by DMA [111].) In addition, those two chosen mechanical test have limitation - as cannot be applied to compare mechanical properties of soft gels (i.e., polyborosiloxanes) [112].

3.2 Main Chemical Analytical Techniques Used in this Research

Infrared spectroscopy (IR spectroscopy) deals with the infrared region of the electromagnetic spectrum that is light and has a longer wavelength and lower frequency than visible light. A Perkin-Elmer Varian 800 FT-IR spectrophotometer was used in this investigation. This equipment was capable of recording a mid-infrared spectrum of a wavelength range from 4000 cm^{-1} to 400 cm^{-1}.

Infrared spectroscopy exploits the fact that molecules absorb specific frequencies that are characteristic of their structure. These absorptions are resonant frequencies (i.e., the frequency of the absorbed radiation matches the frequency of the bond or group that vibrates). The energies are determined by the shape of the molecular potential energy surfaces, the mass of the atoms and the associated vibronic coupling. The simplest and most important IR bands arise from the "normal modes," the simplest distortions of the molecule. In some cases, "overtone bands" are observed. These bands arise from the absorption of a phonon that leads to a doubly excited vibrational state. Such bands appear at approximately twice the energy of the normal mode and are always much smaller in magnitude, but sometimes could be very informative as often lay in the area free of other absorption peaks.

The infrared spectroscopy technique works almost exclusively on samples with covalent bonds and if the molecule is symmetrical, for example such as N_2, the band is not observed in the IR spectrum, but only in the Raman spectrum.

Fourier transform infrared (FT-IR) spectroscopy is a measurement technique that allows one to record such infrared spectra. Infrared light is guided through the sample and then through an interferometer. A moving mirror inside the apparatus alters the distribution of infrared light that passes through the interferometer. The signal directly recorded, called an "interferogram", represents light output as a function of mirror position, as shown in Figure 56. Here a beam of infrared light is produced, passed through an interferometer, and then split into two separate beams. One beam passes through the sample and the other through a reference sample. The beams are both reflected back towards a detector, however first they pass through a splitter which quickly alternates which of the two beams enters the detector. The two signals are then compared

and a printout is obtained and such a "two-beam" setup in the result gives very accurate spectra [5, 26].
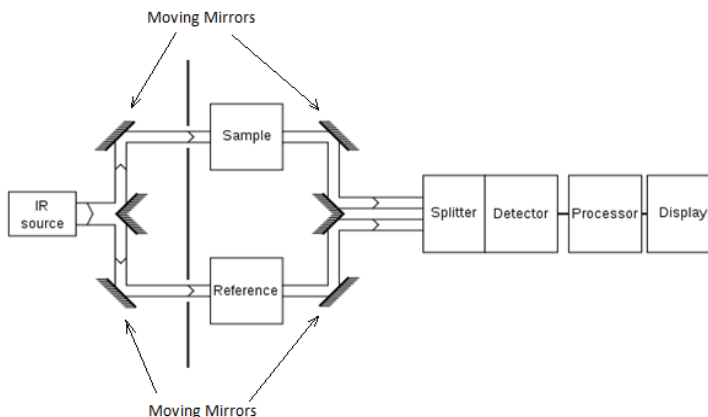
Figure 56: Schematics of a Two-beam Absorption Spectrometer

Nuclear magnetic resonance (NMR) spectroscopy is no less an important analytical tool in this project. NMR spectroscopy is a research technique that exploits the magnetic properties of certain atomic nuclei which can absorb radio-frequency energy when placed in a magnetic field of a strength specific to the identity of the nuclei. Resonant absorption by nuclear spins will occur only when electromagnetic radiation of the correct frequency is being applied to match the energy difference between the nuclear spin levels in a constant magnetic field of the appropriate strength. When this absorption occurs, the nucleus is described as being "in resonance". Different atomic nuclei within a molecule resonate at different frequencies for the same magnetic field strength. The observation of such magnetic resonance frequencies of the nuclei present in a molecule allows the chemical and structural identification of the molecule. So, when placed in a magnetic field, NMR active nuclei, such as ^1H or ^{13}C (about 1 % of all C) absorb electromagnetic radiation at a frequency characteristic of the isotope. The resonant frequency, energy of the absorption and the intensity of the signal are proportional to the strength of the magnetic field.

It might appear from the above that all nuclei of the same nuclide would resonate at the same frequency. However, this is not the case. The most important perturbation of the NMR frequency for applications of NMR is the "shielding" effect of the surrounding electrons. In general, this electronic shielding reduces the magnetic field at the nucleus

(which is what determines the NMR frequency). This shift in the NMR frequency due to the electron molecular orbital coupling to the external magnetic field is called chemical shift and it explains why NMR is able to probe the chemical structure of molecules which depends on the electron density distribution in the corresponding molecular orbitals. If a nucleus in a specific chemical group is shielded to a higher degree by a higher electron density of its surrounding molecular orbital, then its NMR frequency will be shifted "upfield" (that is, a lower chemical shift), whereas if there is less shielding by such surrounding electron density, then the NMR frequency will be shifted "downfield" (that is, a higher chemical shift).

Depending on the local chemical environment, different protons in a molecule resonate at slightly different frequencies. Since both this frequency shift and the fundamental resonant frequency are directly proportional to the strength of the magnetic field, the shift is converted into a field-independent dimensionless value known as the chemical shift. The chemical shift is reported as a relative measure from some reference resonance frequency. (For the nuclei ^1H, ^{13}C and ^{29}Si, tetramethylsilane is commonly used as a reference.) This difference between the frequency of the signal and the frequency of the reference is divided by the frequency of the reference signal to give the chemical shift. The frequency shifts are extremely small in comparison to the fundamental NMR frequency. A typical frequency shift might be 100 Hz, compared to a fundamental NMR frequency of 100 MHz, so the chemical shift is generally expressed in parts per million (ppm).

By understanding different chemical environments, the chemical shift can be used to obtain some structural information about the molecule in a sample. For example, for the ^1H-NMR spectrum for ethanol (CH_3CH_2OH), one would expect three specific signals at three specific chemical shifts: one for the CH_3 group, one for the CH_2 group and one for the OH group. A typical CH_3 group has a shift around 1 ppm, a CH_2 attached to an OH has a shift of around 4 ppm and an OH has a shift around 2-3 ppm depending on the solvent used. The shape and size of peaks are indicators of chemical structure too. In the example above: the proton spectrum of ethanol, the CH_3 peak would

be three times as large as the OH. Similarly the CH_2 peak would be twice the size of the OH peak, but only 2/3 the size of the CH_3 peak, because of number of H involved.

In addition, some of the most useful information for structure determination in a NMR spectrum comes from a spin-spin coupling between NMR active nuclei. This coupling arises from the interaction of different spin states through the chemical bonds of a molecule and results in the splitting of NMR signals. And coupling to n equivalent (spin ½) nuclei splits the signal into a $n + 1$ multiplet with intensity ratios following Pascal's triangle. For example, in the proton spectrum for ethanol described above, the CH_3 group is split into a triplet with an intensity ratio of 1:2:1 by the two neighbouring CH_2 protons and the CH_2 is similarly split into a quartet with an intensity ratio of 1:3:3:1 by the three neighbouring CH_3 protons [5, 23].

4 Experiments

4.1 Experimental Phase 1: Synthesis of Heterogeneous Poly-(boron$_n$-siloxane$_m$) Network

Experimental: All chemicals were purchased from Sigma-Aldrich Fluka Europe supplier and used without further purification, the FT-IR analyses were performed on Perkin Varian 800 FT-IR equipment.

4.1.1 Experiment 1: Hydrolysis of Dichlorodimethylsilane and Subsequent Formation of Heterogeneous Poly-(boron$_n$-siloxane$_m$) Gel

Reagents: Dichlorodimethylsilane (Fluka 80430), distilled water and boric acid (Sigma B7901).

Procedure: First, 20 ml of distilled water and 3.87 g of dichlorodimethylsilane were stirred in an ice cold 50 ml conical flask at 50 rpm for 2 minutes. The reaction is fast and exothermic:

$$n\ [Si(CH_3)_2Cl_2] + n\ [H_2O] \rightarrow [Si(CH_3)_2O]_n + 2n\ HCl \qquad (64)$$

The organic layer was carefully separated by diethyl ether (Et$_2$O) and further washed in a saturated sodium chloride solution ("brine") and further separated by Et$_2$O.

Further, the siloxane and Et$_2$O solution was mixed with 0.12 g of boric acid in a 100 ml conical flask (i.e., proportion of Si ~15 B). The flask was placed on a magnetic stirrer hot plate and the components were mixed at 70 rpm for 5 minutes using a magnetic stir bar.

The mixture was heated gradually to 160 °C and the temperature was kept constant for 15 minutes. The mixture did not become more viscous during these 15 minutes, so the process was continued by raising the temperature to 180 °C with 15 minutes dwelling and then raised further in the same way up to 205 °C. When the gelation process based on the reaction between siloxane and boric acid had occurred (at ~205 °C) (as shown in Figure 57), the magnetic stir bar stopped turning in the flask and kept vibrating. The gel-resin was ready.
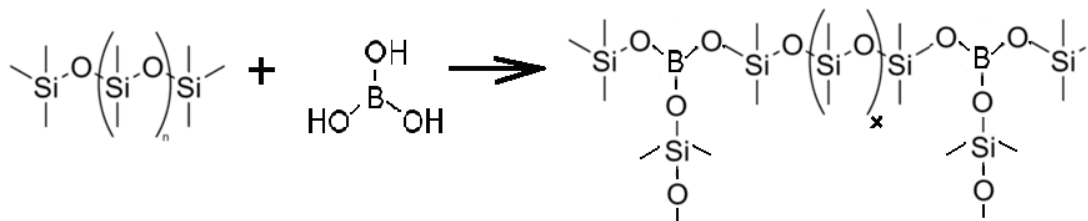
Figure 57: Gelation Process Based on the Reaction between Siloxane and Boric Acid

Results: A soft grey/colourless opaque polymeric gel, FT-IR absorption weak peaks at 2573, 2499 and 2410 cm^{-1} suggest the presence of (Si-O-B) bonds.

An analogous experiment was run but with one change. Boric acid was dissolved in 20 ml of distilled water before being mixed with siloxane. After completion of the gelation, the water and unreacted boric acid were washed away with more distilled water.

The resulting gel was more light-transparent and less opaque. Therefore, in the first case the opaque resulting polymeric gel had a heterogeneous structure with possible incorporations of boric acid crystals, while in the second case the boron-siloxane gel contained boron links in the polymeric backbone and a significantly lower concentration of unreacted boric acid.
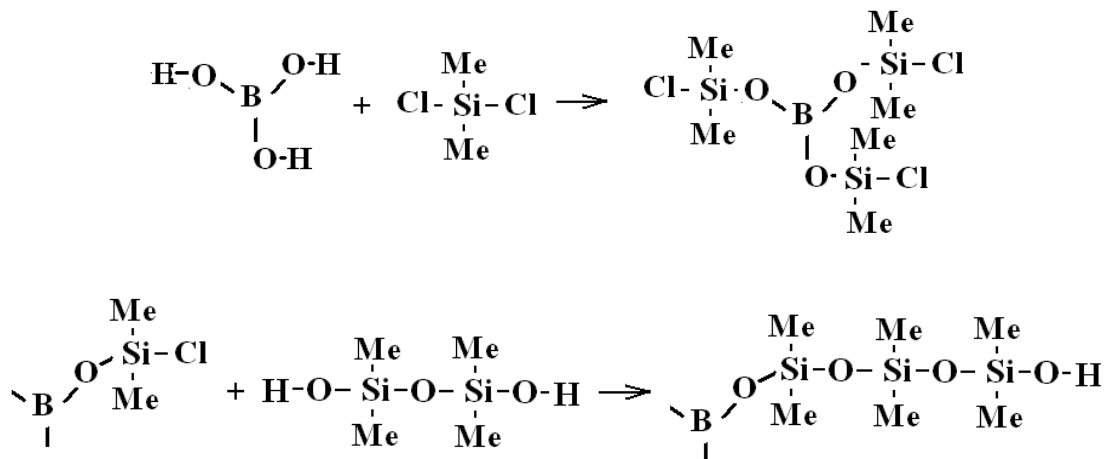
Figure 58: Gelation Process Based on the Simultaneous Reaction between Dichlorodimethylsilane, Boric Acid and Water

4.1.2   Experiment 2: Direct Polycondensation of Heterogeneous Poly-(boron$_n$-siloxane$_m$) Gel from a Dichlorodimethylsilane, Distilled Water and Boric Acid

As a chlorosilane can react with a hydroxyl group attached to boron in the same way as it reacts with a molecule of water, it is possible to introduce boric acid directly into poly-hydrolysis reaction of di/tri-chlorosilanes. The result is a gel-putty of a heterogeneous siloxane, as shown in Figure 58.

Reagents: Dichlorodimethylsilane (Fluka 80430), distilled water and boric acid (Sigma B7901).

Procedure: First, 20 ml of diethyl ether, 0.12 g of boric acid (0.009 mole), 3.87 g of dichlorodimethylsilane (0.03 mole) and 40 ml of distilled water were stirred together at 50 rpm in an ice cold 100 ml conical flask. The mixture was stirred for 2 minutes. The reaction is fast and exothermic. This polycondensation reaction led to the appearance of a colourless/grey water emulsion containing hydrochloric acid, unreacted boric acid and heterosiloxane gel diluted in diethyl ether.

Further, the temperature was risen to 40 °C for 10 minutes to allow for any excess of diethyl ether and hydrochloric acid to evaporate. As a result, a grey hydrophobic siloxane putty formed on the bottom of the flask, where a water solution of hydrochloric and boron acids formed as a top layer.

In order to remove any remains of hydrochloric acid, the boron-siloxane putty was repeatedly washed in a saturated sodium bicarbonate solution and distilled water. The putty was then dried at a room temperature for a week.

Results: As in Experiment 1 a soft grey/colourless opaque polymeric gel was obtained, FT-IR absorption weak peaks at 2573, 2499 and 2410 cm^{-1} suggest the presence of (Si-O-B) bonds.

4.1.3   Experiment 3: Direct Polycondensation of Heterogeneous Poly-(boron$_n$-siloxane$_m$) Gel with Different Concentrations of Boric Acid in the Reaction

The reagent and procedures were identical to Experiment 2. Hetero-boron-polysiloxane was formed with varying boron-silicon proportions.

The results are given in Table 5, the data of the possible mechanical properties such as tear resistance and storage modulus G' was obtained by the techniques discussed in the Experimental Strategy, section 3.1.

Table 5: *Results of Experiment 3, where the Atomic Ratio of Boron to Silicon in the Polymeric Siloxane Backbone Varied from 1:6 up to 1:18*

Formulation	B : Si proportion				Results		
	Number of Atoms		Mass of Components (g)		Appearance	G'	Tear Resistance
	B	Si	H$_3$BO$_3$	Cl$_2$SiMe$_2$		MPa	MPa
1	1	6	0.3	3.582	brittle resin	≈ 1.56	≈ 0.05
2	1	9	0.3	5.376	resin	≈ 0.76	≈ 0.01
3	1	12	0.3	7.02	gel	*(gel)*	*(gel)*
4	1	15	0.3	8.96	liquid/gel	*(gel)*	*(gel)*
5	1	18	0.3	10.75	viscous liquid	*(liquid)*	*(liquid)*

Because oligo/polyborosiloxanes obtained in this experiment are not additionally chemically cross-linked, therefore they still tend to a viscous flow under a constant stress, hence the mechanical tests explained in Experimental Strategy, section 3.1 cannot be applied effectively. Such a mechanical test results have very limited value as formulations 1 and 2 (i.e., the obtained resins) have not been used any further in this research. (All other obtained here oligomeric gels cannot be analysed by the same technique.)

4.1.4 Experiment 4: Formation of Homogenous Cross-linked Polysiloxane Gel by Introducing Tri-functional Halosilanes into the Reaction Mixture of the Poly-hydrolysis of Dichlorodimethylsilane

As tri/tetra functional halosilanes would lead to a branched or cross-linked siloxane (in some cases to a "ladder" polymer), it is possible to obtain a homogenous cross-linked siloxane gel/polymer [20].

Reagents: Dichlorodimethylsilane (Fluka 80430), methyltrichlorosilane (Sigma M85301) and distilled water.

Procedure: Identical to Experiment 2.

<u>*Results*</u>*:* Homogenous polysiloxane branched oligomeric liquids and a soft polysiloxane elastomer (formulation 3) were formed with varying tri-functional and di-functional chloro-siloxane proportions.

Table 6: *Results of Experiment 4, where the Proportion of Tri-functional and Di-functional Chloro-siloxane in the Polymeric Siloxane Backbone Varied from 1:3 up to 1:9*

Formulation	$Cl_3SiMe : Cl_2SiMe_2$ proportion				Results		
	Number of Groups		Mass of Components (g)		Appearance	G'	Tear Resistance
	Cl_3SiMe	Cl_2SiMe_2	Cl_3SiMe	Cl_2SiMe_2		MPa	MPa
1	1	3	1	2.59	very soft elastomer	≈ 0.28	≈ 0.06
2	1	6	0.5	2.59	viscous liquid	*(liquid)*	*(liquid)*
3	1	9	0.3	2.33	liquid	*(liquid)*	*(liquid)*

Because the soft polysiloxane elastomer obtained in this experiment is extremely soft, the mechanical tests explained in Experimental Strategy, section 3.1 cannot be applied effectively. Such a mechanical test result has a very limited value as formulation 1 (i.e., the obtained soft elastomer) has not been used any further in this research.

Discussion: A mixture of dichlorodimethylsilane and trichloromethylsilane with water gives a highly cross-linked polymer. The similarities of the cross-links in the polydimethylsilane oligomeric/polymeric material built by boric acid and tri-functional silane are strong, particularly as boron is slightly more electro-positive than silicon.
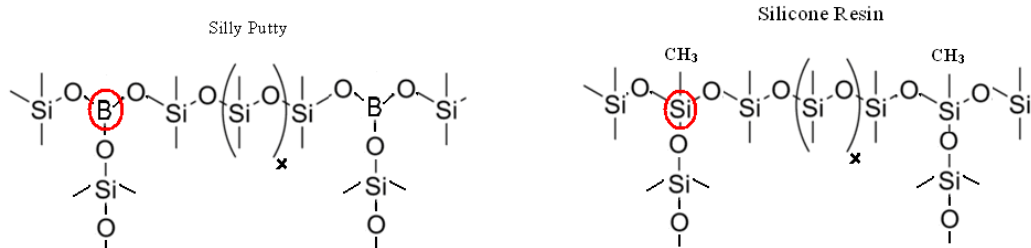
Figure 59: Polymeric Gels Based on Cross-linked Heterogeneous Poly-boron-siloxane and Cross-linked Homogenous Siloxane Resin

The difference between these two branched polymers lies in intermolecular interactions. Boron and silicon atoms are both incorporated into the polymolecule through attachment to three neighbouring oxygen atoms, but boron stays relatively open and tends to form strong hydrogen bonds with neighbouring molecules, where the silicon atom in siloxane is always effectively shielded from other molecules by the methyl/alkyl group, as shown in Figure 59. So, because of the difference in the amount of intermolecular interaction, heterogeneous siloxane cross-linked by tri-functional boron groups gives a significantly harder polymer than a homogenous siloxane with the same number of possible chemical cross-links [23].

4.2   <u>Experimental Phase 2</u>: Synthesis of IPN Based on a Heterogeneous Poly-(boron$_n$-siloxane$_m$) and Soft Polyurethane/urea Polymeric Networks

The byproducts of the reaction of polysiloxane hydrolysis (polycondensation reaction) are hydrochloric acid and water (or alcohols in case of hydrolysis of alkoxy-terminated silanes). It is essential to avoid the presence of a strong acid during formation of polyurethane. Additionally, molecules of water (also hydroxyl-terminated silane) react with isocyanate faster than organo-attached hydroxyl groups, and this reaction leads to the formation of undesirable bubbles of CO_2. The reaction of isocyanate and short (one-side reactive) alcohols leads to a polymeric chain termination [97]. Therefore, in the case of a simultaneous polycondensation reaction in one bath to form polyurethane polymers none of the byproducts of siloxane polycondensation is designed or controllable. Hence, the decision was taken, that the siloxane polymeric network should be completely formed before it is introduced into a polymerization bath of polyurethane, while the polyurethane polymeric network can be just partially formed.

Experimental: All chemicals were purchased from Sigma-Aldrich Fluka Europe supplier and used without further purification, the FT-IR analyses were performed on Perkin Varian 800 FT-IR equipment.

4.2.1   <u>Experiment 5</u>: Formation of a Polyurethane/urea Polymeric Network through a Short Aliphatic Diamine Polymeric Chain Extender

Reagents: Diisocyanate: TDI technical grade 2,4-TDI 80 %, 2,6-TDI 20 % (Aldrich 216836).

Polyols: castor oil $M_n = 340$ (Sigma 259853), polyethylene glycol $M_n = 200$ (PEO $M_n = 200$, Fluka 81150), polyethylene glycol $M_n = 400$ (PEO $M_n = 400$, Fluka 81170), polyethylene glycol $M_n = 600$ (PEO $M_n = 600$, Aldrich 202401).

Chain-extender: 1,6-hexamethylene diamine (Aldrich H11696).

Solvents: ethyl-methyl ketone (2-butanone, Aldrich 48877) 50 % and THF (Aldrich 401757) 50 %. Also before all experiments, the solvents were additionally checked by FT-IR for the presence of water trace (i.e., hydroxyl absorption at 3600-3100 cm^{-1}).

Procedure: In a 50 ml beaker, one polyol at a time and diisocyanate (TDI) were mixed in a ratio of one to two (1:2) according to the number of the reactive-ends (1 hydroxyl group -OH to 2 isocyanate groups O=C=N-). This mixture was stirred for five minutes and heated to 85 °C for two hours.
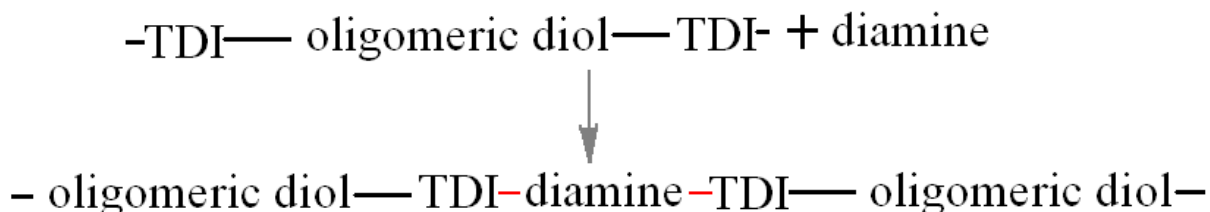
Figure 60: *Polymerization of Linear Polyurethane/urea Polymer through a Diamine Polymeric Chain-extender*

The mixture of isocyanate-ended oligomers was cooled to room temperature and dissolved in the solvent system, and further cooled to 0 °C. Into the solution was added the dissolved ice cold chain-extender 1,6-hexamethylene diamine (the reaction between an aliphatic primary amine and an aromatic isocyanate starts easily at room temperature and is very fast and exothermic [95], the polymerization reaction is schematically shown in Figure 60). The solvent was evaporated at 65 °C for two hours and further under vacuum for 30 minutes.

<u>Results</u>: None of the obtained polyurethane polymers was soft, rubbery and suitable to a further development. All the obtained polymers were hard and brittle. Also the polymers based on castor oil and PEO $M_n = 600$ were slightly softer and less brittle than polymers based on relatively short diols of PEO $M_n = 200$ and PEO $M_n = 400$. The results are given in Table 7.

Discussion:

<u>Formulation 1</u>: As the aim of these series of experiments is to achieve a soft and very flexible polyurethane matrix, therefore any obtained (synthesised) polymeric material which shows brittleness is absolutely unsuitable for a further development. Even though the synthesised in this experiment polyurethane/urea polymer based on castor oil shows slightly better tear resistance and flexibility than polymers based on short liner PEO

$M_n = 200$ and $M_n = 400$, the proportion of the soft polymeric segment may be increased and the short polymeric chain-extender 1,6-hexamethylene diamine could be further changed in order to obtain a softer polymeric matrix.

Table 7: *Results of Experiment 5, where Polyurethane/urea Polymer was Finally Formed by 1,6-hexamethylene diamine Polymeric Chain Extender*

| Formulation | Diisocyanate | Chain-extender | Diol/polyol | Results | | |
				Appearance	G' MPa	Tear Resistance MPa
1	TDI	$H_2N(CH_2)_6NH_2$	castor oil	resin	4.43	0.78
2	TDI	$H_2N(CH_2)_6NH_2$	PEO M_n200	brittle resin	15.53	≈ 0.04
3	TDI	$H_2N(CH_2)_6NH_2$	PEO M_n400	brittle resin	10.62	≈ 0.08
4	TDI	$H_2N(CH_2)_6NH_2$	PEO M_n600	resin	7.05	0.14

Formulation 2: The obtained polyurethane/urea polymer based on short PEO $M_n = 200$ and short polymeric chain-extender 1,6-hexamethylene diamine gave in the result a very brittle resin (i.e., such formulation should be changed), as the proportion of the soft segment was absolutely insufficient.

Formulation 3: The obtained polyurethane/urea polymer based on PEO $M_n = 400$ and short polymeric chain-extender 1,6-hexamethylene diamine gave in the result a brittle resin where the proportion of the soft segment should be significantly increased.

Formulation 4: The obtained polyurethane/urea polymer based on PEO $M_n = 600$ and short polymeric chain-extender 1,6-hexamethylene diamine gave in the result a just slightly flexible resin. Even in this case of slight improvement in comparison with formulations 2 and 3, here the proportion of the soft segment should still be further increased [95-106].

4.2.2 Experiment 6: Formation of a Polyurethane/urea Polymeric Network Based on a Long Linear PEO ($M_n \geq 1000$) and the Polymerization Process Completed through a Short Aliphatic Diamine Polymeric Chain Extender

In order to obtain a softer and more rubbery polyurethane polymer (than polymers which were obtained in Experiment 5) it was decided to increase the proportion of the soft polymeric segment by introducing into the polymer longer polyethylene oxide glycols such as PEO $M_n = 1000$ (Fluka P3515), PEO $M_n = 1500$ (Fluka 243660), PEO $M_n = 3000$ (Fluka 243670) and PEO $M_n = 4000$ (Fluka 243680).

The procedures were similar to Experiment 5, where long PEO oligomers were at first dissolved in the solvent system and introduced into the reaction with short diisocyanate (TDI) (present at twice the molar proportions of PEO used). Further polymerization was completed by the introduction of a short diamine (1,6-hexamethylene diamine).

Results: The obtained polyurethane polymers based on PEO $M_n = 1000$ and PEO $M_n = 1500$ gave rubbery materials, but had insufficient tear resistance. The polymers based on the longer polyethylene oxide blocks PEO $M_n = 3000$ and PEO $M_n = 4000$ tended to form inhomogeneous polymers. The results are given in Table 8.

Table 8: _Results of Experiment 6, where Polyurethane/urea Polymer was Build on Long PEO Blocks ($M_n \geq 1000$) and Finally Polymerized by 1,6-hexamethylene diamine Polymeric Chain Extender_

Formulation	Diisocyanate	Chain-extender	Diol	Results		
				Appearance	G' MPa	Tear Resistance MPa
1	TDI	$H_2N(CH_2)_6NH_2$	PEO $M_n 1000$	resin/ elastomer	1.82	0.16
2	TDI	$H_2N(CH_2)_6NH_2$	PEO $M_n 1500$	elastomer	1.14	0.14
3	TDI	$H_2N(CH_2)_6NH_2$	PEO $M_n 3000$	non-homogeneous elastomer	≈ 0.76	≈ 0.11
4	TDI	$H_2N(CH_2)_6NH_2$	PEO $M_n 4000$	non-homogeneous elastomer	≈ 0.56	≈ 0.06

Discussion: The obtained polyurethane polymers which were based on long polyethylene oxide blocks PEO M_n = 3000 and PEO M_n = 4000 tended to form non-homogeneous polymers, because of the presence of significant crystalline blocks formed by the long and straight sections of linear polyethylene oxide. Therefore, in order to obtain a soft, amorphous and rubbery polyurethane polymer it is necessary to avoid excessively long blocks of homogenous polymeric materials which tend to crystallize at room temperature [17]. Hence, a combination of different kinds of polyols and diols is preferable, such as a combination of linear polyethylene oxide, polypropylene oxide, castor oil, etc. As such a heterogeneous system would be effectively prevented from forming crystalline blocks and will be close to being absolutely amorphous at working temperatures (i.e., room temperature).

From the literature it is also known that introducing some tri-functional castor oil, glycerol or multi-functional sorbitol into the polyurethane formulation should improve the tear resistance of the polymer [95].

In order to obtain soft, amorphous and rubbery polyurethane, all further polyurethane polymers produced have been an amorphous mixture of a few different and relatively immiscible diol and polyol blocks. Therefore, as castor oil does not form crystalline blocks on its own at room temperature nor with TDI, MDI or HDI and long linear polyethylene/propylene oxides [23, 101], it was decided that this tri-functional hydroxyl-ended oligomer may be introduced in the majority of these soft, elastic polyurethane polymeric networks formulations. Also long linear polypropylene oxide (PPO) oligomers are immiscible with polyethylene oxide oligomers [19], so PPO can be used as a combination with PEO in the soft-amorphous segments of such polyurethane polymers.

4.2.3 <u>Experiment 7</u>: Synthesis of Polyurethane Polymers Based on Castor Oil and Different Diisocyanates

Further introduced reagents: 4,4′-Methylene-bis(phenyl isocyanate) (4,4′-MDI, Fluka 33428), 1,6-Diisocyanatohexane (HDI, Sigma 52649).

A number of polyurethane resins were obtained based on castor oil and TDI, MDI, HDI diisocyanates, and the molecular proportion of reactive-ends (functionality) was -OH 1:1 O=C=N-.

Procedure: In a 50 ml beaker, oligomeric castor oil and short diisocyanate were dissolved in the solvent system and stirred for 5 minutes. Further the mixture was heated for 80 minutes to 85 °C (TDI), 125 °C (MDI) and 180 °C (HDI) respectively (polymerization reaction of formation of polyurethane links). The obtained resins were allowed to dry at room temperature for a week.

Results: Polyurethane resins based on castor oil and TDI were slightly softer and had better tear resistance, where resins based on MDI and HDI were comparable. Also, these results are in good agreement with those in the literature [95]. The results are given in Table 9.

Table 9: *Results of Experiment 7, where Polyurethane Polymers were Based on Castor Oil and Different Diisocyanates*

Formulation	Diisocyanate	Polyol	Results		
			Appearance	G' MPa	Tear Resistance MPa
1	TDI	castor oil	resin	2.65	0.75
2	MDI	castor oil	resin	3.19	0.71
3	HDI	castor oil	resin	2.86	0.69

Discussion: Aliphatic diisocyanate HDI does not contain a bulky benzene ring (as compared to TDI or MDI). Because HDI is a straight-chained molecule, the polymer obtained does not increase the free volume (i.e., decrease density) of the polymer and so is able to obtain a high magnitude of intermolecular interaction [95-105]. Therefore, in order to obtain soft rubbery polyurethane material, TDI was chosen as a preferable diisocyanate. (Also in the case of preparation of a pre-polymer based on different kinds of diisocyanates, the final polymerization cannot be based on an aliphatic diisocyanate such as HDI, as it requires an elevated temperature of 180 °C to form such aliphatic

urethane links, where such aromatic diisocyanates in polymeric backbone as TDI may decompose [95].)

4.2.4   Experiment 8: One-step Polyurethane Polymerization Based on TDI and a Heterogeneous Soft Polymeric Segment

A number of polyurethane resins were obtained by one-step polymerization from the given formulations, where the isocyanate-hydroxyl proportion was 1:1.

Formulation 1: (-OH 1:1 O=C=N- *proportion*): TDI (1.74 g), castor oil 30 % (2.1 g), PPO M_n = 425 10 % (0.42 g,), PEO M_n = 400 10 % (0.4 g), PEO M_n = 600 20 % (1.2 g), PEO M_n = 1000 30 % (3 g).

Formulation 2: (-OH 1:1 O=C=N- *proportion*): TDI (1.74 g), castor oil 25 % (1.51 g), PPO M_n = 425 15 % (0.63 g), PEO M_n = 600 20 % (1.2 g), PEO M_n = 1000 30 % (3 g), PEO M_n = 4000 10 % (4 g).

Formulation 3: (-OH 1:1 O=C=N- *proportion*): TDI (1.74 g), glycerol 20 % (0.3 g), PPO M_n = 425 10 % (0.63 g), PEO M_n = 600 20 % (1.2 g), PEO M_n = 1000 30 % (3 g), PEO M_n = 4000 20 % (4 g).

Formulation 4: (-OH 1:1 O=C=N- *proportion*): TDI (1.74 g), sorbitol 30 % (0.3 g), PPO M_n = 425 10 % (0.63 g), PEO M_n = 600 20 % (1.2 g), PEO M_n = 1000 30 % (3 g), PEO M_n = 4000 10 % (4 g).

Procedure: In a 100 ml beaker all components were dissolved in 10 ml of the solvent system and further stirred for 15 minutes. The mixture was heated for 50 minutes at 85 °C. The obtained polymers were further dried for two days at room temperature.

Results: The obtained polyurethane polymers were yellow, slightly light-transparent/cloudy (sample of formulation 3 was particularly cloudy), softer and more rubbery than obtained in Experiment 7, except for those which were based on sorbitol (i.e., formulation 4). Also, the obtained polymers (except formulation 3 and 4) had significantly improved tear resistance. The results are given in Table 10.

Table 10: *Results of Experiment 8, where Polyurethane Polymers were Polymerized by One-step Polymerization from TDI and a Heterogeneous Soft Polymeric Segment*

Formulation	Diisocyanate	Diol M_n	Polyol	Results		
				Appearance	G' MPa	Tear Resistance MPa
1	TDI	high	castor oil	elastomer	0.47	1.06
2	TDI	high	castor oil	elastomer	0.39	1.18
3	TDI	high	glycerol	elastomer/resin	0.96	0.86
4	TDI	high	sorbitol	resin	1.82	0.12

Discussion: These results can be explained by a number of factors: such as, castor oil effectively increases the tear resistance of the polyurethane polymer, and also some small proportion of long prepolymer, when added (as PEO M_n = 4000 is believed creates effective cross-link-bridges between entire blocks of polymolecules). But in case, where such long prepolymer as PEO M_n = 4000 is in high proportion, it tends to form some crystalline blocks even before the gelation process has been completed. That leads to a heterogeneous polymer of poor quality.

In addition, as it was discussed in Literature Review, section 2.3.8, isocyanate 2 of TDI is often unable to react fully (i.e., to reach for the reaction secondary alcohol of sorbitol, glycerol or even castor oil) with secondary alcohol of sorbitol (particularly, when the gelation has already happened), therefore the obtained gel would contain a high proportion of short oligomeric molecules. Such material often gives quite poor mechanical properties [101].

4.2.5 Experiment 9: Two-step Polyurethane Polymerization Based on TDI and a Heterogeneous Soft Polymeric Segment

An additional number of polyurethane resins was produced by two-step polymerization from the same formulations as in Experiment 8, where the isocyanate-hydroxyl proportion (-OH : O=C=N-) was also 1:1.

Procedure: In a 100 ml beaker diisocyanate and polyol (castor oil, glycerol or sorbitol) were dissolved in 40 ml of solvent system and further stirred for 15 minutes. The mixture further was heated for 50 minutes at 85 °C.

Glycerol and sorbitol gave brittle white crystalline prepolymer materials which were not used further.

Prepolymers based on castor oil were further dissolved in 30 ml of the solvent system and mixed with the rest of the polyurethane formulation. The mixture was stirred for 15 minutes and further heated for 50 minutes at 85 °C. The obtained polymers were further dried for two days at room temperature.

Results: The obtained polymers (based on castor oil) were similar to those produced in Experiment 8.

Discussion: An intense yellow colour appeared in the resulting polymers, clearly indicating the presence of a high proportion of urea links [101], which can appear in the reactive system by the reaction of an amine (most probably a primary amine) and isocyanate [23]. As amine groups had been originally absent in the reactive system at the start of the reaction, it means that amine groups were formed during the polymerization reaction. The possible way to form an amine group is a reaction between isocyanate and water [95]:

$$H_2O + O=C=N- \rightarrow H_2N- + CO_2 \qquad (65)$$

Alternatively for a hydrophobic castor oil it may be a reaction of a carboxyl acid group with isocyanate, which also gives a primary amine group and a molecule of carbon dioxide.

Formation of carbon dioxide in the final stages (i.e., gelation) is strictly undesirable, as it would lead to the formation of CO_2 bubbles, which would lead to a non-homogeneous system and reduce such mechanical properties as tear resistance of the final polymer [96]. But, if the formation of any amines may be limited only to during the initial polymerization (i.e., before gelation starts), and the oligomeric mixture is still soft and flexible enough to release all the formed CO_2 gas, such very limited formation of amine can be beneficial, as the formed urea links may improve the tear resistance of the

final polymer. On the other hand, high concentrations of urea and substituted urea links would inevitably lead to a polymer with a high tensile strength and may lead to a polyurethane polymer with insufficient tear resistance.

Unfortunately FT-IR is of very limited help in recognizing traces of moisture in such oligomers as glycerol or sorbitol, as the wide absorption spectrum of hydroxyl of water and hydroxyl attached to a sorbitol or glycerol can interfere as they are in the same absorption area of 3600-3100 cm^{-1}. Experiment 9 was run repeatedly as sorbitol or glycerol had been heated and stirred before the experiment for 5 hours at 130 °C, in order to release all traces of moisture. The resulting prepolymer was still a brittle polymeric resin.

The use of short oligomeric polyols such as sorbitol or glycerol as a final chain-extender can be also very limited. As 2,4-TDI always reacts faster on one side (because of its geometry) then any TDI based prepolymer will be left with unreacted isocyanate partially covered by the neighbouring methyl group. Hence, during gel formation not all such long and bulky 2-TDI-ended prepolymer groups may be able to react with all the hydroxyl groups attached to a bulky sorbitol or glycerol [17]. Also there is quite a low probability that all 2-TDI-ended long oligomeric prepolymer groups would be able to react completely with all the hydroxyl groups attached to castor oil [95]. Therefore, it is desirable to have an isocyanate-ended prepolymer of polyol at the beginning stage of the polymerization process [96].

Castor oil was also checked by FT-IR for the presence of carboxyl groups, which have a wide absorption spectrum at 2800-2200 cm^{-1} [23]. The sample of castor oil used in this experiment did not show any visible absorption at this area. The concentration of carboxyl groups could be extremely low, but at the same time, one carboxyl group is able to change the polyurethane polymerization reaction for a number of isocyanate groups. One carboxyl group reacts with an isocyanate and gives a hydroxyl group and primary amine, where both the resulting hydroxyl group and the resulting primary amine will be involved in the further reactions of polymerization. One primary amine group reacts fast with one aromatic isocyanate and forms a urea group, which may react further to form a substituted urea [97]. Therefore, the original stoichiometry may be lost.

The majority of the sources in the literature on polyurethane suggest the use of a slightly higher proportion of isocyanate than 1:1 (i.e., O=C=N- 1.05 : 1 HO- or O=C=N- 1.1 : 1 HO-) [95-101]. In some applications, such as coatings, it is advisable to use as much as 1.7 isocyanate group to 1 possible reactive hydroxyl group (O=C=N- 1.7 : 1 HO-) [95]. Therefore, at this stage it was decided to start using a higher than 1:1 proportion of isocyanate in the polymeric formulations.

4.2.6 Experiment 10: Multiple Step Polymerization of Polyurethanes Based on Branched Castor Oil, PPO and TDI Prepolymers

In order to obtain a softer and more rubbery polymer with better tear resistance (than in Experiment 8) a number of polyurethane polymers based on a mixture of castor oil/diol copolymers were produced. All the polymerization reaction ingredients (except TDI) were dried at 70 °C for a few days.

Formulation 1: Castor oil (3.4 g) was mixed for 5 minutes with TDI (1.91 g) in a proportion of O=C=N- 2.2 : 1 HO- and allowed to react at 85 °C for 40 minutes. Further the prepolymer was dissolved in the TFH/Et-Me-ketone solvent system (10 ml) and mixed with PPO M_n = 425 (1.1 g) in a proportion 1 PPO diol in 2 castor oil oligomers, in order to obtain prepolymer blocks of PPO M_n = 425 connected through TDI to 2 castor oils, also containing 4 attached unreacted isocyanate groups, as shown in Figure 61.
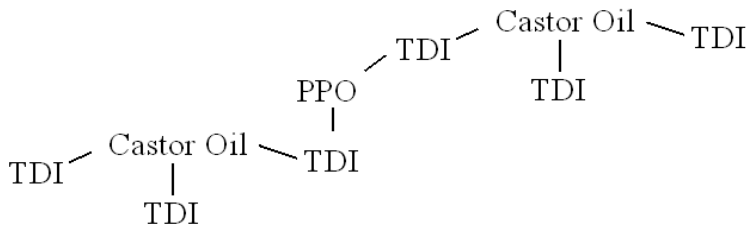
Figure 61: Multiple-isocyanate-ended Prepolymer Based on Castor Oil, TDI and PPO

The oligomeric isocyanate-ended prepolymer was additionally diluted with the solvent system (20 ml) and stirred with PEO M_n = 600 50 % (0.63 g) and PEO

$M_n = 1000$ 50 % (1.05 g). The proportion of O=C=N- : HO- was kept 1.2:1. The mixture was stirred for 10 minutes and heated for 50 minutes at 85 °C. The obtained polymer was further dried for a week at room temperature.

Formulation 2: Castor oil was mixed with TDI (1.39 g) in a molecular proportion of 12 x 5, in order to obtain an isocyanate-ended prepolymer containing 5 castor oil (3.4 g) groups in a row, as shown in Figure 62.
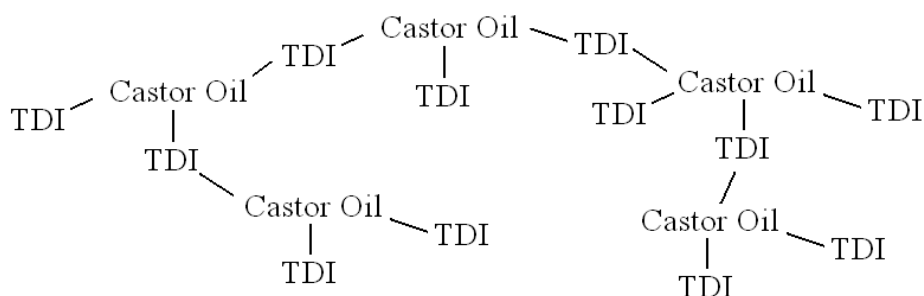
Figure 62: *Multiple-isocyanate-ended Prepolymer Based on Castor Oil and TDI*

The obtained prepolymer was given to react for 50 minutes at 85 °C and further diluted in 10 ml of the solvent system and reacted with PPO $M_n = 425$ 50 % (0.3 g) and PEO $M_n = 1000$ 50 % (0.69 g) as a chain-extender. The overall O=C=N- : HO- proportion was kept 1.2:1.

Formulation 3: In a similar way as in formulation 2, castor oil (3.4 g) was mixed with excessive TDI (1.24 g) in such proportions to obtain 10 castor oil groups in a row connected by TDI. The components were mixed, stirred and allowed to react. The resulting prepolymer formed a rubbery polymer, which was impossible to further dissolve in 70 ml of the solvent system.

Formulation 4: A molar (i.e., active reactive-ends number) mixture of 40 % of PPO $M_n = 425$ (1.06 g), 30 % of castor oil (1.13 g), 25 % of PEO $M_n = 1000$ (1.25 g) and 5 % of PEO $M_n = 3000$ (0.75 g) was dissolved in 10 ml of the solvent system and mixed with 1.74 g of TDI in a O=C=N- : HO- in proportion of 2:1. The solution was further stirred for 15 minutes and allowed to react for 50 minutes at 85 °C. The obtained gel prepolymer was further dissolved in 100 ml of the solvent system and cooled to 0 °C.

In a separate flask, in 70 ml of the solvent system, was dissolved 0.37 g of

1,6-hexamethylene diamine. The molar proportion of the short diamine was of 1 primary amine group to 1.5 isocyanate group of the prepared prepolymer (i.e., because the prepared isocyanate-ended prepolymer already had a yellow colour, and so, inevitably contained some urea groups, an excess of isocyanate groups would be able to further react with urea groups to form substituted urea links).

In an ice bath, in an ice cold 500 ml beaker, both solutions were quickly mixed and stirred for 5 minutes (overall solution volume ~200 ml). Further the obtained solution was constantly stirred and allowed to warm to room temperature where the reaction between aliphatic diamine and aromatic isocyanate happened. The stir bar was taken out from the resultant yellow and light-transparent gel. The polymeric gel was allowed to dry inside the beaker at room temperature for 3 days (because a fast evaporation of the solvent at high temperature would inevitably lead to the formation of undesired bubbles in the polymer).

After 3 days, the gel formed a rubber disc on the bottom of the flask. This rubber disc was carefully taken out and allowed to dry further at room temperature for a week. The obtained polyurethane/urea rubber was yellow, clear and light-transparent. This polymer was further heated for 2 hours at 90 °C in order to complete the polymerization reaction.

Results: The obtained polyurethane polymers were yellow and clearly light-transparent (i.e., cloudiness of these polymers would suggest some incorporations of possible crystalline blocks and therefore non-homogeneity [26].)

These obtained polymers (except formulation 3) had improved tear resistance. The results are given in Table 11.

Discussion:

Formulations 1 and 2: These samples had improved tear resistance in comparison with Experiment 8 (i.e., based on $O=C=N-$: $HO-$ proportion of 1:1). Also those samples stayed soft and rubbery. Hence the same or similar formulation could be further used as polyurethane matrix for the IPN with polyborosiloxane.

Table 11: *Results of Experiment 10, where Branched Polyurethane Polymers were Polymerized by Multiple Step Polymerization from TDI, Castor Oil, PPO and PEO*

| Formulation | Proportion given in reactive-ends | | | | Results | | |
	NCO:OH+NH$_2$	PPO/PEO	Polyol (castor oil)	Amine	Appearance	G' MPa	Tear Resistance MPa
1	1.2:1	0.5	0.5	0	elastomer	0.56	1.56
2	≈1.2:1	≈ 0.4	≈ 0.6	0	elastomer	0.69	2.35
3	the sample was not synthesized completely						
4	≈ 1.35:1	0.35	0.15	≈ 0.15	resin/elastomer	3.6	3.14

Formulation 3: Such long prepolymer (i.e., ≈ 10 castor oil-TDI-blocks together) should be considered as impractical as it increasingly difficult to dissolve for further polymerization.

Formulation 4: Even though the sample got to be quite rigid and less flexible, the tear resistance of the sample was some further improvement in comparison with formulations 1 and 2. Therefore, the polymeric chain-extenders based on primary diamine could be used in a combination with some increase of the soft polymeric segment.

Hence, on a base of short aromatic diisocyanate TDI, it is possible to obtain a suitable polyurethane/urea soft polymeric matrix with the desirable mechanical properties, which is also suitable for further IPN formation. Such a polyurethane polymer can be readily obtained by a two-step polyurethane polymerization, where the mechanical properties can change by the variation of components of the "soft" segment and short/long chain-extender [104].

4.2.7 Experiment 11: Formation of IPN Based on Two-step Polymerization Polyurethane Matrix and Poly-(boron$_n$-siloxane$_m$) Network

Poly-(boron$_n$-siloxane$_m$) gel in all this series of experiments was produced by the method shown in Experiment 1. The atomic boron-silicon proportion was kept to 1:16.

Formulation 1: In a 100 ml conical flask, 5 g of poly-(boron$_n$-siloxane$_m$) gel was dissolved in 75 ml of the 50 %-50 % TFH/Et-Me-ketone solvent system.

In a separate 100 ml flask an isocyanate-ended prepolymer was prepared, as shown in Experiment 10, formulation 1.

In a 200 ml beaker both solutions were carefully mixed and stirred for 5 minutes. Further the final polymeric chain extenders were added (as shown earlier, PPO M_n=425 50 % and PEO M_n=1000 50 %). The mixture was stirred for the next 15 minutes. The solution was gradually heated up to 45 -50 °C in order to reduce the amount of excessive solvent.

When the amount of the solvent had decreased by half, a light-transparent grey rubbery borosiloxane gel started to form separate from the main body of the cloudy-yellow viscous solution.

When the amount of the solvent was reduced significantly the oligomeric components formed a gel. The gel was left to dry in the beaker at room temperature for a day.

The resulting borosiloxane gel (separated from the main solution siloxane gel) was taken out and dried. The yield was 2.7 g of poly-(boron$_n$-siloxane$_m$) from the solution.

The polyurethane-siloxane prepolymer-IPN was heated at 85 °C for 70 minutes, to allow the complete polymerization of polyurethane matrix.

Results: Only a small proportion of borosiloxane gel formed IPN with the given polyurethane matrix. The actual polyurethane-borosiloxane IPN contained borosiloxane just ~15 % of mass in comparison with the planned ~40 %.

The obtained IPN was cloudy and light yellow, which suggests a heterogeneous polymeric system.

Formulation 2: The experiment from formulation 1 was rerun with a different concentration of borosiloxane gel. The mass of the polyurethane matrix was left the same and the mass of the poly-(boron$_n$-siloxane$_m$) gel varied from 4.5 g to 0.5 g.

Results: Only at a concentration of borosiloxane below 10 % (0.75 g) of the IPN mass, a gel separate from the main solution-gel was not formed during solvent evaporation.

Formulation 3: The experiment from formulation 2 was rerun with the polyurethane matrix based on Experiment 10, formulation 2 and also different concentration of borosiloxane gel. The mass of the polyurethane matrix was left the same and the mass of the poly-(boron$_n$-siloxane$_m$) gel varied from 3 g to 0.3 g.

Results: In this experiment also, it was only at a concentration of borosiloxane below 10 % (0.5 g) of the IPN mass, that a gel separate from the main solution-gel was not formed during solvent evaporation.

Discussion: Borosiloxane gel is immiscible with the polyurethane matrix and strongly tends to show phase separation [30]. The possible limited intermolecular forces which formed between boron and nucleophilic groups of the polyurethane matrix were just enough to detain a very limited quantity of borosiloxane oligomer in the formed IPN.

Hence, where a fast reaction between the isocyanate groups of the prepolymer and primary diamines is possible, the gelation process would be much faster and may occur strongly enough to trap all the borosiloxane inside the IPN.

4.2.8   Experiment 12: Formation of IPN Based on Two-step Polymerization Polyurethane/urea Matrix and Poly-(boron$_n$-siloxane$_m$) Network, where the Polyurethane/urea Polymerization Process was Completed through a Fast Reaction with Aliphatic Diamine

In order to trap successfully inside the formed IPN a higher possible concentration of borosiloxane than in Experiment 11 (i.e., $\approx$ 10 % of the IPN mass) the final polyurethane polymerization reaction was changed from a slow reaction between aromatic isocyanate and aliphatic primary hydroxyl (used in Experiment 11) to a much faster reaction between aromatic isocyanate and aliphatic primary amine.

Formulation 1: This experiment was run with a polyurethane/urea matrix based on Experiment 10, formulation 4. Also different concentrations of borosiloxane gel were applied.

Results: As the gelation process was significantly faster than in previous experiments, a higher concentration of borosiloxane was trapped into the formed IPN. The highest successful mass proportion of poly-(boron$_n$-siloxane$_m$) in the produced IPN was 21 %

(1.7 g from 8 g of overall IPN mass).

Formulation 2: At this stage a new α, ω –diamine prepolymer was introduced.
Poly(propylene glycol)-block-poly(ethylene glycol)-block-poly(propylene glycol) bis(2-aminopropyl ether) (shown in Figure 63) average M_n ~2,000 (Aldrich 406635) gave the
opportunity to use very fast gelation based on the reaction of isocyanate of the
prepolymer and primary amine of another long prepolymer. In addition, a use of a such
long α, ω-diamine heterogeneous-block prepolymer has such advantages: it creates a
polyurethane/urea polymer with a high average molecular weight (suitable for a further
chemical cross-linking through a substituted urea formation) and simultaneously gives a
high proportion of the amorphous soft polymeric segment (i.e., PEO and PPO are
immiscible at room temperature, therefore are free from crystalline).
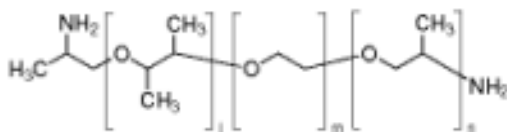
Figure 63: *Poly(propylene glycol)-block-poly(ethylene glycol)-block-poly(propylene glycol) bis(2-aminopropyl ether)*

Formulation 1 was rerun with one exception, the final polymerization was based on the
introduction of dissolved poly(propylene glycol)-block-poly(ethylene glycol)-block-poly(propylene glycol) bis(2-aminopropyl ether) M_n ~2,000 (5 g) instead of a short
diamine, such as 1,6-hexamethyl diamine. Also the resulting proportion of isocyanate-primary amine was shifted to a 2:1 in comparison with 1.35:1 in the previous experiment.

Results: Up to 5 g (29 %) of borosiloxane was incorporated into 16 g of the soft and
rubbery resulting polyurethane/urea-heterosiloxane IPN.

Formulation 3: The solvent system which was used during the gelation process was
changed in such a way as to be less miscible with borosiloxane, therefore it may lead to a
greater concentration of poly-(boron$_n$-siloxane$_m$) inside the body of the formed IPN and
reduce the concentration of borosiloxane in the rest of the solution [30]. The solvent
system was 35 % diethyl ether, 50 % THF and 15 % 2-butanone.

Formulation 2 was rerun, where the final gelation was run in the new solvent system. The highest possible concentration of poly-(boron$_n$-siloxane$_m$) trapped inside the IPN was 44 % (8 g of 17 g of IPN).

The gel-IPN products obtained in formulations 2 and 3 were dried further for 3 weeks at room temperature and further heated at 90 °C for 2 hours to allow the reaction between the formed secondary amines and any possibly remaining isocyanate groups to be completed (i.e., final polymerization as a formation of cross-linked polymeric matrix). During this stage of the polymerization (at elevated temperature) phase separation between borosiloxane and the rest of IPN (polymeric matrix) happened. Borosiloxane previously (at room temperature) successfully trapped inside the IPN started to concentrate on the surface of the polymer. At the end of the heating process, borosiloxane effectively formed a thick layer on the surface of the IPN. In the IPN sample obtained in formulation 3, 3.5 g of borosiloxane was found on the surface of the IPN.

Discussion: In order to successfully introduce a PDMS base polymeric network into IPN based on a soft non-siloxane (here, polyurethane) matrix, the siloxane polymeric matrix should be "anchored" into the second polymeric matrix. One possible way to achieve this is by increasing the molecular mass of the siloxane-based polymeric network, as it may stabilize both polymeric networks and prevent it from a possible separation. Also, in this case, such a cross-linked polymer would be increasingly difficult to dissolve and thoroughly disperse in the second polymeric matrix [20].

Alternatively, the role of the "polymeric anchor" can be played by the introduction of siloxane based polymeric segments into the second non-siloxane (i.e., polyurethane) polymeric matrix. Therefore, it would increase the affinity between the two polymeric matrices and may prevent separation [17]. Another way to stabilize both polymeric networks in the IPN is the introduction of some chemical cross-links between the networks. Currently there exists on the market epoxy-, primary amine-, isocyanate-, alkoxy- and hydroxyl-ended siloxane based prepolymers, suitable for co-polymerization/further polymerization with conventional isocyanate-ended polymers [20, 24].

In this specific application some boron groups should be introduced into a polysiloxane polymer before it further polymerizes with polyurethane polymer [24].

Because of the very high market price of the existing alkoxy-siloxane prepolymers suitable for a copolymerization with polyurethanes, the resulting final polymer may be economically unsuitable. Therefore, it was decided to continue the research along the lines of a more cost-effective way to introduce some degree of chemical cross-linking between soft poly-(boron$_n$-siloxane$_m$) and polyurethane polymeric matrices.

The two most popular ways of introducing organo-functional groups into a siloxane polymer are hydrosilylation (i.e., reaction of double carbon-carbon bond with hydrogen directly attached to the silicon atom) and by Grignard reaction. The first method could be more economically effective (if successful) in an industrial scale production of high quantities of a siloxane polymer [20], while the second method may be efficient in this application.

4.3 <u>Experimental Phase 3</u>: Introduction of Organo-functional Groups, Suitable for Copolymerization with Isocyanates, through Grignard Reaction on Siloxanes

Experimental: All chemicals were purchased from Sigma-Aldrich Fluka Europe and used without further purifications (always, before the experiment, all solvents were checked for traces of moisture by FT-IR), the FT-IR analyses were performed on Perkin Varian 800 FT-IR equipment.

4.3.1 <u>Experiment 13</u>: Synthesis of Me₃Si(CH₂)₆SiMe₃ by a Grignard Reaction of 1,6-dichlorohexane and Chlorotrimethylsilane

Reagents: 1,6-dichlorohexane (Aldrich D63809), chlorotrimethylsilane (Aldrich 386529), magnesium (granular, Grignard reagent, Sigma Aldrich 254126), tetrahydrofuran (THF) anhydrous $\geq$ 99.9 % (Sigma Aldrich 401757), diethyl ether (Et_2O) spectrometric grade $\geq$ 99.9 % (Sigma Aldrich 309958).

<u>*Formulation 1:*</u> In a dry 100 ml conical flask 1.55 g of $1,6\text{-Cl}(CH_2)_6Cl$, 0.48 g of Mg and 40 ml of Et_2O were sealed and stirred at 25 °C for a week, to achieve the reaction shown in Figure 64.
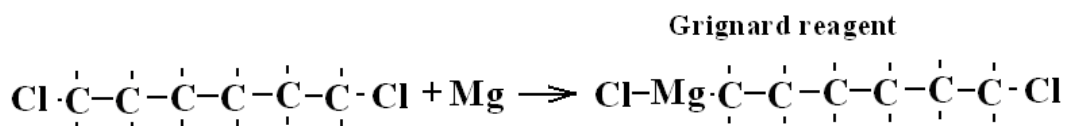
Figure 64: Formation of Grignard Reagent

<u>*Results:*</u> On the bottom of the flask was present almost the full amount of unreacted granular magnesium and no trace of the possible formed white salt ($MgCl_2$). The ingredients had reacted only partially and very slowly. Hence, at room temperature in diethyl ether the reaction between 1,6-dichlorohexane and magnesium is too slow to be applied into the polymerization process.

Formulation 2: The boiling temperature of THF is significantly higher than that of diethyl ether. Temperatures of ≤ 70 °C can be applied without any additional pressure. Therefore, the solvent was changed and the procedures were identical to formulation 1. *Results:* Similar to those in formulation 1, just a very limited amount of magnesium granules had reacted during a week of stirring at such temperature.

Formulation 3: Alternatively, this Grignard reaction can be run by the simultaneous introduction of halosilanes into the reaction bath. This normally speeds the reaction, where the resultant Grignard reagent is further able to react with dichlorodimethylsilane [72]:
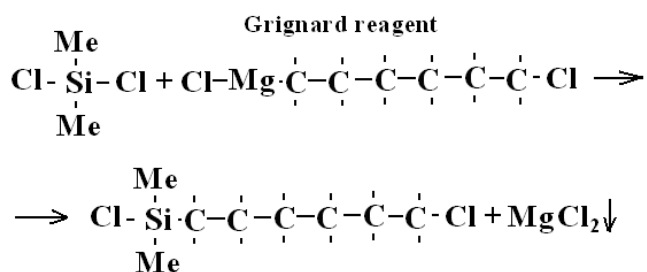
Figure 65: Reaction between Grignard Reagent and Chlorosilane

In a dry 100 ml conical flask 1.55 g of $1,6\text{-}Cl(CH_2)_6Cl$, 0.48 g of Mg, 2.17g of chlorotrimethylsilane and 40 ml of THF were sealed and stirred at 65 °C for 2 weeks. *Results:* On the bottom of the flask some particles of granular magnesium were present (though reduced in size) and a very limited proportion of a white salt had formed. The ingredients had reacted just partially, and the principle reaction is shown in Figure 65.

Discussion: The reaction between 1,6-dichlorohexane and magnesium at 65-67 °C was still too slow to be applied into the polymerization process.

4.3.2 Experiment 14: Synthesis of Me₃Si(CH₂)₅ SiMe₃ by a Grignard Reaction of 1,5-dibromopentane and Chlorotrimethylsilane

Further introduced reagent: 1,5-dibromopentane (Fluka 34260).

In a dry 100 ml conical flask 2.3 g of $1,5\text{-}Br(CH_2)_5Br$, 0.48 g of Mg and 40 ml of Et_2O were sealed and stirred at 25 °C for 5 hours.

The solution instantly became light-yellow in colour which indicates formation of the bromide anion Br^- [23]. The first reaction appeared after 40 minutes of stirring where about a half of the magnesium granules had visibly reacted and gave a grey coloured solution. Further the solution had been stirred for ~2 hours at ~30 °C before the remaining magnesium granules started to react with ϵ-Br of $BrMg(CH_2)_5Br$ compound.

Discussion: As the reaction with magnesium is much faster with α-Br of 1,5-dibromopentane than with ϵ-Br (the detailed explanation of the applied chemistry is given in the Literature Review, section 2.3.4), it is possible to expect that with molar proportions of 1:1 for 1,5-dibromopentane and magnesium, the reaction would predominantly run on one side (i.e., predominantly gives $BrMg(CH_2)_5Br$ instead of less predictable $BrMg(CH_2)_5MgBr$) [23, 72].

Hence, it may be possible to synthesise a stable enough halosiloxane monomer -$(Me)_nSi(CH2)_mX$ which is further introduced into polycondensation of di-functional halosilanes.
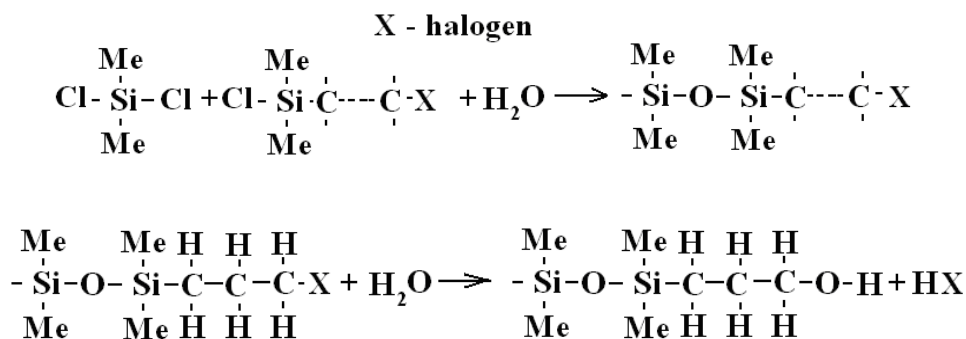
Figure 66: Reaction between Halide and Water

Such a halogen-ended (organo-functional) silane can be further transformed into a hydroxyl-ended siloxane suitable for a copolymerization with isocyanates, as shown in Figure 66.

4.3.3 Experiment 15: Two-step Synthesis of Me₃Si(CH₂)₅OH by a Grignard Reaction of 1,5-dibromopentane and Chlorotrimethylsilane

Formulation 1: In a dry 100 ml conical flask, 2.3 g of $1,5\text{-}Br(CH_2)_5Br$, 0.24 g of Mg and 40 ml of Et_2O were sealed and stirred at 25 °C for 2 hours. A light-transparent grey solution (with no trace of magnesium granules) was observed to form. $BrMg(CH_2)_5Br$ crystallized on the bottom of the flask.

The amount of Et_2O was increased by 50 % and further additionally by 100 %, but the resulting organo-salt of $BrMg(CH_2)_5Br$ was not dissolved.

Formulation 2: As in formulation 1, $BrMg(CH_2)_5Br$ organo-salt was obtained in 40 ml of Et_2O, but in this experiment 1.1 g of chlorotrimethylsilane was added. Me_3SiCl had dissolved the organo-salt of $BrMg(CH_2)_5Br$ and further reacted with it for 4 hours. This resulted in a white $ClMgBr$ salt forming on the bottom of the flask and an organo-layer of $Me_3Si(CH2)_5Br$ dissolved in Et_2O, as shown in Figure 67.

Figure 67: *Results of a Grignard Reaction of 1,5-dibromopentane, Magnesium and Chlorotrimethylsilane in Et₂O, where $ClMgBr$ Salt Formed on the Bottom*

Then 650 ml of ice cold distilled water was placed in a 1000 ml flask and stirred continuously in an ice bath. All contents from the reaction were slowly poured into the water and stirred for 3 minutes.

The flask was left for the next 10 minutes for phase separation to occur and the top organic layer was collected from a separation funnel.

An additional 20 ml of diethyl ether was added to the flask and stirred for 3 minutes. The flask was further left for 10 minutes for phase separation to take place and the newly formed organic layer was collected into the same separation funnel.

In the separation funnel the organic layer was washed repeatedly with brine (concentrated $NaCl$ solution) until the organic layer was at a pH of about 7.

This organic solution was dried continuously by stirring at 70 °C for 2 hours and further under vacuum at 35 °C for 15 minutes.

Results: A colourless oil (slightly cloudy) was observed, FT-IR spectrum 1: Si-Me bond gives a very strong sharp peak 1260 cm^{-1}; weak wide absorption of hydroxyl group -OH 3400 cm^{-1}; CH_2-H bond (in Me) gives a strong sharp peak of absorption at 2962 cm^{-1} (about 70 % of magnitude of the Si-Me peak); 2900 cm^{-1} and 2860 cm^{-1} absorption belongs to methylene groups of pentanol attached to a siloxane chain (about 20 % of magnitude of the Si-Me peak), as shown in Figure 68.
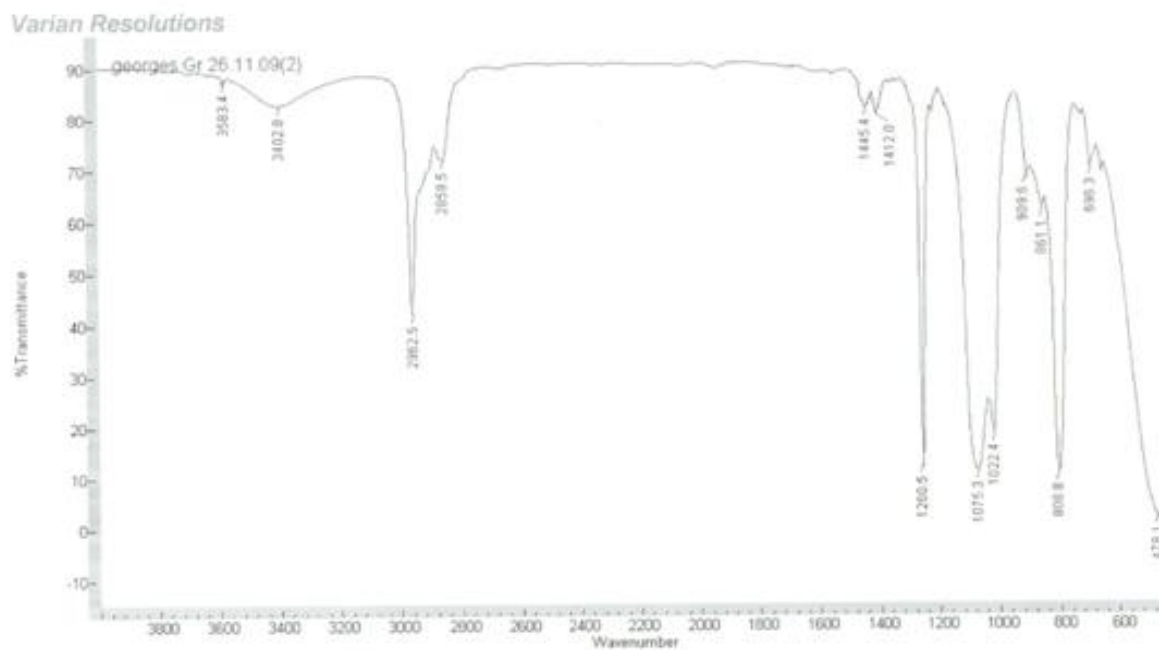
Figure 68*: <u>FT-IR Spectrum 1</u> Me₃Si(CH₂)₅OH Obtained by Grignard Reaction from Me₃SiCl, Mg and Br(CH₂)₅Br*

124

Discussion: This experiment was run repeatedly a number of times. Some of the FT-IR spectra obtained gave a weak absorption peak at 3100-3000 cm^{-1}, suggesting the presence of some double carbon-carbon bonds [23]. Here, such undesirable carbon-carbon bonds may appear as a result of an elimination reaction, which is normally significantly slower than Grignard reaction of short linear $BrMg(CH_2)_5Br$ with chlorosilanes [23, 72]. This slower elimination reaction may succeed because the resultant crystal of $BrMg(CH_2)_5Br$ in Et$_2$O prevents full access to some of Me_3SiCl reagent, so the slower reaction had time to take place.

4.3.4   Experiment 16: Reaction of Chlorotrimethylsilane, Dichlorodimethylsilane, Trichloromethylsilane and Magnesium

Formulation 1: In a dry 100 ml conical flask, 2.16 g of Me_3SiCl and 0.24 g of Mg were dissolved in 40 ml of Et$_2$O, sealed and stirred at 25 °C for 2 days.

Results: No visual changes to the magnesium granules were observed as the solution stayed clear and colourless.

Formulation 2: The same experiment was run with Me_2SiCl_2 and $MeSiCl_3$. The results were the same as in formulation 1. These results are in good agreement with theory [20, 72].

Discussion: As magnesium does not react (i.e., does not produce a stable compound [23]) with chlorosilanes without the presence of halo-organo compounds, hence an excess amount of halosilanes may be used as an additional solvent system to this Grignard reaction [72].

4.3.5   Experiment 17: One-step Synthesis of Me$_3$Si(CH$_2$)$_5$OH by a Grignard Reaction of 1,5-dibromopentane and Chlorotrimethylsilane

Formulation 1: The reaction of Experiment 15, formulation 2 was rerun, where all the reagents (i.e., 2.3 g of $1,5\text{-}Br(CH_2)_5Br$, 0.24 g of Mg and 1.1 g of Me_3SiCl) were simultaneously dissolved in Et$_2$O, sealed and stirred at 25 °C for 3 hours. Then the reaction was allowed to run until completion.

Results: The resulting FT-IR spectrum did not show any absorption peaks in the area of a possible carbon-carbon double bond.

Formulation 2: The reaction of formulation 1 was rerun, where 1.1 g chlorotrimethylsilane (Me_3SiCl) was substituted with 1.3 g of dichlorodimethylsilane (Me_2SiCl_2). It took 45 minutes for the reaction to reach completion.

Formulation 3: The reaction of the experiment of stage 2 was rerun, where Me_3SiCl was substituted with 1.5 g of trichloromethylsilane ($MeSiCl_3$). It took less than 20 minutes for the reaction to reach completion.

Results: These results are in good agreement with theory [20, 72], as tri-halosilanes normally have higher reactivity than di-halosilanes and particularly mono-halosilanes (i.e., tri-organo substituted halosilanes).
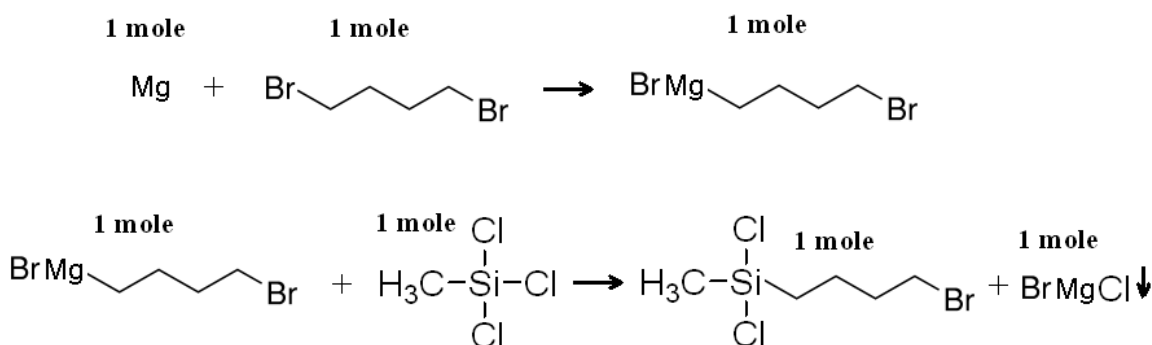
Figure 69: *Grignard Organo-substitution of One of Chlorine of Trichloromethylsilane*

Discussion: Trichloromethylsilane reacts much faster than dichlorodimethylsilane. If both of these halosilanes are present in a Grignard reaction bath, the reaction with dichlorodimethylsilane normally begins only when the reaction with trichloromethylsilane has been completed. Therefore, it is possible to expect that in a mixture with molar proportions of 1 mole of magnesium, 1 mole of 1,5-dibromopentane, 1 mole of trichloromethylsilane and $\geq$ 1 mole of dichlorodimethylsilane, the Grignard organo-substitution would run predominantly on an organo-substitution of one of the chlorines of trichloromethylsilane [72], as shown in Figure 69. Hence, it is possible to predict that the resulting polysiloxane polymer (after polycondensation reaction) would

be an alternating and random polysiloxane. Also by changing the amount of di-functional halosilanes in the reaction bath it is possible to control the average distance between the attached ε-pentanol groups.

4.3.6 <u>Experiment 18</u>: Formation through a Grignard Reaction of a Poly-(alkyl-siloxane) Polychain with Attached ε-pentanol Groups, which are Suitable for a Further Copolymerization Reaction with Isocyanate Groups

Formulation 1: In a dry flat-bottom 500 ml conical flask were placed 0.97 g of Mg (0.04 moles), 45 ml of diethyl ether ($\geq 4 \times 10$ moles solvent), 9.2 g of 1,5-dibromopentane (0.04 moles), 6.0 g of trichloromethylsilane (0.04 moles), 5.2 g of dichlorodimethylsilane (≥ 0.04 moles) (i.e., trichloromethylsilane is more reactive, therefore dichlorodimethylsilane works here as an additional solvent for the system). The flask was sealed by a rubber-stopper and the mixture was stirred with a magnetic Teflon stir-bar very slowly for 10 minutes. The temperature of the flask was further reduced from room temperature to 15 °C.

For a short period of time (~30 seconds) the liquid inside the flask became slightly yellow (due to the formation of free bromine anion Br^-) and instantly started to become cloudy grey due to the reaction between the bromine anion and magnesium). As the reaction is quite exothermic [23], the temperature inside the flask soon started to rise, the stirring was stopped and the flask was kept in an ice bath for 2 minutes to reduce the temperature of the flask to ~19 °C.

As the temperature of the flask had dropped, the liquid was then stirred continuously at ~20 °C for the next 1 hour.

A white powder of bromo-magnesium-chlorine salt was observed in the flask together with some dark-grey particles of unreacted magnesium turnings.

The temperature of the flask was increased to 27 °C and stirred continuously for 2 hours until all the magnesium turnings had disappeared and white $BrMgCl$ salt formed at the bottom. Therefore, the reaction had run into completion.

The temperature of the flask was then reduced to ~0 °C in an ice bath and a hydrolysis reaction (the experimental technique is fully described in the previous experiment) was then allowed to take place:

$$n\ [Si(CH_3)_2Cl_2] + n\ H_2O \rightarrow [Si(CH_3)_2O]n + 2n\ HCl \qquad (66)$$

$$n\ [Si(CH_3)(C_5H_{10}Br)Cl_2] + n\ H_2O \rightarrow [Si(CH_3)\ (C_5H_{10}Br)O]n + 2n\ HCl \qquad (67)$$

$$n\ [Si(CH_3)(C_5H_{10}Br)O] + n\ H_2O \rightarrow [Si(CH_3)(C_5H_{10}OH)O]n + n\ HBr \qquad (68)$$
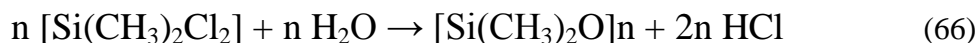
Results: A heavy, slightly cloudy, colourless oil, which was a mixture of cyclo and linear siloxane oligomers, was observed. The obtained FT-IR spectrum 2 (shown in Figure 70) shows peaks of absorption at 2924 and ~2855 cm^{-1} indicating the presence of a high proportion of methylene groups from the attached alkane group [102]. Additionally, the fact that FT-IR showed the absorption peaks to be slightly shifted to lower than theoretical absorption frequencies clearly suggests that the structure attached to the siloxane chain is a straight alkane chain [110].
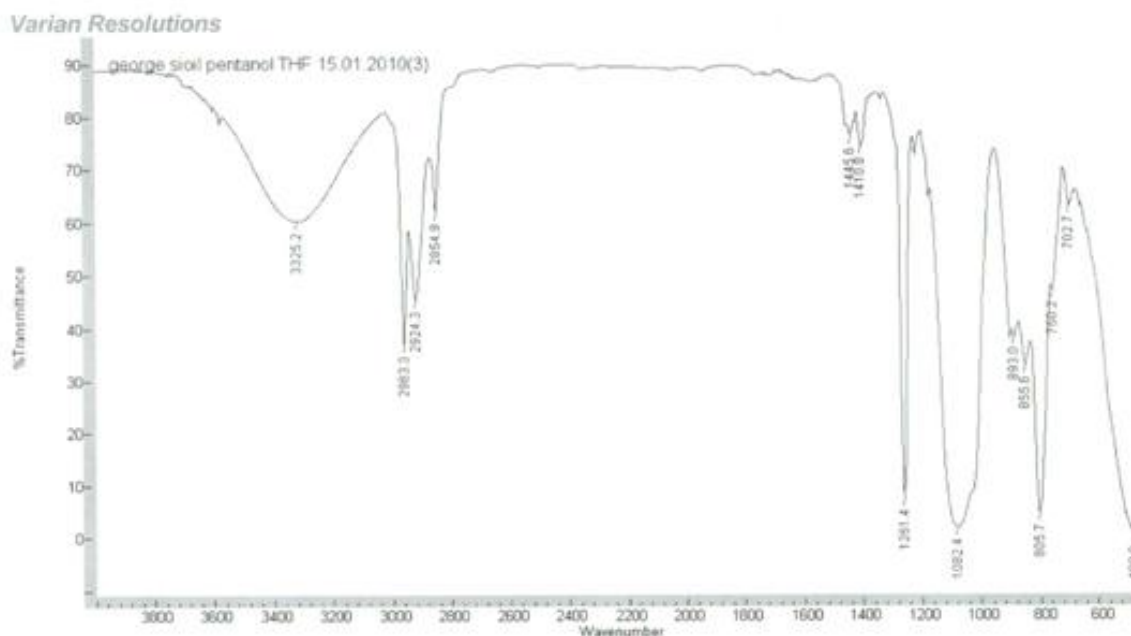
Figure 70*: FT-IR Spectrum 2 -O-(Me$_2$Si-O)$_n$-(MeSi(CH$_2$)$_5$OH)$_m$- Siloxane Polymeric Structure, Obtained by Grignard Reaction from MeSiCl$_3$, Mg and Br(CH$_2$)$_5$Br and Co-hydrolysis with Me$_2$SiCl$_2$*

The mass of the obtained siloxane oil was 7.5 g. The theoretical prediction was 8.8 g. The yield was lower because the tetrapentanol-tetramethyl-tetracyclosilane ($[-O-MeSi(CH_2)_5OH]_4$) formed during the hydrolysis reaction is much less hydrophobic than the rest of the resulting silanes, and therefore it was difficult to separate all of it from water.

Formulation 2: The previous formulation was rerun with a different proportion of dichlorodimethylsilane in the reaction bath. The molar proportion of Me_2SiCl_2 towards $MeSiCl_3$ varied from a ratio of 2:1 to 1:2. The obtained FT-IR spectra are shown in spectrum 3 (shown in Figure 71) for a molar proportion of 2 :1 Me_2SiCl_2 to $MeSiCl_3$ and spectrum 4 (shown in Figure 72) for the proportion of 1:2 Me_2SiCl_2 to $MeSiCl_3$.
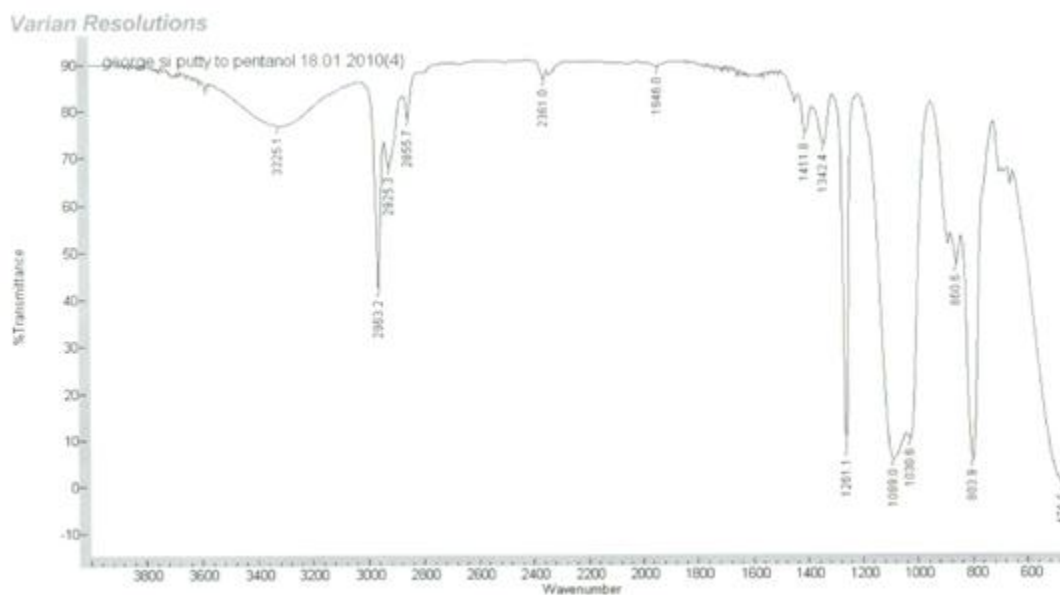
Figure 71: <u>FT-IR Spectrum 3</u> -O-(Me₂Si-O)ₙ-(MeSi(CH₂)₅OH)ₘ- Siloxane Polymeric Structure, Obtained by Grignard Reaction from MeSiCl₃, Mg and Br(CH₂)₅Br and Co-hydrolysis with 2 moles equivalent of Me₂SiCl₂

It is possible to see an absorption peak of methylene groups at ~2925 cm^{-1} and a wide absorption at 3600-3100 cm^{-1} of hydroxyl at higher magnitude in spectrum 4 than in spectrum 3, where other absorption peaks, such as ~1260 cm^{-1} of the silicon-methyl

129

bond have quite a similar magnitude. Therefore, it clearly suggests, that the proportion of dimethyl-silane in poly-(alkyl-silane) of spectrum 3 is greater than in spectrum 4.
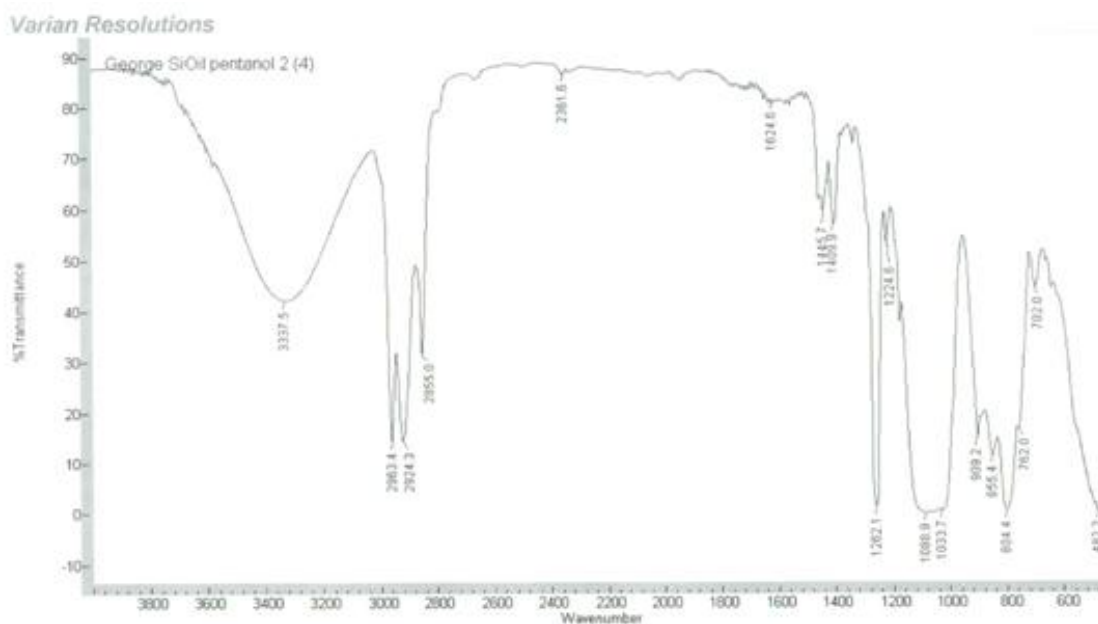
Figure 72: *FT-IR Spectrum 4* -O-$(Me_2Si$-$O)_n$-$(MeSi(CH_2)_5OH)_m$- *Siloxane Polymeric Structure, Obtained by Grignard Reaction from* $MeSiCl_3$, *Mg and* $Br(CH_2)_5Br$ *and Co-hydrolysis with 1/2 mole of* Me_2SiCl_2

Formulation 3: Formulation 1 was rerun, but with 5.5 g (1 mole) of di-hydroxyl-ended PDMS ($M_n \approx 550$ g/mole) added to the hydrolysis reaction in a flask of ice cold distilled water.

The obtained FT-IR spectrum given in spectrum 5 (shown in Figure 73) suggests that the siloxane formed has predominantly dimethyl-silane polymeric backbone members, and methyl-pentanol-silane members are randomly incorporated into the backbone.

Discussion: By the simple incorporation of PDMS prepolymers, such as dichlorodimethylsilane or di-hydroxyl-ended PDMS prepolymers at different stages, it is possible to control quite precisely the amount of pentanol groups attached to the resulting poly-(alkyl-siloxane) polymeric backbone.
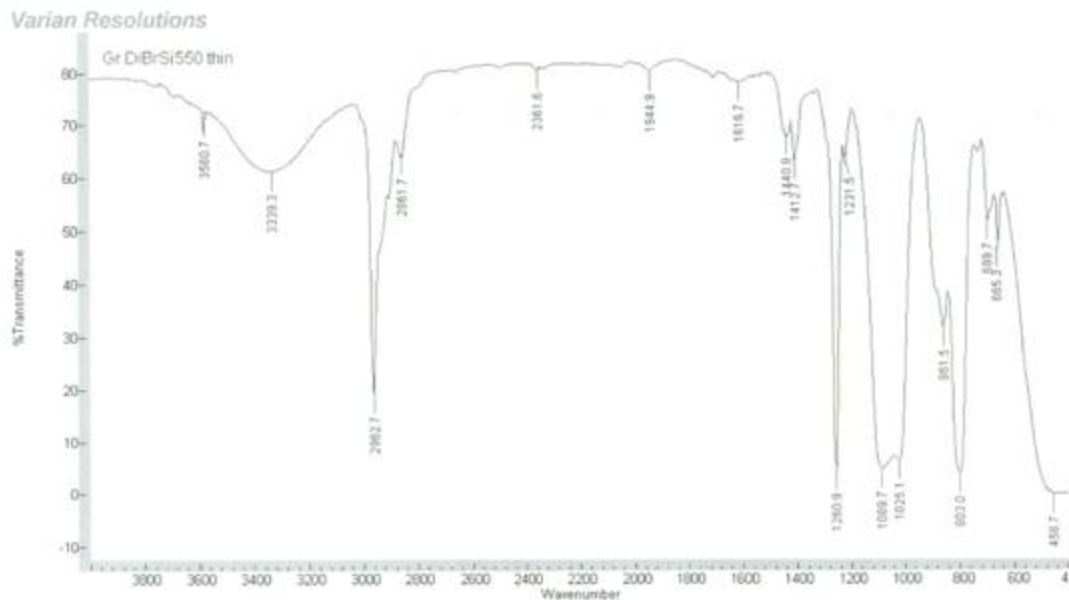
Figure 73*: <u>FT-IR Spectrum 5</u> -O-(Me$_2$Si-O)$_n$-(MeSi(CH$_2$)$_5$OH)$_m$- Siloxane Polymeric Structure, Obtained by Grignard Reaction from MeSiCl$_3$, Mg and Br(CH$_2$)$_5$Br and Co-hydrolysis with HO-(Me$_2$SiO)$_{5-7}$-OH*

<u>Formulation 4:</u> A few experiments were run in order to obtain an alkoxy-ended oligo(alkyl-siloxane) prepolymer based on Me/Et-O-(Me$_2$Si-O)$_n$-(MeSi(CH$_2$)$_5$OH)$_m$-Me/Et, but none of the attempts so far have given a satisfactory result.

4.4 <u>Experimental Phase 4</u>: Formation of Poly-[(boron)$_n$-(alkyl-silane)$_m$] Containing Alternating Pentanol Groups Polymeric Network, Suitable to a further Formation of Scarcely Cross-linked semi-IPN with Polyurethane Network

In the presence of a weak Lewis acid (i.e., boric acid) and an elevated temperature (or a strong catalyst) oligomeric cyclo-siloxanes tend to break the silicon-oxygen bond and form polymeric chains. Because boron is also able to form stable chemical bonds through oxygen in a siloxane polymeric chain tri-functional boron forms a cross-linked network of poly/oligo-(boron-siloxanes) [90]. As well as in Experimental Phase 1, here it is also preferable to have a proportion of 1boron atom to 16 atoms of silicon in the siloxane backbone in order to have a soft bouncy oligomeric putty.

PDMS gives a chemically fairly stable polymer as a methyl group attached directly to a silicon atom of the siloxane backbone is more stable than a methyl group attached to a polyolefin, such as polypropylene. However, it also known that longer organic groups attached to the silicon of a siloxane backbone (i.e., ε-pentanol) do not have such stability. For example, the presence of a strong alkaline group in a water solution normally leads to hydrolysis of silicon-carbon bonds between a siloxane polymeric backbone and the attached pentanol groups. On the other hand, an acid attack (i.e., Lewis acid - boric acid) on this bond is known to be less effective (harmful) in cleaving the silicon's α-carbon bond of an attached alkyl [20, 72].

The purpose of these experiments was to ensure that the formation of borosiloxane (i.e., boron-oxygen-silicon bond) does not cleave a previously formed silicon-carbon bond on the attached ε-pentanol group.

4.4.1 <u>Experiment 19</u>: Formation of Poly-[(boron)$_n$-(alkyl-silane)$_m$] Oligomeric Gel from Boric Acid and Poly-[(ε-pentanol/methyl)$_n$dimethyl$_m$]siloxane

(Poly-[(ε-pentanol/methyl)$_n$dimethyl$_m$]siloxane was obtained in the previous experiment, FT-IR spectrum 2).

Procedure: 0.2 g of boric acid was dissolved in 20 ml of distilled water in a conical 200 ml flask at 70 °C.

In a separate 100 ml flask 8 g of poly-[(ε-pentanol/methyl)$_n$dimethyl$_m$]siloxane was dissolved in 50 ml of acetone at room temperature.

The acetone-polysiloxane solution was then added to the water - boric acid solution and stirred continuously. The temperature of the flask with the emulsion was raised to 175 °C and stirred continuously for 15 minutes.

The emulsion was then poured into an open 200 ml beaker in order to evaporate the excess solvent and water. 20 ml of THF was added in order to reduce the viscosity of the resulting emulsion/solution.

Boiling acetone, water and THF create bubbles on the surface of the siloxane mass. At first the bubbles were normally smaller than 5 mm in diameter and broke in less than a second. Gradually the bubbles increased in size to 20 mm in diameter and lasted up to 5-10 seconds, and the viscosity of the solution significantly increased. The boron-siloxane putty was ready.

The resulting putty was cooled to room temperature and washed in distilled water in order to remove traces of unreacted boric acid and any pentanol which may have formed. The resultant borosiloxane putty was dried at 70 °C for 3 hours and further at room temperature for 12 hours.
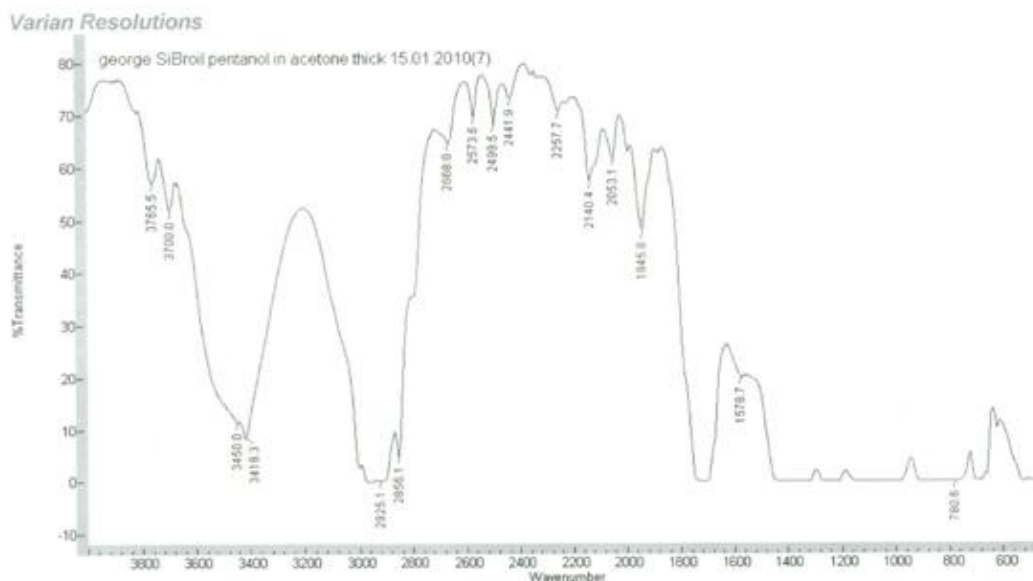
Figure 74: *FT-IR Spectrum 6*

Poly-boron$_x$[(ε-pentanol/methyl)$_n$dimethyl$_m$]siloxane Gel

Results: A soft grey/colourless oligomeric putty (which was slightly cloudy) was formed. The borosiloxane putty was quite similar to the borosiloxane putties obtained in Experimental Phase 1, but was visually less cloudy and more light transparent (probably because the hydroxyl groups of the attached ε-pentanol groups formed hydrogen bonds with the incorporated boron and so reduce the nonhomogeneity of the resulting oligomeric gel). There was also some observed shift in FT-IR absorption of hydroxyl present, shown in spectrum 6 in Figure 74.

The obtained FT-IR spectrum suggests that a proportion of ε-pentanol was not reduced (the strong absorption at 2925 cm^{-1} was still present). So, if some of the silicon-carbon bonds between the siloxane backbone and the attached ε-pentanol groups were cleaved, this process was at a low level and was insignificant to the proportion of ε-pentanol still attached to the siloxane backbone.

Analysis of ^{13}C NMR and ^{1}H NMR spectra given in Figure 75 and Figure 76 confirmed the data indicated by FT-IR spectrum 6, given in Figure 74. The obtained structure is a poly-boron$_x$[(ε-pentanol/methyl)$_n$ dimethyl$_m$]siloxane, as shown in Figure 77.
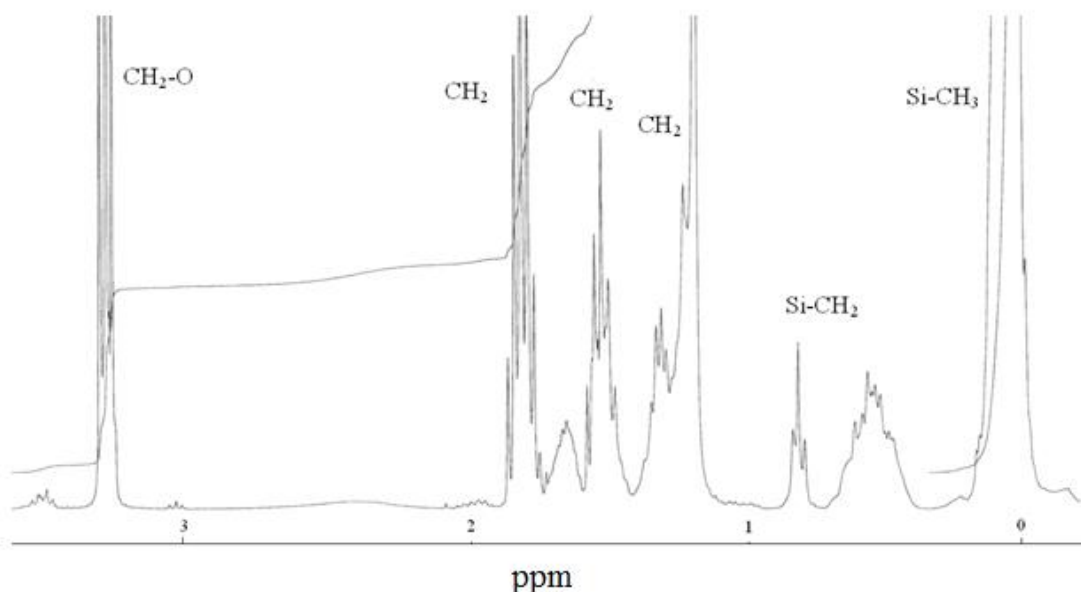
Figure 75: *^{1}H NMR Spectrum of*

Poly-boron$_x$[(ε-pentanol/methyl)$_n$ dimethyl$_m$]siloxane Gel
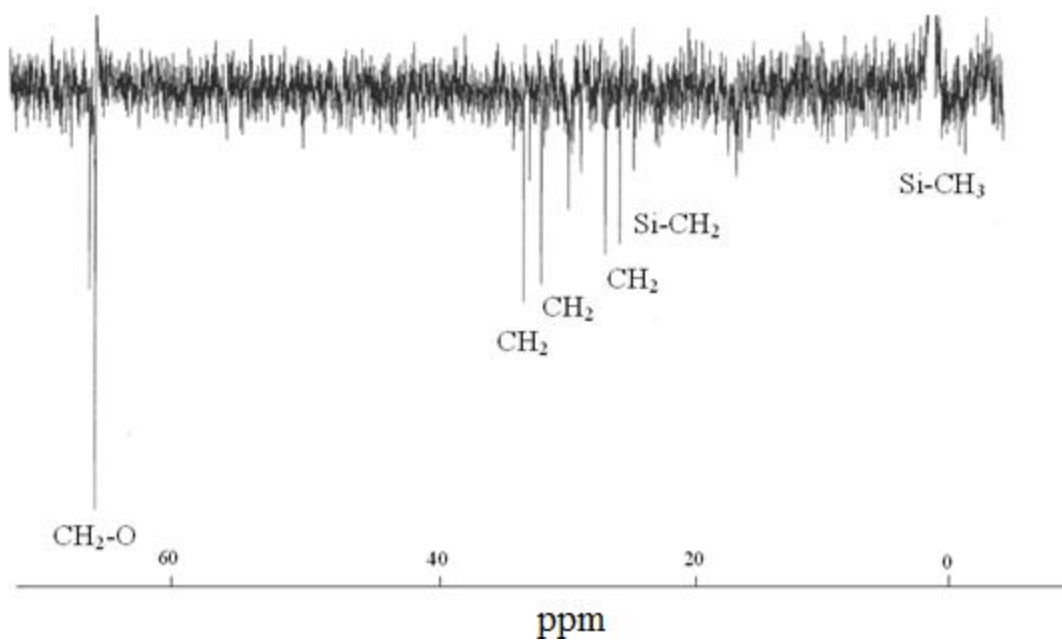
Figure 76: ^{13}C *DEPT-135 NMR Spectrum of*

Poly-boron$_x$[(ε-pentanol/methyl)$_n$ dimethyl$_m$]siloxane Gel
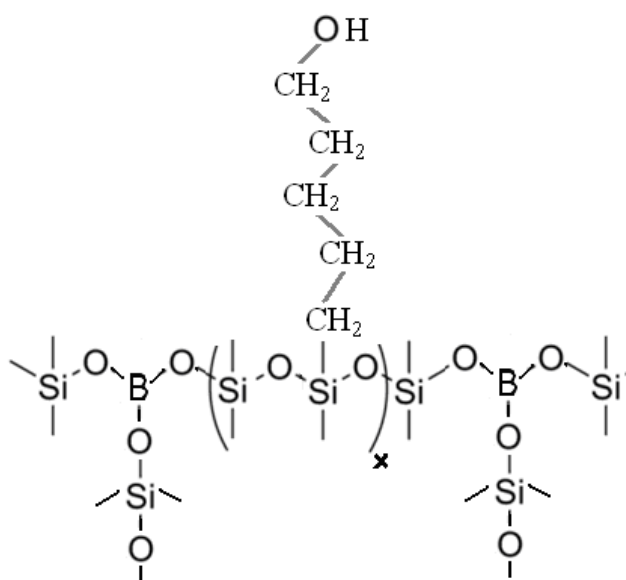
Figure 77: *Possible Structure of the Obtained*

Poly-boron$_x$[(ε-pentanol/methyl)$_n$ dimethyl$_m$]siloxane

4.5 <u>Experimental Phase 5</u>: Formation of Scarcely Cross-linked through Urethane Groups semi-IPN, Based on Poly-boron$_x$[(ϵ-pentanol/methyl)$_n$ dimethyl$_m$]siloxane and Polyurethane/urea Network

4.5.1 <u>Experiment 20</u>: (<u>*Sample 1*</u>) Formation of a Semi-IPN Based on a Poly-boron$_x$[(ϵ-pentanol/methyl)$_n$ dimethyl$_m$]siloxane and a Soft Polyurethane/urea Network

Procedure: 7.5 g of poly-[(ϵ-pentanol/methyl)$_n$ dimethyl$_m$]siloxane (FT-IR spectrum 5) was dissolved in 50 ml of acetone and mixed with 0.2 g of boric acid dissolved in 50 ml of distilled water. The resulting emulsion/solution was stirred continuously while the temperature was raised to 175 °C. The resulting emulsion/solution was stirred for 40 minutes.

The resulting gel of poly-boron$_x$[(ϵ-pentanol/methyl)$_n$ dimethyl$_m$]siloxane was repeatedly washed in distilled water and dried at 70 °C for 20 hours.

The FT-IR analysis of the resulting borosiloxane gel showed absorption at 2925 cm^{-1} suggesting the presence of ϵ-pentanol attached to the siloxane chain, and also peaks in the area between 2700-2400 cm^{-1}, which are characteristic absorption peaks of a boron-siloxane bond.

The mass of one molar/polymeric-segment of dimethylsiloxane group -O-SiMe$_2$- is 72.159 g/mole(polymeric segment) and the mass of the similar ϵ-pentanolmethylsiloxane group -O-Si([CH$_2$]$_5$OH)Me- is 146.269 g/mole(polymeric segment). When boron is incorporated into the siloxane polymeric backbone the segment's mass for a block of the resulting polymer will increase by ~50 g/mole on each 10 dimethylsiloxane groups. Therefore, in this experiment it was decided to count one active ϵ-pentanol group (i.e., active hydroxyl group -OH) for each ~840 g/mole(polymeric segment) of the obtained prepolymer.

The polyurethane prepolymeric network was formed from a preparation of tri-isocyanate prepolymer based on a castor oil molecule with 3 attached molecules of TDI, with one unreacted isocyanate functional group on each attached TDI.

Therefore, 1.5 moles of castor oil (5.1 g) and 1.5 moles of TDI (2.61 g) were stirred for 15 minutes and heated at 80 °C for 60 minutes. This isocyanate-ended prepolymer was then dissolved in 50 ml of dry THF and cooled to 0 °C.

In a separate flask 7.7 g of the resulting poly-boron$_x$[(ε-pentanol/methyl)$_n$ dimethyl$_m$]siloxane gel was dissolved in 50 ml of dry THF and cooled to 0 °C.

In a third flask 2 g of poly(propylene glycol)-block-poly(ethylene glycol)-block-poly(propylene glycol) bis(2-aminopropyl ether) M_n ~2,000 was dissolved in 15 ml of dry THF.

In an ice cold 500 ml beaker polyurethane prepolymer and poly-boron$_x$[(ε-pentanol/methyl)$_n$ dimethyl$_m$]siloxane gel were stirred together for 15 minutes in an ice bath. Further dissolved poly(propylene glycol)-block-poly(ethylene glycol)-block-poly(propylene glycol) bis(2-aminopropyl ether) M_n ~2,000 was added into the solution. The final proportion of isocyanate and hydroxyl/primary-amine groups was 1.4:1. The solution was stirred in an ice bath for ~2 minutes before the polymerization reaction between the primary amine of the block copolymer and the isocyanate groups began. A yellow cloudy gel quickly formed.

In a 200 ml beaker the gel was allowed to dry at room temperature for 3 days until it formed a soft rubbery polymer on the bottom.

This polymeric gel was dried for 3 weeks at room temperature and further heated at 95 °C for 70 minutes in order to form urethane links between the poly-boron$_x$[(ε-pentanol/methyl)$_n$ dimethyl$_m$]siloxane polymeric network and the polyurea-polyurethane/castor oil based polymeric matrix.

Results: A soft opaque rubbery yellow polymer (further called Sample 1) was formed (mechanical properties analysed by DMA). As shown in FT-IR spectrum 7, shown in Figure 78, the strong absorption at ~2360 cm^{-1} of the unreacted isocyanate is still present (about 15 % of overall the absorption of isocyanate before copolymerization had started), therefore in order to obtain a better quality (and also non-toxic) polymer the isocyanate-hydroxyl proportion should be further reduced.
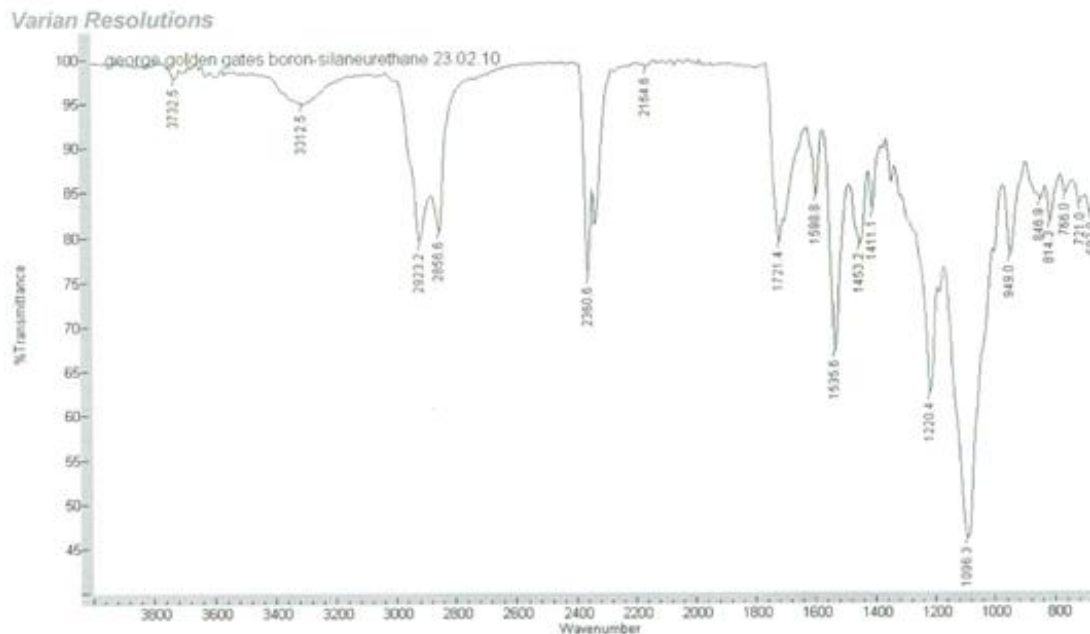
Figure 78: *"Golden-Gate"* <u>*FT-IR Spectrum 7*</u> *semi-IPN Based on Poly-boron$_x$[(ε-pentanol/methyl)$_n$ dimethyl$_m$]siloxane and Polyurea-urethane Networks*

The absorption peak at 1721 cm^{-1} is due to a $C{=}O$ bond of urethane and the absorption at lower frequencies is due to the $C{-}N$ stretching of an amide (of both urea and urethane groups), and also absorption in the area of 1570-1500 cm^{-1} is due to the in-plane $N{-}H$ bending. All IR absorption of the urethane groups (also here of isocyanate groups) is slightly shifted to the left suggesting a strong hydrogen bond which may be formed between boron groups of the borosiloxane network and urethane groups of polyurethane polymeric networks [110]. Hence, it is possible to predict a very complex stress relaxation process, as the reconformations of hydrogen bonds would be a function of deformation of both polymeric networks of the resulting IPN. (Also, these FT-IR results are in good agreement with the contemporary theoretical models [58, 62].)

After 3 months of storage of this polymer an FT-IR spectrum was taken (shown in FT-IR spectrum 8 in Figure 79) and according to the FT-IR spectrum 8 the proportion of unreacted isocyanate groups (also as THF) visually decreased in comparison with FT-IR spectrum 7 taken before the storage.

Unfortunately ^{1}H NMR and ^{13}C NMR spectra did not give any satisfactory results; because of the number of compounds in the final polymer the obtained spectra showed strong interferences which made it difficult for precise interpretation.
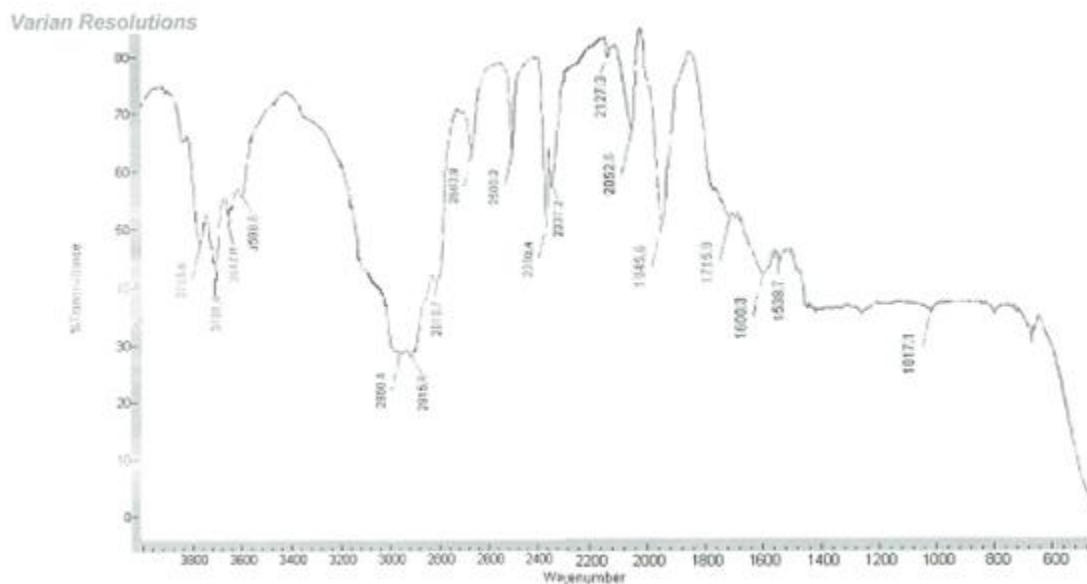
Figure 79: *Thin Polymeric Layer* <u>*FT-IR Spectrum 8*</u> *Obtained on $NaCl$ Crystals of semi-IPN Based on Poly-boron$_x$[(ε-pentanol/methyl)$_n$ dimethyl$_m$]siloxane and Polyurea-urethane Networks, after 3 Month of Storage*

4.5.2   <u>Experiment 21</u>: Formation of Scarcely Cross-linked Semi-IPN/co-polymer Based on an Isocyanate-ended Poly-boron$_x$[(ε-pentanol/methyl)$_n$ dimethyl$_m$]siloxane Polyurethane Prepolymer and a Soft Polyurethane/urea Network

Formulation 1: (**<u>Sample 2</u>**) The polyborosiloxane obtained in Experimental Phase 4 (1 boron for every16 silicon atoms in the polymeric backbone gel prepolymers poly-boron$_x$[(ε-pentanol/methyl)$_n$ dimethyl$_m$]siloxane as shown on FT-IR spectrum 4) was dissolved in dry acetone (checked additionally by FT-IR) and mixed with TDI. The poly-boron$_x$[(ε-pentanol/methyl)$_n$ dimethyl$_m$]siloxane (2.1 g) and acetone (10 ml) solution was mixed in a proportion of 1 TDI molecule (1.74 g) for each

210 g/mole(polymeric segment) of borosiloxane, as it was predicted that one ε-pentanol alternating group was attached to each second silicon atom of the siloxane polymeric backbone. Therefore, the backbone of the resulting polymer may be a random block copolymer of poly-(dimethylsilane/ε-pentanolmethylsilane) with an equal proportion of dimethylsilane and ε-pentanolmethylsilane blocks.

The solution was stirred for 15 minutes and heated up to 80 °C for 60 minutes. The FT-IR spectrum of the resulting siloxane prepolymer gel (after drying in vacuum for 30 minutes) is shown in FT-IR spectrum 9 in Figure 80.
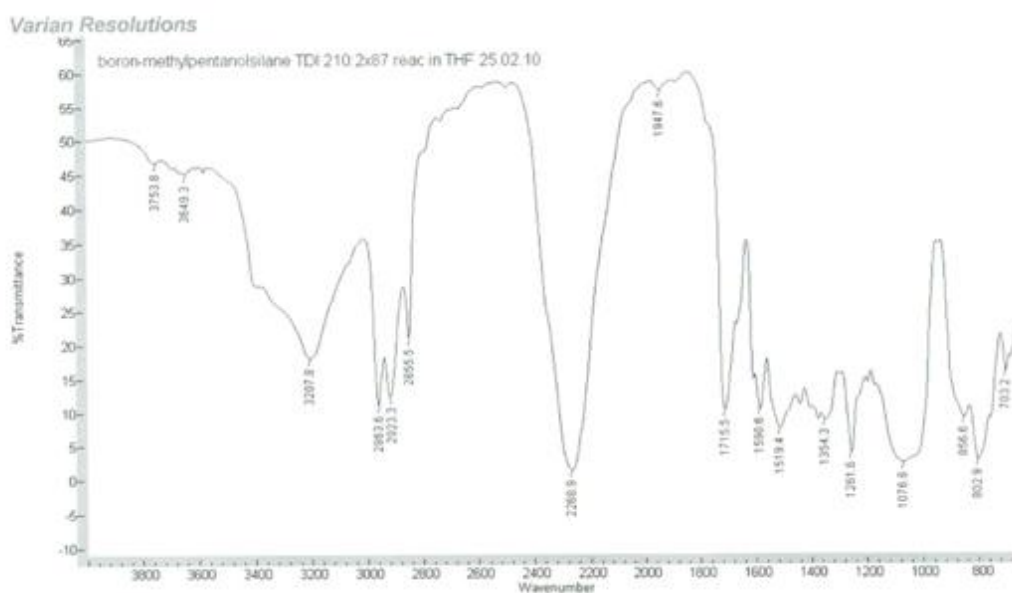
Figure 80: Thin Layer of Gel, FT-IR Spectrum 9 Obtained on $NaCl$ Crystals of Isocyanate-ended Prepolymer Based on Poly-boron$_x$[(ε-pentanol/methyl)$_n$ dimethyl$_m$]siloxane Obtained at Experimental Phase 4

A castor oil (1.7 g) and TDI (0.87 g) based isocyanate-ended prepolymer was separately prepared by the same experimental technique shown in the previous experiment.

In an ice bath in a 200 ml beaker both isocyanate-ended prepolymers were dissolved in 20 ml dry acetone and stirred continuously.

In a separate 50 ml flask 2 g of poly(propylene glycol)-block-poly(ethylene glycol)-block-poly(propylene glycol) bis(2-aminopropyl ether) M_n ~2,000 and 0.5 g of

1,6- hexamethylene diamine were dissolved in 20 ml of dry acetone. This resulting solution of di-primary amine prepolymers was added to the beaker with the isocyanate-ended prepolymers.

The stirring was continued for 5 minutes and then the temperature was allowed to rise to room temperature as the beaker with the solution was taken out of the ice bath. Gel formation appeared at ~7 °C and the gelation formation was swift.

Then the resultant yellow, light-transparent and rubbery gel was filled into a Teflon form and dried at room temperature for 3 days. After that, the rubbery sample was taken from the form and dried further at room temperature for 2 months.

After 2 months, the yellow and opaque hard rubbery sample was additionally heated for 70 minutes at 95 °C in order to complete the polymerization process (i.e., to form a substituted urea from the still unreacted isocyanate groups and secondary amine groups of formed urea links).

<u>Results:</u> The resultant borosiloxane-urea/urethane polymer is a very hard (storage modulus $G' = 12.21$ MPa) and inflexible yellow opaque polymer. Therefore, such hard polymeric material (Sample 2) is unsuitable for the original application. Hence, the proportion of urea and urethane cross-links should be significantly reduced in order to obtain a softer and more rubbery polymer.

*Formulation 2: (**Sample 3**)* Similarly to formulation 1, 4.54 g of the poly-boron$_x$[(ε-pentanol/methyl)$_n$ dimethyl$_m$]siloxane prepolymer obtained in Experimental Phase 4 was dissolved in 20 ml of dry acetone and mixed with 0.87 g of TDI. This gives a proportion of 1 isocyanate group for every10 silicon atoms of the siloxane.

The prepolymer was heated to 80 °C for 60 minutes. An FT-IR spectrum of the obtained isocyanate-ended prepolymer is shown in FT- IR spectrum 10 in Figure 81.

Further, similarly to formulation 1, the borosiloxane isocyanate-ended prepolymer was formed into a rubbery gel with 2 g of poly(propylene glycol)-block-poly(ethylene glycol)-block-poly(propylene glycol) bis(2-aminopropyl ether) M_n ~2,000 and 0.5 g of 1,6- hexamethylene diamine.

The resulting polymer was also dried for 2 months and further additionally heated for 70 minutes at 95 °C in order to complete the polymerization process.
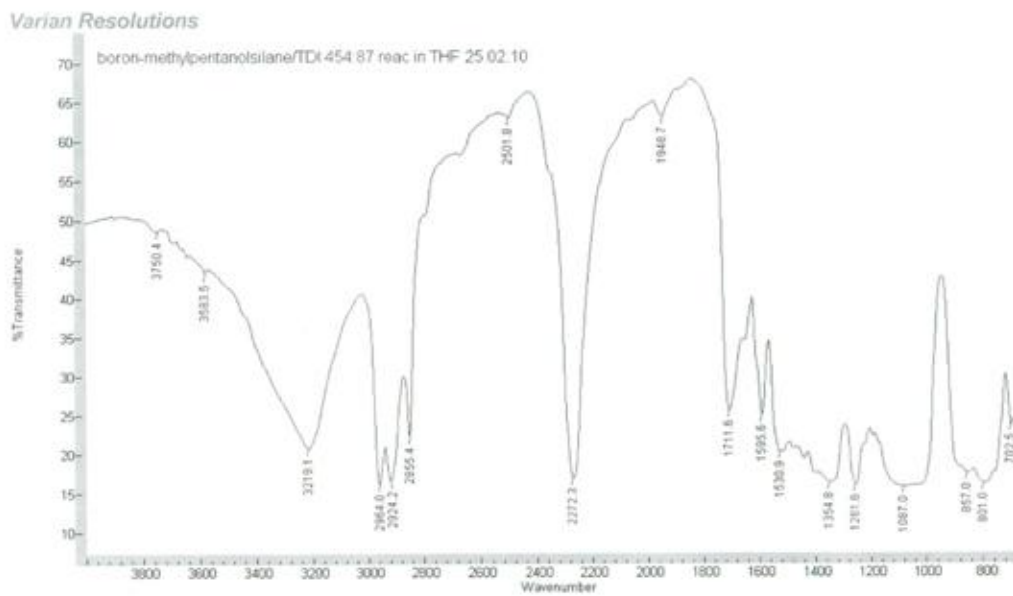
Figure 81: Thin Layer of Gel, <u>FT-IR Spectrum 10</u> Obtained on $NaCl$ Plates of Isocyanate-ended Prepolymer Based on Poly-boron$_x$[(ε-pentanol/methyl)$_n$ dimethyl$_m$]siloxane Obtained at Experimental Phase 4

<u>Results:</u> After 3 months of storage of a thin slice (0.8 mm) of this cloudy yellow rubbery semi-IPN, the resulting rubber (mechanical properties analysed by DMA) became a clear light-transparent yellow polymeric material. But after the DMA test (i.e., multiple deformations) the same light-transparent polymeric sample became cloudy once more (i.e., as the original one). Therefore, it is possible to suggest that over a longer time polymolecules of both polymeric networks are able to form a kind of homogenous polymer (i.e., light-transparent) instead of IPN. Deformation leads to restoration of two separate immiscible and incompatible polymeric networks.

<u>Discussion:</u> From the attempts to obtain a suitable soft rubbery polymeric material based on poly-boron$_x$[(ε-pentanol/methyl)$_n$ dimethyl$_m$]siloxane and soft polyurethane polymeric matrix only the series of Sample 1 and Sample 3 polymers gave a satisfactory results. Also, after 3 months of storage all of the resultant polymers still contained some trace of unreacted isocyanate (where the proportion of unreacted isocyanate in Sample 1 is ≈5 % and Sample 3 ≈15 % of the original IR absorption). Therefore, in order to obtain a prototype polymeric material suitable for industry further research is needed.

4.6   <u>Experimental Phase 6</u>: Dynamic Mechanical Analysis (DMA)

<u>Experimental:</u> All DMA tests were carried on PerkinElmer DMA 8000 analytical equipment.

Four samples were tested. Sample 1 and Sample 3 were described in Experimental Phase 5. Polyurethane elastomer (based on castor oil, TDI and poly(propylene glycol)-block-poly(ethylene glycol)-block-poly(propylene glycol) bis(2-aminopropyl ether) M_n ~2,000, with the final proportion of isocyanate to hydroxyl/primary amine 1.2 : 1) was also chosen as a polymeric material appropriately similar to the polyurethane matrix of Sample 1. In addition, a random sample of silica fines reinforced natural rubber from Office Depot supplier, product number No980553 was tested.

Procedure: All the samples were cut in strips of 0.8 mm thick, 5.6 mm wide and 12.5 mm length.

The oscillating stress was applied at different frequencies and amplitude values of 0.05 mm, 0.1 mm and 0.25 mm (that were equivalent to sample percentage deformation of 0.4%, 0.8% and 2%). Storage modulus G' and $\tan \delta$ (i.e., $\tan \delta = G''/G'$, where G'' is a loss modulus, as discussed in the Literature Review, section 2.2.2) were repeatedly measured at different temperatures and the average values are presented.

DMA Results 1 (shown in Figure 82) present average values of the storage modulus and $\tan \delta$ for Sample 1 at room temperature at an oscillating stress at different frequencies and amplitudes.

Data collected from Sample 1 at deformation of 0.25 mm shows the behaviour of an elastomer at multiple frequencies of oscillating stress, where G' is rising by a magnitude of 100 (from a deformation at 1 Hz to 100 Hz). The sharp rise of the storage modulus related to T_g of the given elastomer starts after 55 Hz.

In addition, Sample 1 shows a very specific rise of the storage modulus between 7.5 Hz and 15 Hz stress, where there is a greater than 6-fold increase and the value of $\tan \delta$ falls by about a factor of 10.
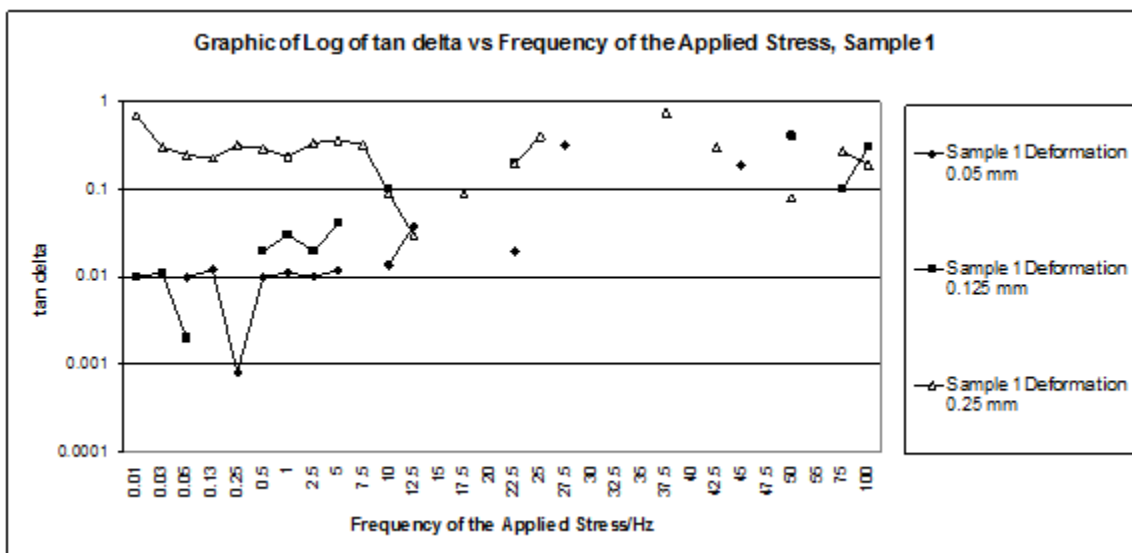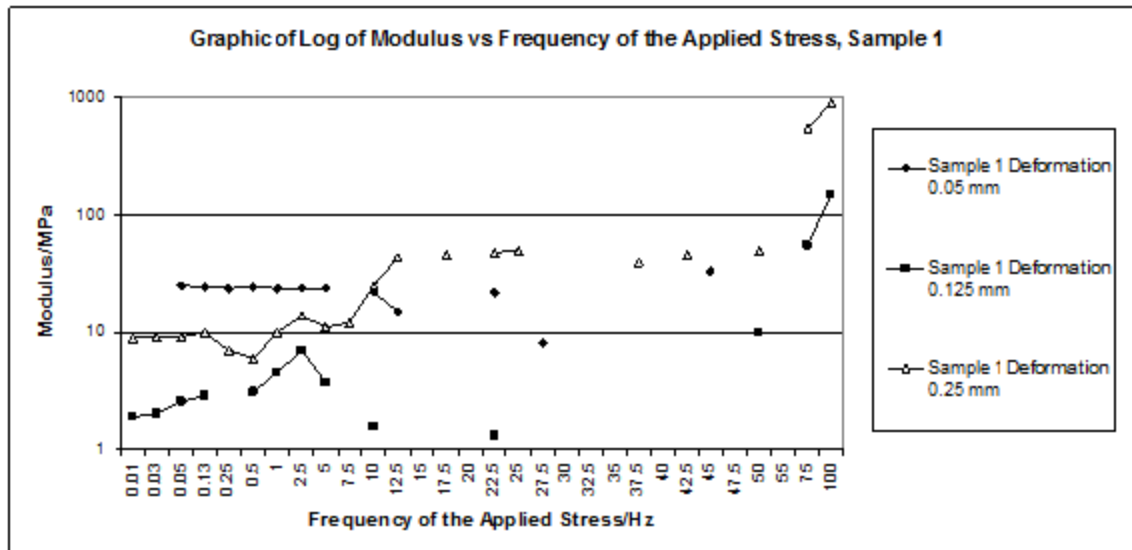
Figure 82: <u>*DMA Results 1*</u> *(Sample 1) Log of the Storage Modulus (top) and Log of tan δ (bottom) vs Frequency of the Applied Stress*

At all amplitudes (0.05 mm, 0.1 mm and 0.25 mm) in the area between 0.0125 Hz and 1 Hz Sample 1 behaves as a shear thinning polymer. This shear thinning behaviour can be possibly explained by a combination of factors. First, intermolecular bonds formed during a relatively long time of relaxation were disconnected by the initial deformation and the moving telechelic parts of the IPN may form loops predicted by Indei's models [64]. In addition, such stationary formed intermolecular bonds could form a kind of

polymeric gel, which also disappears when the deformation of the material exceeds certain values [67, 70]. In support of this hypothesis is the appearance of very different dynamic behaviour of this polymer at different amplitudes of the applied stress. At a deformation of 0.25 mm the polymer exhibits shear thinning and also $\tan \delta$ falls twice, when at a deformation of 0.1 mm the material generally shows shear thickening at those frequencies.

Sample 1, Deformation 0.1 mm, Applied Stress 0.125 Hz
Dynamic Properties vs Temperature
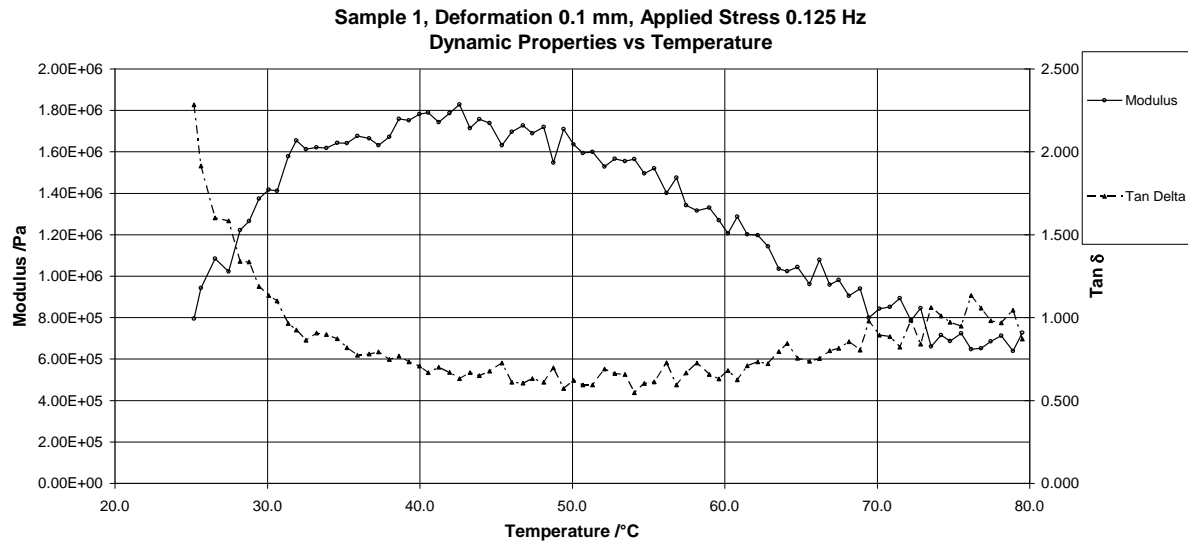
Figure 83: <u>DMA Results 2</u> (Sample 1) the Storage Modulus and $\tan \delta$ vs Temperature, Frequency of the Applied Stress 0.125 Hz, Deformation 0.1 mm

DMA Results 2 (shown in Figure 83) present data collected from Sample 1 at a deformation of 0.1 mm at constant frequency stress of 0.125 Hz. With an initial rise of temperature from room temperature up to ~43 °C, the storage modulus rises from 0.8 MPa to1.8 MPa and the value of $\tan \delta$ drops from 2.25 to 0.5. This rise of the storage modulus can possibly be explained by the fact that at higher temperatures earlier disconnected intermolecular bonds are able to rearrange much faster, so the storage modulus rises. Above ~43 °C, the storage modulus starts to decrease and $\tan \delta$ rises. At this temperature and deformation of 0.1 mm the polymer behaves similarly to branched polyethylene above 130 °C, where the storage modulus drops dramatically as the amount of the crystalline structure rapidly decreases with the rising temperature (as discussed in the Literature Review, section 2.2.2).

Figure 84: <u>DMA Results 3</u> *(Sample 1) the Storage Modulus and* $\tan \delta$ *vs Temperature, Frequency of the Applied Stress 1 Hz, Deformation 0.25 mm*

Figure 85: <u>DMA Results 4</u> *(Sample 1) the Storage Modulus and* $\tan \delta$ *vs Temperature, Frequency of the Applied Stress 12.5 Hz, Deformation 0.25 mm*

DMA Results 3 (shown in Figure 84) present the dynamic stress data for

Sample 1 at a deformation of 0.25 mm and at a constant frequency stress of 1 Hz. At this frequency the polymer no longer shows a drop in G' above 45 °C. And even at 80 °C the storage modulus only rises with the rise of temperature.

In the frequency area from 7.5 Hz to 12.5 Hz, the storage modulus rises dramatically to 65 MPa and the value of $\tan \delta$ drops (shown in DMA Results 4 in Figure 85). This sharp rise of G' may be related to boron substitutions in the polysiloxane backbone, as, at the given frequency, the polymer does not have sufficient free volume for fast rearrangements of strong hydrogen bonds [17]. In support of this hypothesis is the fact that with temperatures up to 80 °C (when infrared oscillation of the polymolecules starts effectively to speed up polymolecular reconfirmations and also the amount of free volume increases [26]) the value of the storage modulus drops about by 20 %.

As it is possible to see in the data given in DMA Results 1, G' drops from 65 MPa at 12.5-25 Hz to 40 MPa at 37.5-40 Hz (value of $\tan \delta$ rises in this area). This drop in the storage modulus may be related to the fact that the deformation inside the polymer happens so quickly that strong intermolecular hydrogen bonds tend to form dangling loops in the backbone chains in the telechelic parts of the polymeric material instead of rearrangements to the intermolecular bonds. Such behaviour was predicted by Indei in his theoretical model [64].

Between 55 Hz and 100 Hz, the storage modulus rises from 40-50 MPa to 1 GPa. This significant rise in G' value could be related to the fact that the entire polymer does not have sufficient free volume and as all the molecules of the semi-IPN are no longer capable of relaxation, the polymer goes below its T_g at the given oscillating stress and temperature. Such a sharp rise in storage modulus at higher frequencies is universal for any elastomeric polymer, and even an absolutely amorphous ideal elastomer would exhibit such rise in the value of the modulus [19].

The amount of boron substitution in the siloxane backbone may decrease the actual frequency of the applied stress at which the polymer goes below its T_g, as molecules containing strong intermolecular hydrogen bonds would normally require more free polymeric volume and time for molecular rearrangement [17].
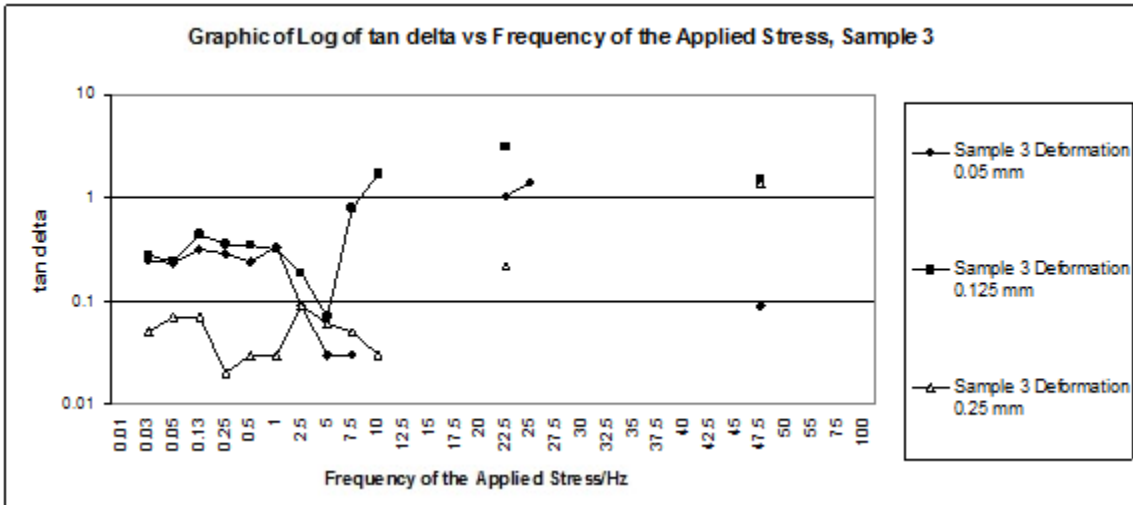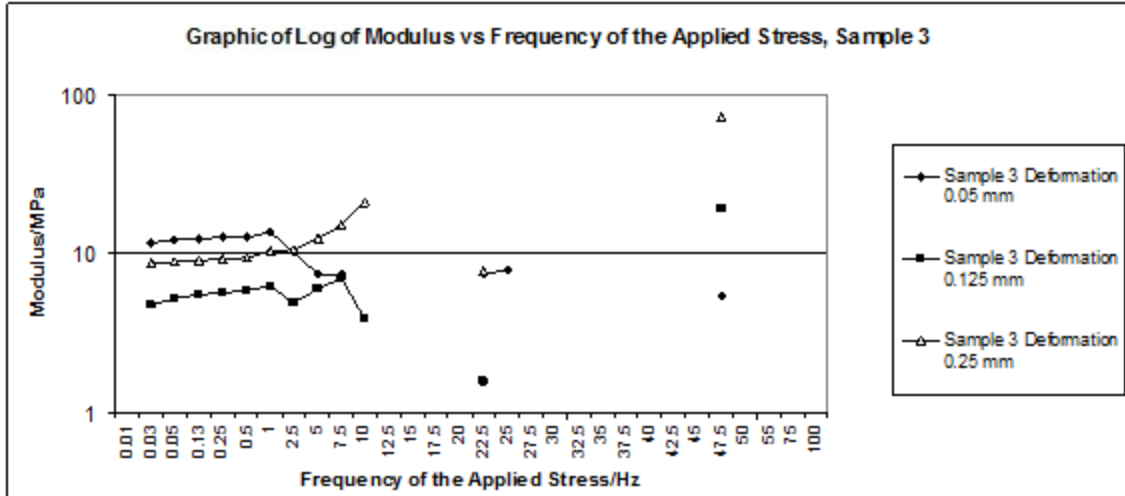
Figure 86: <u>*DMA Results 5*</u> *(Sample 3) Log of the Storage Modulus (top) and Log of*
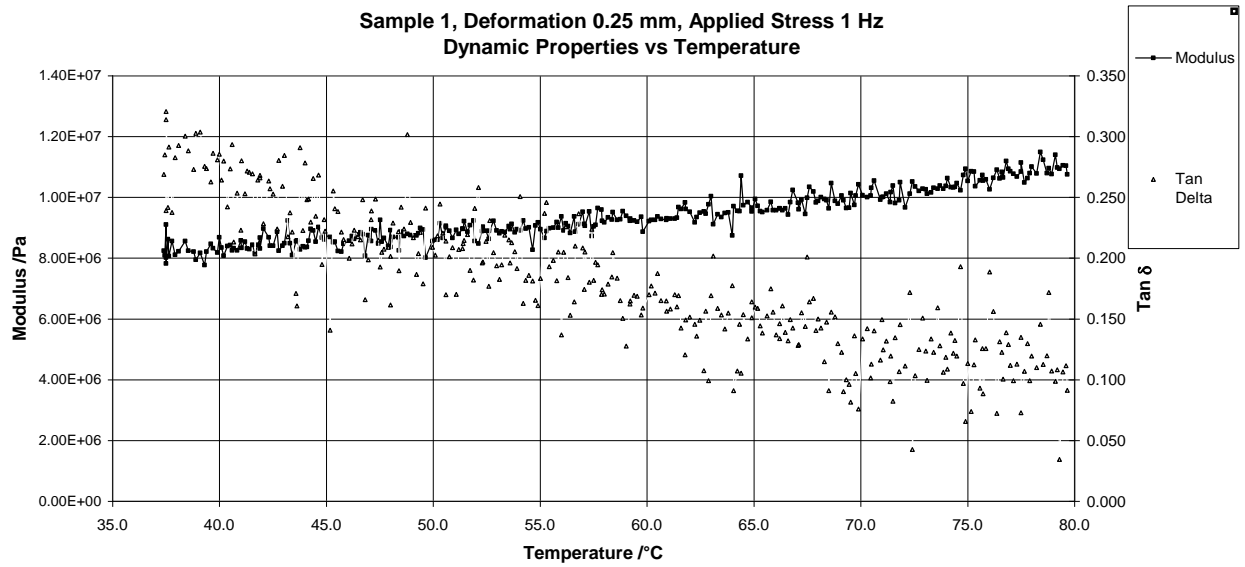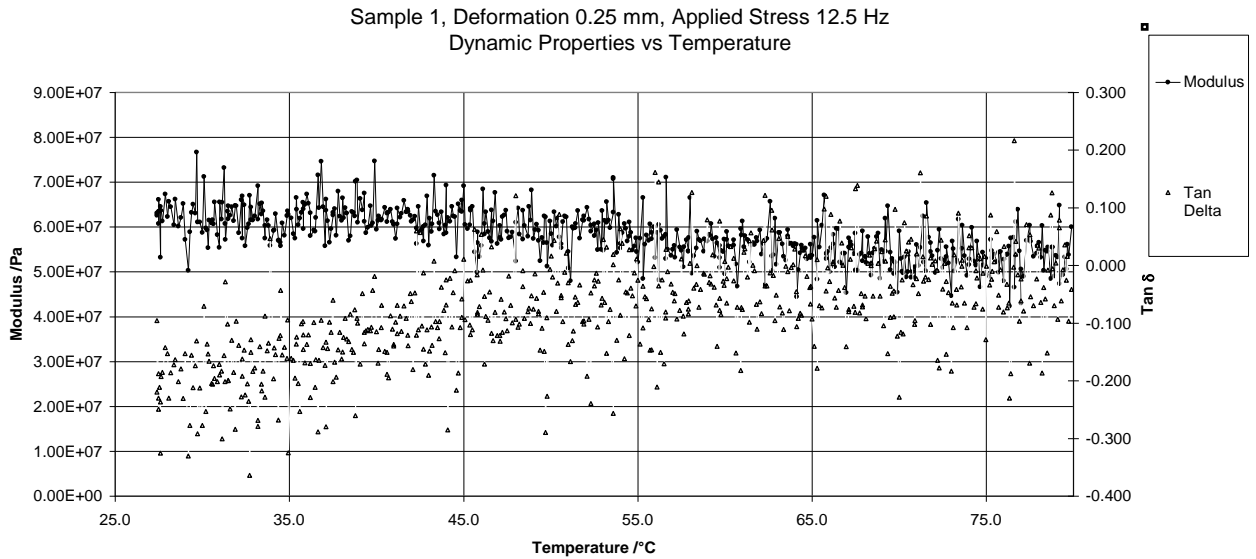*tan δ (bottom) vs Frequency of the Applied Stress*

DMA Results 5 (shown in Figure 86) present data for the storage modulus G' and
tan δ of Sample 3 versus the frequency of the applied deformational stress. In general,
the spectra of G' and tan δ for Sample 3 are similar to the spectra of the storage modulus
and tan δ for Sample 1, where the initial sharp rise in the value of G' starts at ~7 Hz and
leads to a drop in tan δ values followed by a decrease of the modulus at 22-40 Hz and a
final sharp rise at frequencies above 55 Hz.

The difference between these two polymeric materials is that the actual rise in G' value for Sample 3 (from 8 MPa up to 35 MPa) is nearly half that for Sample 1 (from 8 MPa up to 65 MPa). A decrease in the storage modulus value also appears at lower frequencies (for Sample 1 ~40 Hz and for Sample 3 ~22 Hz).

This difference may be explained by the fact that the proportion of rigid urea groups is significantly higher in Sample 3 than in Sample 1, therefore the polymolecules are less flexible to allow fast rearrangement in intermolecular hydrogen bonds [104], hence the formation of the dangling chains and the loops in the telechelic chains of the polymeric material appears at lower frequencies. These results are in good agreement with Indei's theoretical model [64].

In addition, there is a similarity in both samples regarding to the values of G' at very low frequencies of the oscillating deformational stress. Both samples show very similar G' at deformations of 0.05 mm, 0.1 mm and 0.25 mm between 0.25 Hz to1 Hz, where the storage modulus at 0.05 mm is ~12 MPa, ~8 MPa at 0.25 mm and ~5 MPa at 0.1 mm. This factor suggests that at very low frequency oscillating stress and a very limited deformation of 0.01 mm, a significant number of stationary formed bonds (i.e., formed during very long time) have still not been broken, therefore the material exhibits reasonably high values of the storage modulus. Further deformation leads to an effective breakage of such intermolecular bonds and G' sharply decreases - at deformation of 0.1 mm the values of storage modulus in both samples were less than half that at 0.05 mm. Finally when the deformation increases further to 0.25 mm, G' rises as strong intermolecular bonds (most probably boron bonds) require more time and free volume for effective molecular rearrangements. These results are in good agreement with model described by Xu et al (as given in the Literature Review, section 2.2.3) [70, 71].

DMA Results 6 (shown in Figure 87) present data for the storage modulus and $\tan \delta$ of the Polyurethane Matrix versus frequency of the applied deformational stress. In contrast with Sample 1 and Sample 3, the Polyurethane Matrix does not give a sharp rise of the storage modulus in any area of frequencies of the oscillating deformational stress lower than ~47-50 Hz (i.e., the frequency of the stress which leads to T_g of the polymer).
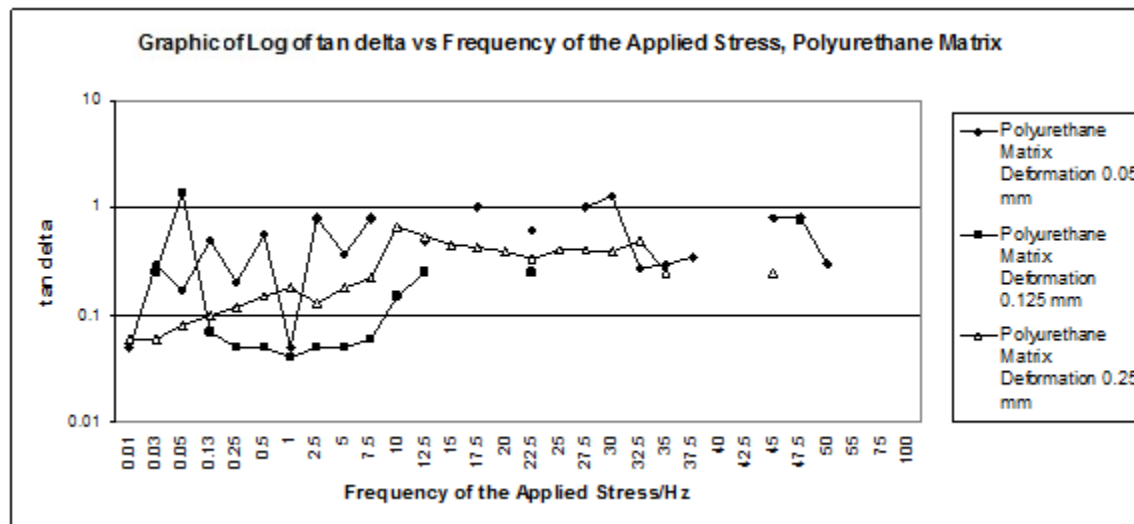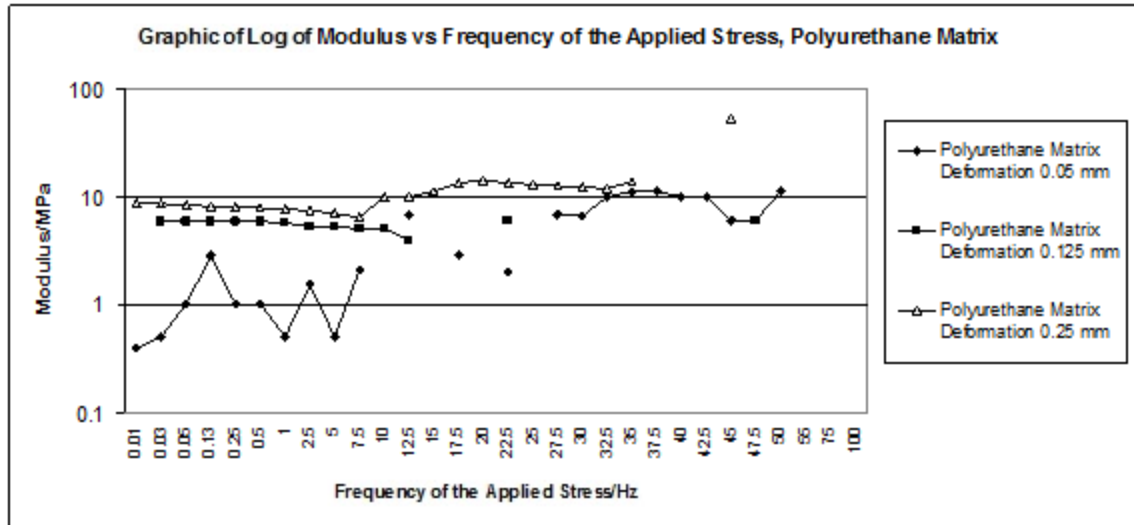
Figure 87: <u>*DMA Results 6*</u> *(the Polyurethane Matrix) Log of the Storage Modulus (top) and Log of* $\tan\delta$ *(bottom) vs Frequency of the Applied*

An insignificant decrease in the values of the storage modulus for deformational stresses at 0.1 mm and 0.25 mm at low frequencies (0.125-10 Hz) may be caused by the fact that the Polyurethane Matrix is quite inhomogeneous (i.e., contains immiscible parts as polyester parts, like castor oil, rigid urethane-urea blocks and soft PPO-PEO-PPO block copolymer). Xu et al and other researchers [70, 71] considered such a factor as a shear thinning effect of non-homogeneous polymeric materials (as given in the Literature Review, section 2.2.3).
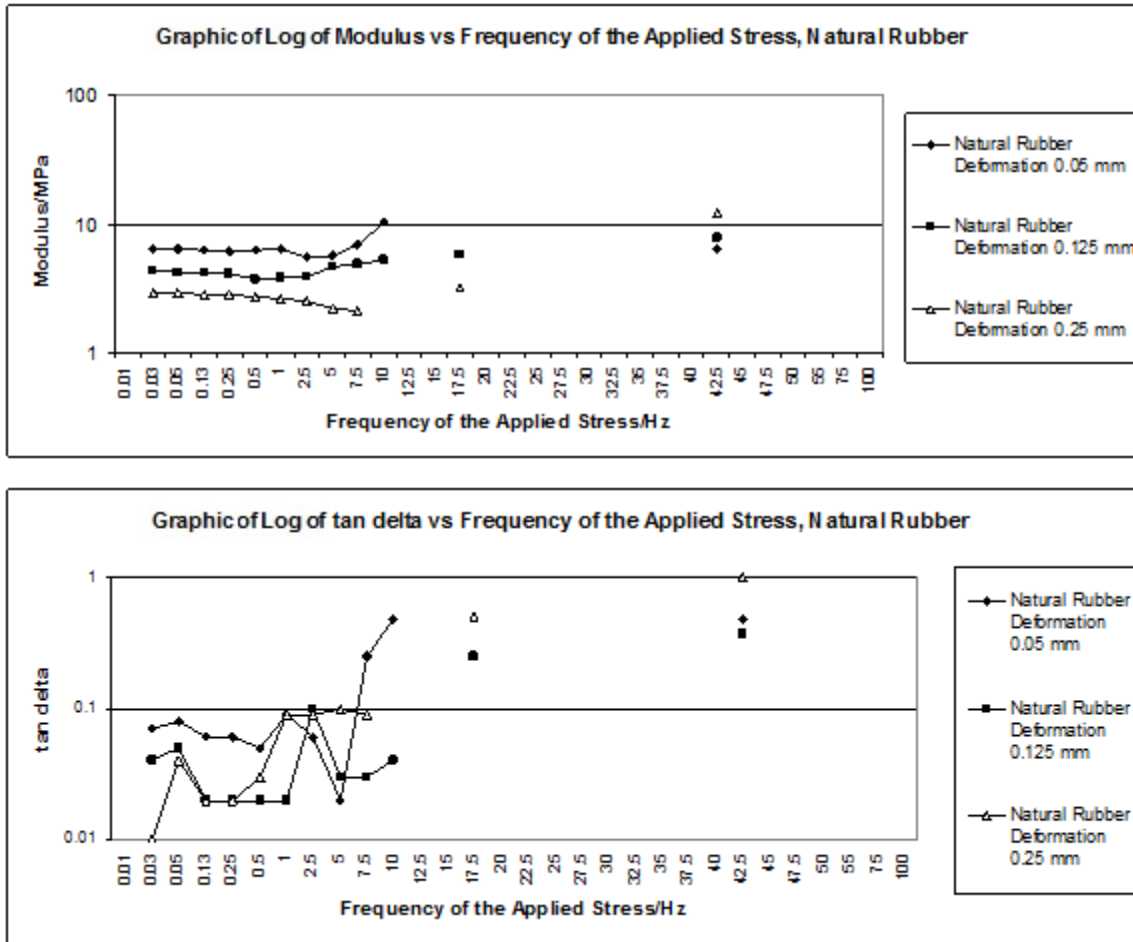
Figure 88: <u>DMA Results 7 (a Random Sample of Natural Rubber) Log of the Storage Modulus (top) and Log of $\tan \delta$ (bottom) vs Frequency of the Applied</u>

DMA Results 7 (shown in Figure 88) present data of the storage modulus and $\tan \delta$ of a random sample of natural rubber reinforced by filler versus frequency of the applied deformational stress. This sample of random reinforced natural rubber shows a shear thinning behaviour at stress of low frequencies from 0.125 Hz up to 10 Hz, therefore it suggests a non-homogeneous structure to the polymer [62, 70]. In addition, no sharp rise of the storage modulus has appeared at those frequencies where Sample 1 and Sample 3 had shown sharp increases in G' (as shown in DMA Results 8 presented in Figure 89).

This factor may also be able to prove the suggestion that the rise in values of the modulus for Sample 1 and Sample 3 in oscillating deformational stress at 7-40 Hz frequencies was related to the boron polymeric backbone substitutions.
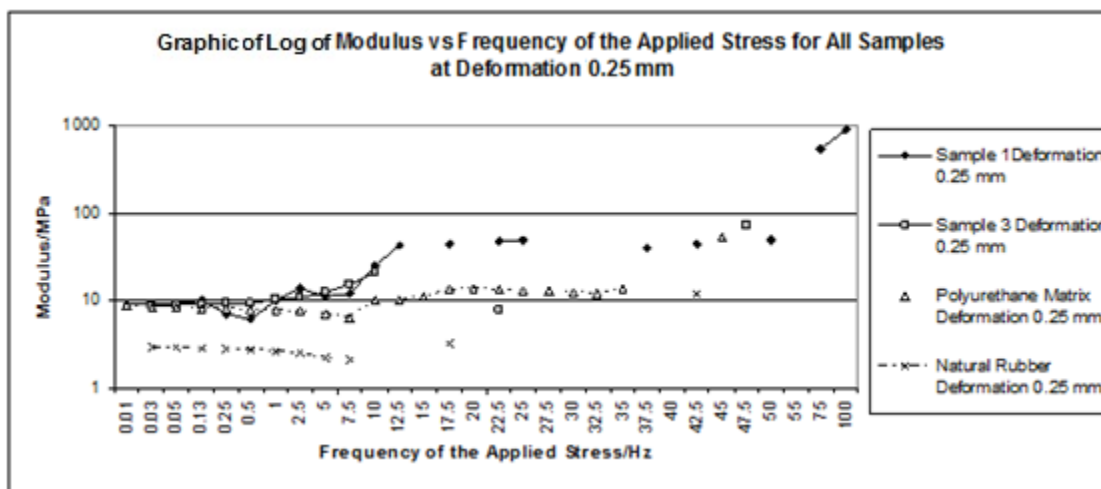
Figure 89: <u>DMA Results 8</u> Log of the Storage Modulus vs Frequency of the Applied, Deformation 0.25 mm, Comparison of All Samples Taken

DMA Results 8 (shown in Figure 89) present comparable data for all samples in this test at oscillating deformational stress of multiple frequencies and deformation of 0.25 mm. This figure shows that Sample 1 and Sample 3 have a similar dynamic behaviour with a sharp rise in the values of G' at frequency intervals between 7.5 Hz and 40 Hz.

Samples of polyurethane matrix and natural rubber also show some similarities such as an insignificant decrease in storage modulus between 0.125 Hz and ~7.5 Hz, that suggest a non-homogeneous polymeric structure for these materials [70].

Discussion: Sample 1 and Sample 3 show a sharp rise in storage modulus at applied oscillating stresses from ~7.5 Hz to 25-40 Hz. This sharp and significant rise in values of G' may be directly related to boron substitutions into the siloxane polymeric backbone, as neither the chosen sample of reinforced natural rubber nor the polyurethane matrix show such dynamic behaviour.

5 <u>Discussion</u>

5.1   Discussion of Chemical Synthesis of the Polymeric Material

A soft colourless oligomeric/polymeric gel of poly-boron$_n$-dimethylsiloxane$_m$ (where m ≈ 16 n) can be readily synthesised by two different ways; (i) by simple substitution of some of polysiloxane chain member at elevated temperature (≥ 200 °C) where the siloxane polymeric backbone of PDMS is no longer stable and boron substitutions through oxygen bonds onto the polymeric backbone to give a more thermally stable polymer or (ii) by simultaneous copolymerization (in a reaction bath) of dimethyldichlorosilane, water and boric acid. The latter method gives better control over the polymerization process, but molecules of hydrochloric acid (which is a byproduct of the reaction) may be trapped in the polymeric gel. The presence of such a strong acid is highly undesirable in this application, as 1 mole of a strong acid may be able to decompose up to 500 isocyanate groups. Therefore at this stage polyborosilane prepolymers (including those where some of the methyl groups were substituted by ε-pentanol groups) were exclusively produced by a substitution of a siloxane into borosiloxane at elevated temperatures.

In order to obtain a more controlled structure of the resulting polyborosiloxane prepolymer, it was suggested to use instead of dimethyldichlorosilane, a hydroxyl (or alternatively alkoxy) terminated short silane which does not give such a corrosive byproduct. So far, oligomeric dihydroxyl terminated oligomeric siloxanes (generally M_n ≈ 550) were successfully used in combination with dimethyldichlorosilane monomers, but in such a case hydrochloric acid was still a byproduct albeit in smaller quantities. All the attempts to use alkoxy-terminated monomers (given in Experimental Phase 4) have been unsuccessful.

A soft and rubbery polyurethane polymeric matrix can be obtained by numerous ways. The important factor is that a better tear resistance is possible in a polymer with a higher degree of chemical cross-links than in a polymer cross-linked by physical cross-

links [101]. Therefore, the soft segment of the polymer may be based on a combination of flexible and immiscible (i.e., prevent crystallisation) prepolymers such as PPO, PEO, castor oil, etc. TDI and isophorone diisocyanate may be used as an effective diisocyanate in order to create a soft and highly flexible polyurethane polymeric network. Even though soft polyurethanes based on castor oil normally show quite good tear resistance, in this application such polymers may be commercially undesirable because of a possible strong odour of the final product [99]. Hence, it is proposed that in further research castor oil could be substituted by a siloxane or PPO/PEO based highly flexible polyols with a high molecular weight. The proportion of urea links should be limited in any soft polyurethane formulation, as a material containing a high proportion of rigid urea links usually shows high tensile strength and often quite low tear resistance [101].

Traces of solvent trapped in the polymeric gel often lead to a significant reduction of mechanical properties of the final polymer [19], but in this application of the IPN between absolutely immiscible polymeric networks based on polyurethane and PDMS, use of a solvent during the final formation of the IPN is inevitable. So far all the obtained samples were dried for a very long time (i.e., a couple of months) before the DMA tests, but further research is needed in order to find some technological approaches to reduce the amount of the required solvent or alternatively reduce the solvent evaporation time without formation of a foam-like polymeric system.

A soft polymeric matrix based on PDMS strongly tends to phase separation in the IPN with polyurethane network. All possible attempts to stabilize those networks without introduction of chemical cross-links (as shown in Experimental Phase 2) so far have not been successful. Even when a high proportion of polyborosilane was successfully trapped in the formed polyurethane network of the IPN by use of an "unfriendly" solvent system [30], a phase separation happened at elevated temperature (90 °C) when the sample was additionally heated in order to allow unreacted isocyanate groups to react with unreacted hydroxyl and secondary amine groups (i.e., final polymerization of the polyurethane network). Therefore, at that stage it was decided that the PDMS based polyborosilane should be modified so that it would be capable of creating some chemical cross-links with the neighbouring polyurethane polymeric network.

In PDMS based polyborosilane some of the methyl groups attached to the polymeric siloxane backbone were substituted by ε-pentanol which contains a primary hydroxyl group attached to olefin (i.e., pentane) and such a primary hydroxyl group of ε-pentanol can readily react with isocyanate of the polyurethane network and as a result create a urethane cross-link between both polymeric networks.

The actual substitution of methyl groups attached to the polymeric siloxane backbone was performed by Grignard reaction, where a novel synthesis method was used (i.e., on side reaction of short 1,5-dibromopentane) in order to attach a halogen-ended short olefin to a siloxane prepolymer. The resulting halogen-ended olefin was further modified into hydroxyl-ended ε-pentanol. S_N2 substitution reaction of halogen with water was used; the strong acid by-product acted as a catalyst for this.

Furthermore the PDMS with alternating ε-pentanol groups was allowed to react with boric acid at elevated temperature (≥ 200 °C) in order to create poly-boron$_n$-[(ε-pentanol/methyl)$_n$dimethyl$_m$]siloxane prepolymer which is suitable for further polymerization through isocyanates. Even though some of the ε-pentanol groups which are attached to the siloxane polymeric backbone were lost during the reaction between siloxane and boric acid, the proportion of the lost ε-pentanol substitution was small and insignificant in comparison with the number of ε-pentanol groups still attached to the resulting borosiloxane polymeric backbone. In Experimental Phase 4 FT-IR, ^{1}H NMR and ^{13}C NMR spectra of the resulting novel are presented.

The use of our own polyurethane polymeric matrix instead of a readily available commercial one has a great advantage because in this way the final number of available isocyanate groups can be precisely controlled. Hence, all physical properties of the resulting semi-IPN can be controlled much more effectively.

5.2   Discussion of DMA Tests

DMA tests were performed on four different samples, where two of these contained a high proportion of telechelic polyborosilane in the polymeric formulation (about 50 % of the polymer mass). By such comparison of dynamical behaviour of a polymeric matrix based on polyurethane and a sample based on a very similar polyurethane matrix which formed the IPN with polyborosilane, it may be possible to estimate the effect on the dynamical properties of the IPN caused by incorporation of high proportion of telechelic polyborosilane. The actual effect on the dynamical properties of such IPN will be caused by a combined effect of telechelic behaviour of polyborosilane as well as co-influence of both polymeric networks. Such a strong co-influence on the dynamic behaviour of both polymeric networks was predicted by Gotlib et al [61, 62].

According to Indei's theoretical model [64], the telechelic behaviour of polyborosilane may be explained as follows: during very low frequencies of an applied oscillating stress very little change in the values of G' and G'' should be observed, but when the frequency of the applied oscillating stress rises, a sharp rise in the value of the storage modulus is expected. When the frequency of the stress rises further the members of the soft polymeric backbone which tend to form strong intermolecular bonds are expected to start to form dangling and loop chains instead of intermolecular rearrangements and the value of G' is expected to fall.

The pattern of the dynamical behaviour of the polyurethane matrix was difficult to predict, because of the high number of possible factors which may influence the dynamical behaviour involved. First, the polyurethane matrix contains a high proportion of soft and generally amorphous segments based on polyester of castor oil and blocks of PPO/PEO polyethers. The hard segment was based on aromatic diisocyanate, where some of isocyanates reacted to form urethane and/or even more rigid urea groups. According to a model by Xu et al [70], during the application of an oscillating stress and with increasing stress frequency, the value of the storage modulus is expected to drop, as a gel-like matrix which was formed by predominantly hard segments of the polymer and

such a gel-like matrix is expected to effectively disintegrate when polymolecules start to move.

By contrast, the value of G' is expected to rise with the increase of the frequency of the applied oscillating stress, because of an increasing number of polymolecular entanglements. The number of such entanglements at one given moment of time should increase dramatically, when the stress is applied faster than the time which is required for reptation relaxation of the molecules involved [54].

In addition, the amount of intermolecular interactions in a soft polymeric segment should rise significantly with an increase of the deformation, because (as shown in the Literature Review, section 2.1.5) polymolecules which tend to form coils between polymeric junctions in a relaxed stage will be forced to obtain new configurations where the number of possible molecular conformations is reduced (i.e., may cause an increase in the amount of crystalline in the amorphous part of polymer). In addition, there is a reduction in the free polymeric volume and hence the amount of intermolecular interaction may be significantly higher [17]. However before the DMA test was performed, it was difficult to predict the actual magnitude of such an increase in the intermolecular interaction in the soft segment.

Some effect may also be predicted by Gotlib's model [62] that suggests that polymolecules of the second polymeric network of IPN (i.e., which was fully cured only inside the IPN after the first polymeric network was formed) are able to only partially form coils between junctions during very long relaxation times and thus always stay stretched. The original Gotlib's model was for two ideal amorphous polymeric networks where intermolecular interaction can be neglected. Gotlib predicted that the relaxation time in IPN is somewhat longer than in a homogenous polymer and the time of relaxation for different junctions of the polymer will be widely dispersed. In this particular semi-IPN where there is hydrogen bonding between the two polymeric networks (i.e., shown by significant shifts to the lower IR absorption frequencies at IR absorption spectra of urethane, amine and carboxyl groups, as described in Literature Review, section 2.3.9) and some chemical cross-links between the two networks, the actual time of relaxation for different junctions of both polymeric networks were expected to be dispersed even stronger. A wide dispersion of values of G' and $\tan \delta$ in the DMA graphs given in

Figure 84 and Figure 85 may be explained by this theoretical prediction.

The exact pattern of dynamical behaviour is expected to be very complex. Therefore, the comparison of the dynamical behaviour of samples of the semi-IPN polyurethane polymeric matrix containing telechelic polyborosilane and polyurethane matrix seems to be the most beneficial option.

DMA Results 9 (shown in Figure 90) present results of the DMA test for all four samples of the DMA test, where Sample 1 and Sample 3 contain a high mass proportion of polyborosilane.

Areas of frequency of the applied oscillating stress are separated in Figure 90 in such order that to show which specific pattern of the polymeric dynamical behaviour thought to be predominant at given frequencies.
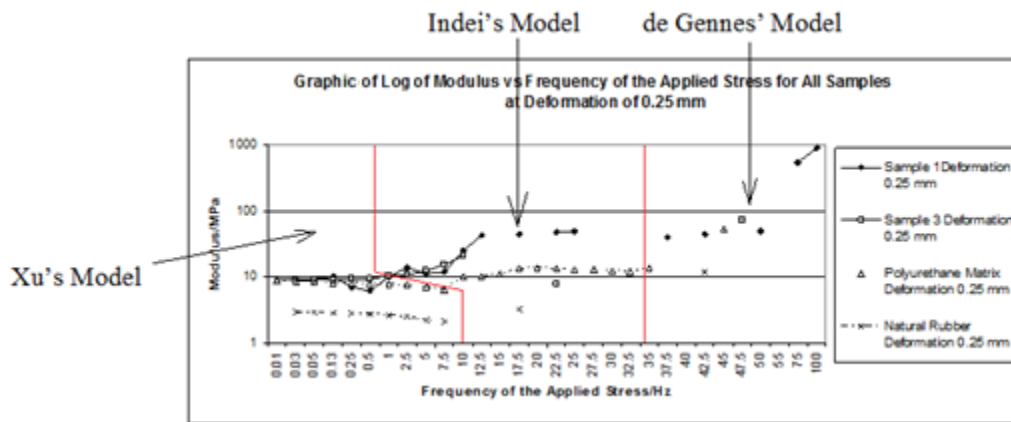
Figure 90: DMA Results 9 Log of the Modulus vs Frequency of the Applied Stress, Deformation 0.25 mm, the Areas of Frequencies are Separated in Order to Show Predominance of the Local Pattern of the Dynamic Polymeric Behaviour

All samples show a similar drop in G' values at frequencies between 0.01 and 1 Hz. For samples of natural rubber and polyurethane matrix such a drop in G' continued up to 7.5 Hz. The decrease in the G' value for all the samples may be explained by the failure of the gel-like matrix formed in those samples during very long relaxation time of molecules containing segments which tend to strong intermolecular interactions. This model was described by Xu et al [70]. For the sample of natural rubber, such gel-like

matrix is expected to be predominantly based on the co-interaction of particles of the reinforcing filler and for the polyurethane matrix (including Sample 1 and Sample 3). Such a gel-like matrix is expected to be based generally on the hard blocks of polymolecules (here boron substitution in polysiloxane must also be considered as a hard polymeric block).

At frequencies between 7.5 and 22.5 Hz for Samples 1 and 3, a sharp rise in G' values was observed followed by a drop after 25 Hz. This pattern of dynamic behaviour is in good qualitative agreement with Indei's theoretical prediction [64]. No such significant rise in G' values was observed in the dynamic behaviour of the polyurethane matrix or in the sample of natural rubber. Therefore, it is possible to suggest that this sharp rise in G' values for Sample 1 and Sample 3 was due to the presence of the polyborosilane network. This sharp rise in G' values in the behaviour of Samples 1 and 3 may also be due to an effect of interaction between the polyurethane and polyborosilane polymeric networks. Most probably this pattern of dynamic behaviour is a combination of both factors, where the influence of the former factor is predominant.

Further, the sharp rise in the values of G' for all samples at frequencies of the applied oscillating stress above 55 Hz is due to the rising number of polymolecular entanglements at the higher rate of deformation. The possible influence of increasing crystalline in a soft polymeric segment should also be considered [17]. In order to understand the influence of all the factors concerned further research is essential.

6 <u>Conclusions</u>

During this research a novel poly-[(boron)$_n$-(siloxane)$_m$-urea/urethane] soft polymeric material was successfully synthesised and the predicted structure of the obtained polymer was confirmed by a number of chemical analytical techniques, such as FT-IT, ^{13}C NMR and ^{1}H NMR spectroscope. The produced polymeric material combines properties of IPN where two soft and immiscible polymeric networks are interpenetrated together. In addition, in order to prevent a possible phase separation of siloxane from the main polymer body, both soft networks were chemically cross-linked through urethane cross-links. The final polymer is a soft cross-linked polymeric gel.

Polydimethylsilane (PDMS) based polymer is highly immiscible with any purely organic polymer and also exhibits very high polymolecular backbone mobility, therefore such polymer inevitably tends strongly to a phase separation. The performed during this research experiments have clearly shown that even in IPN based on a highly cross-linked organic polymeric system (here polyurethane block copolymer) and PDMS based cross-linked gel, such phase separation will have some (limited) place. One way to improve adhesion between the polymeric networks in such IPN was to increase the number of physical cross-links by introducing more polar boron substitutions in the poly-[(boron)$_n$-(siloxane)$_m$] network. But in such case valuable rheological properties of the given polymer will suffer or may be lost, as predicted in the theoretical model of Indei [64].

Therefore, it was decided to introduce some chemical bonding between the polymeric networks of the IPN. Hence, in this application poly-[(boron)$_n$-(siloxane)$_m$] gel was modified through the attachment of ε-pentanol groups to silicon atoms of siloxane polymeric backbone. Therefore this prepolymer contained reactive hydroxyl groups and was suitable to further copolymerization reaction with a prepolymer containing reactive isocyanate groups (i.e., formation of polyurethane links). The attachment of ε-pentanol to silicon of the polymeric backbone was performed by Grignard reaction. Chemical analysis was performed by means of FT-IT, ^{13}C NMR and ^{1}H NMR spectroscopy and showed that the product had the predicted chemical structure.

After the final copolymerization reaction between the poly-[(boron)$_n$-(siloxane)$_m$] and the urethane/urea-ether/ester prepolymer, the novel soft polymeric material was produced. This novel polymeric, scarcely cross-linked semi-IPN was tested by means of DMA. The material exhibited a significant rise in the value of its storage modulus G' (up to 10 times) in a diapason of frequency of the applied oscillating deformational stress between 7.5 Hz to 40 Hz and deformation about 2 % of the length of the sample (while at deformations between 0.25 to 1.5 % of the length of the sample, no increase in the storage modulus was detected). A decrease in the values of storage modulus G' was recorded between maximum values of 25 Hz (65 MPa) and about 20 % lower values of the storage modulus at 40 Hz (~ 48 MPa). So, further research is essential in order to obtain a more reliable polymeric material for body protection.

In addition, all samples of the obtained poly-[(boron)$_n$-(siloxane)$_m$-urea/urethane] semi-IPN contained some unreacted isocyanate groups (shown by FT-IR spectrum), where in Sample 1 the proportion of unreacted isocyanate was the lowest. Therefore, at this stage the obtained polymeric material is not suitable for use as a protective polymer for body protection as toxic unreacted isocyanate groups could potentially harm the human body. Because the final application can be considered as a direct contact of such polymeric system with human skin, further research is essential in order to obtain polyurethane (or other polymer) based polymeric gel which is completely free from any potentially toxic and/or irritant groups.

7 __Further Work__

Further research is essential in order to obtain a polymeric material which is able to increase its modulus of elasticity at a wider range of deformations, because the existing polymeric sample reliably increases its storage modulus just at quite narrow diapason of deformations ~2-2.5 % of the sample length. Further research is also needed in order to decrease the magnitude of the drop (decrease) of the value of the storage modulus at applied oscillating stress at frequencies around 40 Hz. The current sample decreases its storage modulus around 20 % from the maximum value at 25 Hz (~ 65 MPa).

A new formulation of polyurethane pre-polymeric matrix is essential in order to achieve the final polymer with a proportion of isocyanate and hydroxyl/primary amine groups closer to 1:1. In such a case all the isocyanate groups would have to react to produce the final polymer which will there be free of any potentially toxic and/or irritant groups.

In addition, here has been considered a possibility to obtain a soft polyborosilane polymeric system in which the boron atoms of the polychain would be able to trap the introduced anion groups. Therefore, it would be possible to receive a polymer where electrical conductivity depends on the momentum physical stage (i.e., stress relaxation). As a result, it may be possible to obtain a polymeric material which is able to register a mechanical impact on its surface as an electromagnetic signal, etc. But, in such a case, the entire chemical formulation of the current working polymer should be changed, as ester and urethane groups included in the current formulation could be chemically unstable during a cationic or an anionic attack.

8 <u>References</u>

1. A. N. Tarle; (1968) "Theoretical Mechanics" High School, USSR

2. Prof. A. Kuzmickis; (1996) "Theoretical Mechanics for Mechanical Engineers" Vilnius Gedimino Technical University Press, Lithuania

3. Doc. K. Zukauskas; (2007) "Technology for Sport's Applications" Press of Kaunas' Technological University, Kaunas, Lithuania

4. M.C. Bishop, (2002) "Lorica Segmentata Volume I" A Handbook of Articulated Roman Plate Armour, Armotura Press

5. The illustration was taken from www.wikipedia.org

6. Prof. V. Pliaukste and doc. S. Navickas; (1998) "History of a Gradual Development of the World's Military's Mind-part: Ancient World" Academic Book, Vilnius, Lithuania

7. Bor Z. Jang; (1994) "Advanced Polymer Composites" ASM International

8. On-line Journal of University of Exeter, www.exeter.ac.uk/news/featurednews/title,85818,en.html

9. Auxetic Ltd [GB] and Hook Patrick (2006)"Uses of Auxetic Fibres" patent No WO 2006021763, Published online in European Patent Office, (www.epo.org)

10. Yoshio Nakagawa Naoaki Higuchi Kenji Sano Hiroshi Nagami Yasushi Buzojima Tatsuya Suzuki Katsuya Kume Tomohide Banba Makoto Kai; (2009) "Impact Absorption Sheet for Flat Panel Display, Process for Producing the Same,

and Flat Panel Display" Patent Application Number: 20090087647 Published online in Internet FAQ Archives (www.faqs.org)

11. Patent DE 100 10 182 A1; (2000) "Improvements in shock absorbing ethylene vinyl acetate copolymer materials" Published online in The German Patent and Trade Mark Office (DPMA) (www.dpma.de)

12. Lawrence J. Rhoades, John M. Matechen and Mark J. Rosner; (2004) "Smart Padding System Utilizing an Energy Absorbent Medium and Articles Made Therefrom" Patent US 6,701,529 B1 Published online in The German Patent and Trade Mark Office (DPMA) (www.dpma.de)

13. Graham Budden; (2006) "Defence and Comfort: New Advancement in Impact-Protection Textiles" Dow Corning Corp.

14. Palmer Richard Martin and Green Philip Charles; "Design Blue" (d3o) European Patent Office's Patent Nr. A41D31/00C8: HK1065228; EP1832186; KR20060041185

15. On-line Journal of Russian Chemical Industrial Engineering Society, the e-Site Published by Number of RF Universities, leading by the University of Novosibirsk, Russian Federation (www.xumuk.ru)

16. Bruno Volmert; (1973) "Polymer Chemistry" Springer-Verlag, Berlin

17. Paul C. Painter and Michael M. Coleman; (1997) "Fundamentals of Polymer Science" A Technomic Publishing Company

18. T. Fang and D. A. Shimp; (1995) "Interpenetrating Polymers Networks" Progress in Polymer Science 20, pp. 61-118

19. Alfred Rubin; (1998) "The Elements of Polymer Science and Engineering" Academic Press, University of Waterloo

20. Stephen J. Clarson and J. Anthony Semlyen; (1993) "Siloxane Polymers" PTR prentice Hall, Englewood Cliffs, New Jersey

21. Arie Ram; (1997) "Polymer Engineering" Plenum Press, New York

22. George Odean; (1981) "Principles of Polymerization" John Wiley&Son, New York

23. Andrew Streitwieser, Clayton H. Heathcoch and Edward M. Kosower; (1998) "Introduction to Organic Chemistry" Prentice Hall, New Jersey

24. Fluka- Sigma Aldrich on-line catalogue (includes Charles J. Pouchert; (1975) "The Aldrich Library of IR Spectra")

25. Robert O. Ebewele; (2000) "Polymer Science and Technology" CRC Press LLC, USA

26. Prof. J. Storasta; (2002) Course of Lectures for Postgraduate Students in a Light Absorption in Polymolecular Materials, Physics Faculty, Vilnius University

27. Paul J. Flory; (1953) "Principles of Polymer Chemistry" Cornell University Press, Ithaca, New York

28. Kozo Shinoda; (1978) "Principles of Solution and Solubility" Marcel Dekker, Inc, New York

29. H. Yamakawa; (1971) "Modern Theory of Polymer Solution" Harper and Row, New York

30. Partha Majumdar and Dean C. Webster; (2006) "Influence of Solvent Composition and degree of Reaction on the formation of Surface Microtopography in a Thermoset Siloxane-Urethane System" Polymer, Volume 47, Issue 11, pp. 4172-4181

31. Edward M. Kosower; (1968) "Physical Organic Chemistry" John Wiley & Sons, Inc.

32. G. G. Freeman; (1962) "Silicones an Introduction to Their Chemistry and Applications" published for the Plastic Institute, London

33. John R. Dutcher and Alejandro G. Marangoni; (2005) "Soft Materials Structure and Dynamics" Marcel Dekker, New York

34. L. Treloar; (1975) "Physics of Rubber Elasticity" Third Edition, Clarendon Press, Oxford

35. Hideaki Takahashi, Yoshitaka Ishimuro and Hiroshi Watanabe; (2007) "Viscoelastic Behaviour of Scarcely Crosslinked Poly(dimethyl siloxane) Gels: 2. Effects of Sol Component and Network Strand Length" Journal of the Society of Rheology, Vol. 35, No 4, pp. 147-153

36. F. Albert Cotton and Geoffrey Wilkinson; (1976) "Basic Inorganic Chemistry" John Wiley & Sons, Inc

37. K. Dean, W.D. Cook, M.D. Zipper and P. Burchill; (2001) "Curing Behaviour of IPN Formed from Model VERs and Epoxy Systems I." Amine Cured Epoxy, Polymer 42, pp 1345-1359

38. L. H. Sperling; (1981) "Interpenetrating Polymer Networks and Related Materials" Plenum Press, New York

39. Nilhan Kayaman-Apohan, Ramazan Demirci, Mustafa Cakir and Atilla Gungor; (2005) "UV-curable Interpentrating Polymer Networks Based on Acrylate/vinylether Functionalized Urethane Oligomers" Radiation Physics and Chemistry, Volume 73, Issue 5, pp. 254-262

40. J. J. Fitzgerald and C. J. T. Landy; (1990) "Vitrification and Curing Studies of a Photopolymerizable Semi-interpenetrating Polymer Networks" Applied Polymer Science 40, pp 1727-1743

41. Daniel Brandell, Heiki Kasemagi and Alvo Aabloo; (2009) "Poly(ethylene oxide)-poly(butadiene) interpenetrated networks as electroactive polymers for actuators: A molecular dynamics study" Electochimica Acta, Volume 55, Issue 4, pp. 1333-1337

42. P. C. Barbosa, L. C. Rodrigues, M. M. Silva, M. J. Smith, A. J. Parola, F. Pina and C. Pinheiro; (2009) "Solid-state electrochromic devices using pTMC/PEO blends as polymer electrolytes" Electochimica Acta, Volume 55, Issue 4, pp. 1495-1502

43. Haiyan Pan, Hongting Pu, Decheng Wan, Ming Jin and Zhihong Chang; (2009) "Proton exchange membranes based on semi-interpenetrating networks of fluorine-containing polyimide and Nafion" Journal of power Sources, Volume 195, Issue 10, pp. 3077-3083

44. G. Gallego Ferrer, M. Monleon Pradas, J. L. Gomez Ribelles, F. Romero Colomer, I. Castilla-Cortazar and A. Vidaurre; (2009) "Infulence of the nature of the porous confining network on the sorption, diffusion and mechanical properties of hydrogel IPNs" European Polymer Journal, Volume 46, Issue 4, pp. 774-782

45. Dale J. Waters and Curtis W. Frank; (2009) "Hindered diffusion of oligosaccharides in high strength poly(ethyle glycol)/poly(acrylic acid)

interpenetrating network hydrogels: Hydrodynamic vs. obstruction models"
Polymer, Volume 50, Issue 26, pp. 6331-6339

46. Lichen Yin, Jieying Ding, Jing Zhang, Chunbai He, Cui Tang and Chunhua Yin;
    (2010) "Polymer integrity related absorption mechanism of superporous hydrogel
    containing interpenetrating polymer networks for oral delivery of insulin"
    Biomaterials, Issue 12, pp. 3347-3356

47. Takanori Shimizu, Tatsuro Goda, Norihiko Minoura, Madoka Takai and
    Kazuhiko Ishihara; (2010) "Super-hydrophilic silicone hydrogels with
    interpenetrating poly(2-methacryloyoxyethyl phosphorylcholine) networks"
    Biomaterials, Volume 31, Issue 12, pp. 3274-3280

48. Jinghong Ma, Bing Fan, Borun Liang and Jian Xu; (2009) "Synthesis and
    characterization of Poly(*N*-isopropylacrylamide)/Poly(acrylic acid) semi-IPN
    nanocomposite microgels" Journal of Colloid and Interface Science, Volume 341,
    Issue 1, pp.88-93

49. Jun-long Wang, Chuang Wang, Geng-sheng Jiao and Qiu-ya Wang; (2009)
    "Study of SiO_2/PMMA/CE tri-component interpenetrating polymer network
    composites" Material Science and Engineering: A, Volume 527, Issue 7-8, pp.
    2045-2049

50. F. N. Cogswell; (1994) "Polymer Melt Rheology a Guide for Industrial Practice"
    Woodhead publishing Limited, Cambridge, England

51. Alfeus Sunarso, Takehiro Yamamoto and Noriyasu Mori; (2004) "Numerical
    Analysis of Elangation Behaviour of Melt Flow in Contraction Channels with
    Cylindrical Barriers" Journal of the Society of Rheology, Vol. 33, No 3, pp. 135-
    140

52. Sachio Matsumoto; (2005) "Pioneer Works on Rheology of Foodstuffs in Japan" Journal of the Society of Rheology Vol. 33, No 2, pp. 61-66

53. Haifa El-Sadi, Nabil Esmail and Ibrahim Hassan; (2007) "Numerical Modelling of Non-Newtonian Flow in Viscous Micropump" Journal of the Society of Rheology Vol. 36, No 1, pp 51-58

54. M. Doi and S. F. Edwards; (1986) "The Theory of Polymer Dynamics", Clarendon Press, Oxford

55. Toshiaki Sawada, Xiuying Qiao and Hiroshi Watanabe; (2006) "Viscoelastic Relaxation of Linear Polyisoprenes: Examination of Constrain Release Mechanism" Journal of the Society of Rheology, Vol. 35, No 11, pp. 11-20

56. L. E. Nielsen and R. F. Landel; (1994) "Mechanical Properties of Polymers & Composites" 2nd edition, Marcel Dekker, New York

57. J. D. Ferry; (1980) "Viscoelastic Properties of Polymers" Third edition, Wiley, New York

58. P. G. de Gennes and J. Badoz; (1996) "Fragile Objects : Soft Matter, Hard Science and the Thrill of Discovery" Copernicus

59. L. E. Nielsen; (1962) "Mechanical Properties of Polymer" Reinhold, New York

60. R. Zallen; (1983) "The Physics of Amorphous Solids" John Wiley & Sons, New York

61. Yu. Ya. Gotlib; (1981) "Some Problems of the Theory of Relaxation Phenomena in Polymer Networks with Account for Intersegment Friction" Pushchino, USSR

62. Yu. Ya. Gotlib, I. A. Torchinkii, V. P. Toshchevikov and V. A. Shevelev; (2010) "Theory of Relaxation Spectra for Two Identical Interpenetrating Polymer Networks" ISSN 0965-545X, Polymer Science, Ser A, Vol. 52, No 1, pp. 82-93

63. J. J. Aklonis and W. J. MacKnight; (1983) "Introduction to Polymer Viscoelasticity" Second Edition, Wiley Interscience, New York

64. Tsumotu Indei; (2007) "Effect of nonlinearity Strength in Chain Tension on Shear-Thickening of Associating Polymer Networks" Journal of the Society of Rheology, Vol. 35, No 3, pp. 147-153

65. Alfeus Sunarso and Takehiro Yamamoto; (2006) "Prediction of Rheological Properties of Associative Polymeric Fluids Using a Reversible network with Non-Interacting FENE Dumbbell Model" Journal of the Society of Rheology, Vol. 35, No 3, pp. 129-136

66. Richard A. Pethrick; (1993) "Viscoelastic and Ultrasonic Studies of Linear and Cyclic Polydimethylsiloxane" PTR Prentice Hall, Inc, New Jersey

67. Yoshiaki Takahashi and Yoshihiko Akazawa; (2004) "Hysteresis in Domain Size of Immiscible Polymer Blends under Shear Flow and Related Viscosity Behaviour" Journal of the Society of Rheology, Vol. 33, No 1, pp. 17-21

68. Yoshiaki Takahashi, Shuhei Yahata, Atsushi Takano and Yushu Matsushita; (2006) "Annealing Effects on the Elastic Properties of Sphere-forming ABA and ABC Triblock Copolymers" Journal of the Society of Rheology, Vol. 34, No 3, pp. 177-180

69. Kenzo Okamoto and Masaoki Takahashi; (2007) "Effects of Interface Velocity on the Stress Tensor in Immiscible Polymer Blends: Retraction of Spheroidal

Droplets and Stress Relaxation" Journal of the Society of Rheology, Vol. 36, No 1, pp. 43-49

70. Xiaoming Xu, Chuanhua Gao, Qiang Zheng and Xian Jang; (2007) "Linear/Nonlinear Rheological Properties and Percolation Threshold of Polydimethylsiloxane Filled with Calcium Carbonate" Journal of the Society of Rheology, Vol. 35, No 5, pp. 283-291

71. Howard See and Andrei Gordin; (2007) "Response of Carbonyl Iron-based Magneto-rheological Suspensions Under Step Changes in Magnetic Fields" Journal of the Society of Rheology, Vol. 36, No 1, pp. 59-64

72. R. J. H. Voorhees; (1967) "Organohalosilanes Precursors of Silicones" Elsevier Publishing Company, Amsterdam

73. S. Fordham; (1960) "Silicones" George Newnes Limited, London

74. Clayden, Greeves, Warren and Wothers; (2001) "Organic Chemistry" Oxford, University Press

75. Ernest W. Colvin; (1988) "Silicone Reagents in Organic Synthesis" Academic Press, London

76. E. Colvin; (1981) "Silicon in Organic Synthesis" Butterworths

77. Shunji Aoki; (2009) "Silicone Pressure -Sensitive Adhesive Composition" Patent Application Number: 20090305036 Published online in Internet FAQ Archives (www.faqs.org)

78. Tsuneo Kimura, Norio Kameda and Hideyoshi Yanagisawa; (2009) "Room Temperature Curable Organopolysiloxane Composition" Patent Application

Number: 20090159203. Published online in Internet FAQ Archives (www.faqs.org)

79. Mengqui Jia, Chaobo Wu, Wei Li and Dahai Gao; (2009) "Synthesis and Characterization of a Silicone Resin with Silphenylene Units in Si-O-Si Backbones" Journal of Applied Polymer Science, Vol. 114, pp. 971-977

80. Raquel Pena-Alonso and Gian Domenico Soraru; (2007) "Synthesis and Characterization of Hybrid Borosiloxane Gels as Precursors for Si-B-O-C Fibres" J Sol-Gel Sci Technol, Vol. 43, pp. 313-319

81. Vrena Liebau, Ralf Hauser and Ralf Riedel; (2004) "Amorphous SiBCO Ceramics Derived from Novel Polymeric Precursors" C. R. Chimie, Vol. 7, pp. 463-469

82. D. F. Shriver, P. W. Atkins and C. H. Langford; (1994) "Inorganic Chemistry" Oxford, University Press

83. Gary L. Miessler and Donald A. Tarr; (1991) "Inorganic Chemistry" Prentice-Hall, Inc

84. George Ferguson, Simon E. Lawrence, Lorraine A. Neville, Brian J. O'Leary and Trevor R. Spalding; (2007) "Synthetic and X-ray Diffraction Studies of Borosiloxane cages [R'Si(ORBO)$_3$SiR'] and the adduct of [Bu^{t}Si(O(PhB)O)$_3$SiBu^t] with Pyridine or *N, N, N', N'*-tetramethylethylenediamine" Polyhedron, Vol. 26, pp. 2482-2492

85. Earl L. Muetterties; (1967) "Chemistry of Boron and Its Compounds" John Wiley & Sons, Inc

86. R. Kurono, M. A. Mehta, Takayoshi Inoue and T. Fujinami; (2001) "Preparation and Characterization of Lithium Ion Conducting Borosiloxane Polymer Electrolytes" Electrochimica, Acta 47, pp. 483-487

87. Tatsuo Fujinamo, Daisuke Miyamo, Tadaaki Okamoto, Masahiko Ozawa and Akinori Konno; (2004) "Proton Conducting Borosiloxane-poly(ether-sulfone) Composite Electrolyte" Electrochimica, Acta 50, pp. 627-631

88. Eiji Higuchi, Hiroyuki Uchiba, Tatsuo Fujinami and Masahiro Watanabe; (2004) "Gas Diffusion Electrodes for Polymer Electrolyte Fuel Cells Using Borosiloxane Electrolytes" Solid State Ionics, Vol. 171, pp. 45-49

89. Qian Wang, Liying Fu, Zhijie Zhang, Zemin Xie; (2006) "Preparation and properties of Borosiloxane Gels" Journal of Applied Polymer Science, Vol. 99, pp. 719-724

90. Gian Domenico Soraru, Nicola Dallabona, Christel Gervais and Florence Baboneau; (1999) "Organically Modified SiO2-B2O3 Gels Displaying a High Content of Borosiloxane (B-O-Si) Bonds" Chem. Mater., Vol. 11, pp. 910-919

91. Alexis R. Brunner, Duane R. Bujalski, Eric S. Moyer, Kai Su and Larry G. Sneddon; (2000) "Synthesis and Ceramic Conversion Reactions of Pinacolborane- and Diethylborazine-Modified Poly(vinylsiloxane)s. The Development of a Processable Single-Source Polymeric Precursor to Boron-Modified Silicon Carbide" Chem. Mater., Vol. 12, pp. 2770-2780

92. Robert M. Silversteir, Francis X. Webster and David J. Kiemle; (2005) "Spectrometric Identification of Organic Compounds" John Wiley & Sons, Inc

93. Koji Nakanishi and Philippa H. Solomon; (1977) "Infrared Absorption Spectroscopy" Holden Day Inc

94. Stefan Schnabel, Denis Roizard, Trong Nguyen, Pierre Lochnon and Phillipe Aptel; (1998) "Synthesis of Novel Block Siloxane Polymers for the Removal of Butanols from Aqueous Feed Solutions" Colloids and Surfaces A: Physicochemical and Engineering Aspects, Vol. 138, Issue 2-3, pp. 335-343

95. Paul F. Bruins; (1969) "Polyurethane Technology" Polytechnic Institute of Brooklyn, New York

96. L. N. Phillips and D. B. V. Parker; (1964) "Polyurethanes Chemistry, Technology and Properties" published for the Plastic Institute, London

97. J. M. Buist and H. Gudgeon; (1968) "Advances in Polyurethane Technology" Maclaren and Sons Ltd, London

98. Mahsa Dabagh, , M. J. Abdekhodaie, M. T. Khorasani; (2005) "Effect of Polydimethylsiloxane Grafting on the Calcification, Physical Properties and Biocompatibility of Polyurethane in Heart Valve" Journal of Applied Polymer Science, Vol. 98, pp. 758-766

99. M. Fernandes, M. C. Goncalves, V. de Zea Bermudez, R. A. Sa Ferreira, L. C. Carlos, A. Charas and J. Morgado; (2008) "Optical Material Componed of a di-urethanesil Host Hirbid and Europium Complex" Journal of Alloys and Compounds, Vol. 451, Issue 1-2, pp. 201-205

100. Marica Ivankovic, Ivan Brnardic, Hrvoje Ivankovic, Miroslav Huskic and Andreja Gajovic; (2009) "Preparation and Properties of Organic-inorganic Hybrids Based on poly(methylmethacrylate) and Sol-gel Polymerized 3-glycidyloxypropyltrimethoxysilane" Polymer, Vol. 50, Issue 12, pp. 2544-2550

101. Piotr Krol; (2006) "Synthesis Method, Chemical Structures and Phase Structures of Linear Polyurethanes. Properties and Applications of Linear Polyurethanes in Polyurethane Elastomers, Copolymers and Ionomers" Progress in Materials Science, Volume 52, Issue 6, pp. 915-1015

102. F. S. Chuang, W. C. Tsen and Y. C. Shu; (2004) "The Effect of Different Siloxane Chain-extenders on the Thermal Degradation and Stability of the Segmented Polyurethanes" Polymer Degradation and Stability, Vol. 84, Issue 1, pp. 69-77

103. S. Ioan, G. Grigorescu and A. Stanciu; (2001) "Dynamic-mechanical and Differential Scanning Calorimetry Measurements on Crosslinked Poly(ester-siloxane)- urethanes" Polymer, Vol. 42, Issue, pp. 3633-3639

104. Aurelian Stanciu, Victor Bulacovschi, Miora Lungu, Stelian Vlad, Sorin Balint and Stefan Oprea; (1999) "Mechanical Behaviour of Crosslinked Poly(ester-siloxane)urethanes" European Polymer Journal, Vol. 35, Issue 11, pp. 2039-2044

105. D. Gomes, K. V. Peinemann, S. P. Nunes, W. Kujawski and J. Kozakiewicz; (2006) "Gas Transport Properties of Segmented Poly(ether siloxane urethane urea) Membranes" Journal of Membrane Science, Vol. 281, Issue 1-2, pp. 747-753

106. Gisbet Riess and Hans-Werner Schmidt; (2005) "Novel Urea-Siloxane Polymers as Gelling Agents for Silicone Fluids: Influence of the Hard segment" Monatshefte fur Chemie, 137,pp. 935-941

107. Hamid Javaherian Naghash, Ahmad Reza Massah and Masoud Arman; (2009) "Silicone Secondary Cross-linked IPN Based on Poly(vinyl-co-hydroxyethyl methycrylate) and SiO_2" Progress in Organic Coating, Vol. 65, Issue 2, pp. 275-280

108. S. S. Pathak, A. Sharma, A.S. Khanna; (2009) "Value Addition to Waterborne Polyurethane Resin by Silicone Modification for Developing High Performance Coating of Aluminium Alloy" Progress in Organic Coating, 65, pp. 206-216

109. Lin Ye, Ling Ju, Chuan Wu, Ting Feng, Wei Mo, Feng Wu, Ying Bai and Zeng-guo Feng; (2009) "Synthesis and Characteristics of a Silicon-Containing Polymer, Manufacture of an Electrolyte Membrane from the Polymer and Poly(vinylidene fluoride-co-hexafluoropropene), and Property Testing of the Membrane" Journal of Applied Polymer Science, Vol. 144, pp.1086-1093

110. S. C. Nunes, V. de Zea Bermudez, D. Ostrowkii and Nuno V. Martins; (2007) "Vibrational Spectra and Microstructure of Poly(ε-caprolactone)/siloxane Biohybrids Doped with Lithium-triflate" Journal of Molecular Structure, Vol. 879, Issue 1-3, pp. 72-80

111. Prof. G. Guiga; (2011) Course of Lectures for Postgraduate Students in a Mechanical Properties of Polymolecular Materials, Faculty of Mechanical Engineering, Brazil's Federal University of Santa Catarina

112. Yu-Chi Tseng and Syang-Peng Rwei; (2011) "Synthesis and Characterization of Feed Ratio of Polyethylene Oxide (0 ~ 10 Wt % PEO) in the Nylon-6/PEO Copolymer System" Journal of Applied Polymer Science, Vol. 123, pp.796-806